Electronic Supplementary Material (ESI) for Physical Chemistry Chemical Physics.
This journal is © the Owner Societies 2021

# Experimental Measurement and Prediction of Ionic Liquid Ionisation Energies

Jake M. Seymour,[1] Ekaterina Gousseva,[1] Alex Large,[1] Coby J. Clarke,[2] Peter Licence,[2] Richard M. Fogarty,[3] David A. Duncan,[4] Pilar Ferrer,[4] Federica Venturini,[4] Roger A. Bennett,[1] Robert G. Palgrave,[5] Kevin R. J. Lovelock.[1]

[1] Department of Chemistry, University of Reading, Reading, RG6 6AD, UK
[2] School of Chemistry, University of Nottingham, Nottingham, NG7 2RD, UK
[3] Department of Materials, Imperial College London, SW7 2AZ, UK
[4] Diamond Light Source, Didcot, Oxfordshire, OX11 0DE, UK
[5] Department of Chemistry, University College London, UK
Contact E-mail: k.r.j.lovelock@reading.ac.uk

## 1. Ionic Liquids Studied and Synthesis

Table S1 gives the ionic liquids (ILs) studied. All 60 ILs were liquid at room temperature, making XPS experiments relatively straightforward, as no heating was required for any IL studied here. Compared to the ILs studied in reference [1], two new cation cores were studied here, $[C_nC_1Pyrr]^+$ and $[C_nPy]^+$. Furthermore, 20 new anions were studied, with a variety of properties/reasons to study.

- $I^-$ vs $[I_3]^-$.
- Nine halozincate ILs with different ligands, different number of zinc atoms and different countercation.
- Five transition metal complexes, four tetrahedral and one octahedral.
- $[BF_4]^-$ vs $[PF_6]^-$.
- $[PF_6]^-$ vs $[FAP]^-$.
- $[PF_6]^-$ vs $[SbF_6]^-$.
- Three main group-based anions: $[SnCl_3]^-$ vs $[InCl_4]^-$ vs $[SbF_6]^-$.
- 12 ILs with post-transition centres in total.
- Cation-anion combinations selected to potentially give the cation as the HOMO.

$[C_8C_1Im]_2[FeCl_4]$, $[C_8C_1Im]_2[CoCl_4]$, $[C_8C_1Im]_2[CoBr_4]$, $[C_8C_1Im]_2[Co(NTf_2)_4]$, $[C_8C_1Im]_2[NiCl_4]$, $[C_8C_1Im]_2[Zn_3Br_8]$ and $[C_8C_1Im]_2[ZnCl_2Br_2]$ were prepared using the following method. 1-Octyl-3-methylimidazolium chloride, $[C_8C_1Im]Cl$, and 1-octyl-3-methylimidazolium bromide, $[C_8C_1Im]Br$, were purchased from Iolitec, and dried on a Schlenk line at $<2 \times 10^{-2}$ mbar at 70°C for 48 h before being transferred to a LABstar (MBraun) glovebox with <0.5 ppm of $O_2$ and $H_2O$. These viscous ILs were gently heated to 40°C; next, 2-3 g of the appropriate IL was decanted into a series of 30 mL screw top glass vials. The desired amount of metal salt (ESI Table S2 for metal salt sources, used as received) was calculated and weighed into each vial, stirrer bars were added, and the temperature was raised to 70°C. Masses are given in ESI Table S3. The vials were periodically handled to wash any solid particles from the sides until clear solutions persisted (typically < 48 h). For both laboratory and synchrotron measurements, the samples were mounted in air; exposure to air was limited to <10 minutes. For $[C_8C_1Im]_2[ZnCl_2Br_2]$, 1-octyl-3-methylimidazolium bromide and zinc(II) chloride were used.

**Table S1.** ILs investigated in this work.

| IL no. | Abbreviation | Structure | Name | Synthesis |
|---|---|---|---|---|
| 1 | $[C_8C_1Im]Cl$ | 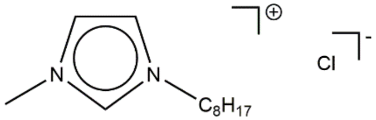 | 1–octyl–3–methylimidazolium chloride | Ref. [1] |
| 2 | $[C_8C_1Im]Br$ | 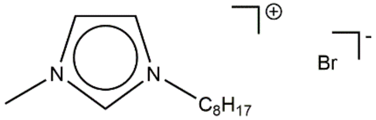 | 1–octyl–3–methylimidazolium bromide | Ref. [1] |
| 3 | $[C_6C_1Im]I$ | 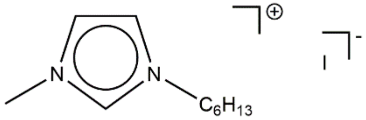 | 1–hexyl–3–methylimidazolium iodide | Ref. [1] |
| 4 | $[P_{6,6,6,14}]Cl$ | 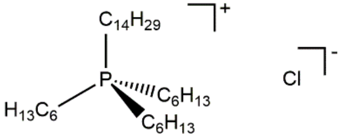 | tetradecyl(trihexyl)phosphonium chloride | Ref. [1] |
| 5 | $[P_{6,6,6,14}]Br$ | 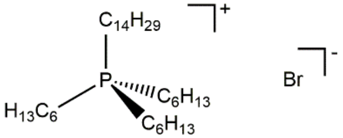 | tetradecyl(trihexyl)phosphonium bromide | Ref. [1] |
| 6 | $[C_4C_1Im][SCN]$ | 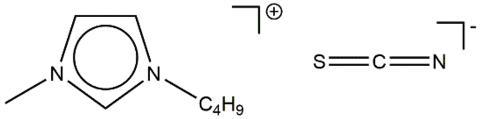 | 1–butyl–3–methylimidazolium thiocyanate | Ref. [1] |
| 7 | $[C_8C_1Im][SCN]$ | 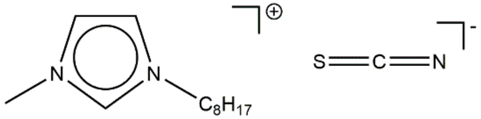 | 1–octyl–3–methylimidazolium thiocyanate | Ref. [1] |
| 8 | $[C_4C_1Im][N(CN)_2]$ | 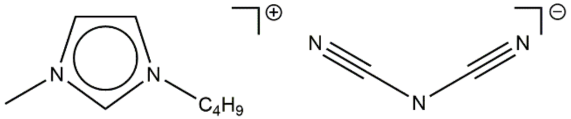 | 1–butyl–3–methylimidazolium dicyanamide | Ref. [1] |

|  |  |  |  |  |
|---|---|---|---|---|
| 9 | $[P_{6,6,6,14}][N(CN)_2]$ | 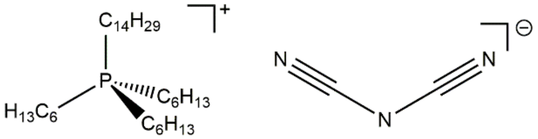 | tetradecyl(trihexyl)phosphonium dicyanamide | Ref. [1] |
| 10 | $[C_8C_1Im][C(CN)_3]$ | 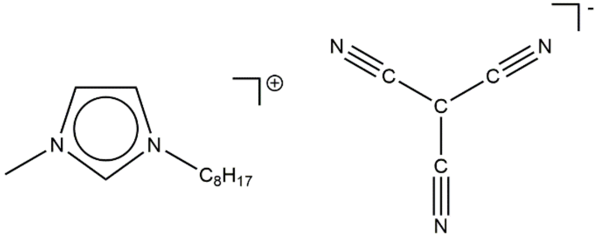 | 1–octyl–3–methylimidazolium tricyanomethanide | Ref. [1] |
| 11 | $[C_6C_1Im][B(CN)_4]$ | 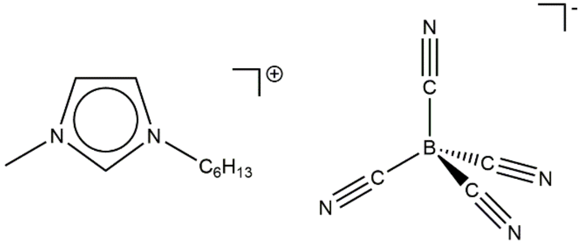 | 1–hexyl–3–methylimidazolium tetracyanoborate | Ref. [1] |
| 12 | $[C_8C_1Im][BF_4]$ | 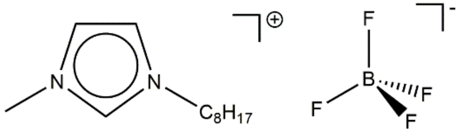 | 1–octyl–3–methylimidazolium tetrafluoroborate | Ref. [1] |
| 13 | $[P_{6,6,6,14}][NO_3]$ | 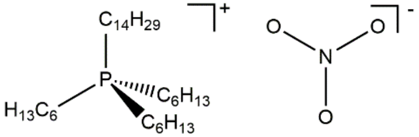 | tetradecyl(trihexyl)phosphonium nitrate | Ref. [1] |
| 14 | $[C_4C_1Im][HSO_4]$ | 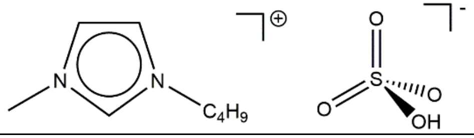 | 1–butyl–3–methylimidazolium hydrogensulfate | Ref. [1] |

| | | | | |
|---|---|---|---|---|
| 15 | $[C_8C_1Im][HSO_4]$ | 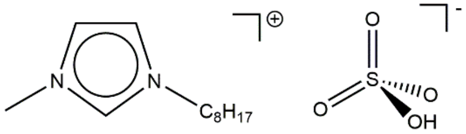 | 1–octyl–3–methylimidazolium hydrogensulfate | Ref. [1] |
| 16 | $[C_4C_0Im][HSO_4]$ | 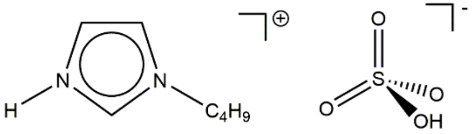 | 1–butyl–imidazolium hydrogensulfate | Ref. [1] |
| 17 | $[N_{4,1,1,0}][HSO_4]$ | 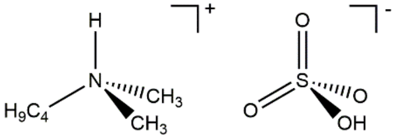 | butyl(dimethyl)ammonium hydrogensulfate | Ref. [1] |
| 18 | $[N_{8,1,1,0}][HSO_4]$ | 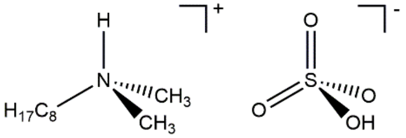 | octyl(dimethyl)ammonium hydrogensulfate | Ref. [1] |
| 19 | $[C_4C_1Im][MeSO_4]$ | 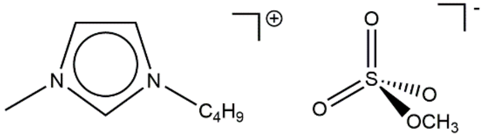 | 1–butyl–3–methylimidazolium methylsulfate | Ref. [1] |
| 20 | $[C_4C_1Im][OcSO_4]$ | 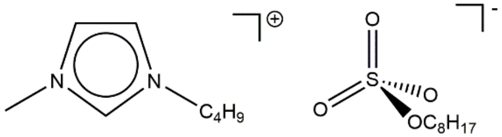 | 1–butyl–3–methylimidazolium octylsulfate | Ref. [1] |
| 21 | $[C_2C_1Im][MeSO_3]$ | 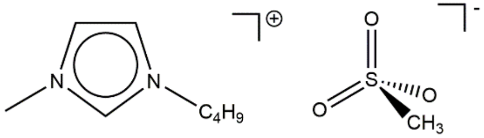 | 1–ethyl–3–methylimidazolium methanesulfonate | Ref. [1] |
| 22 | $[C_4C_1Im][Me_2PO_4]$ | 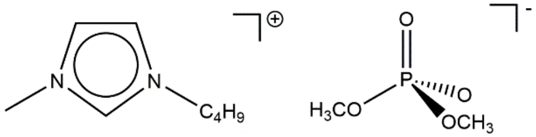 | 1–butyl–3–methylimidazolium dimethylphosphate | Ref. [1] |

|  |  |  |  |  |
|---|---|---|---|---|
| 23 | $[C_4C_1Im][TfO]$ | 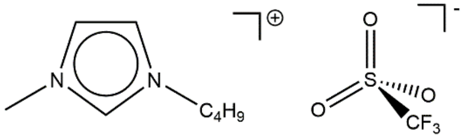 | 1–butyl–3–methylimidazolium trifluoromethylsulfonate | Ref. [1] |
| 24 | $[C_8C_1Im][TfO]$ | 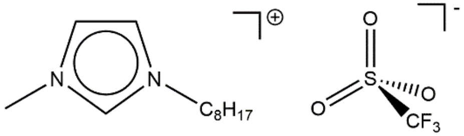 | 1–octyl–3–methylimidazolium trifluoromethylsulfonate | Ref. [1] |
| 25 | $[N_{2,2,1,0}][TfO]$ | 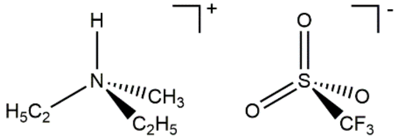 | diethyl(methyl)ammonium trifluoromethylsulfonate | Ref. [1] |
| 26 | $[N_{2OH,2OH,2OH,1}][TfO]$<br>or<br>$[N_{(2OH)3,1}][TfO]$ | 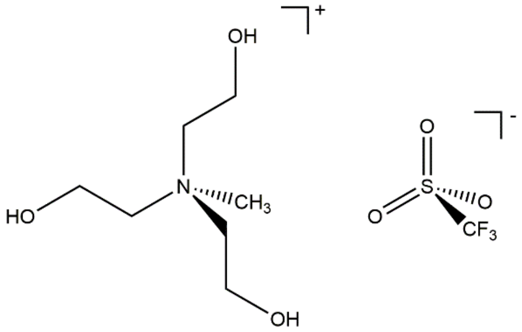 | triethanol(methyl)ammonium triflate | Ref. [1] |
| 27 | $[C_4C_1Im][NTf_2]$ | 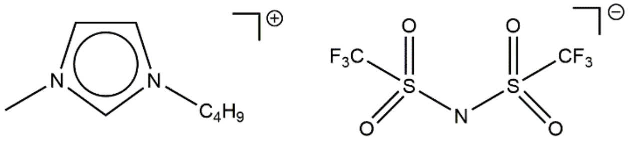 | 1–butyl–3–methylimidazolium bis[(trifluoromethane)sulfonyl]imide | Ref. [1] |
| 28 | $[C_6C_1Im][NTf_2]$ | 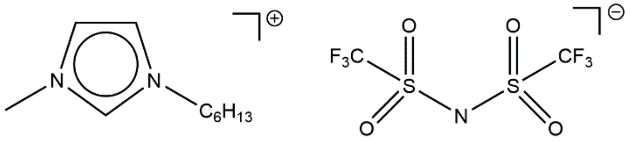 | 1–hexyl–3–methylimidazolium bis[(trifluoromethane)sulfonyl]imide | Ref. [1] |
| 29 | $[C_8C_1Im][NTf_2]$ | 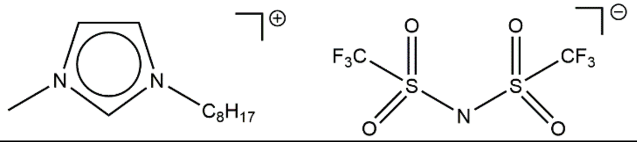 | 1–octyl–3–methylimidazolium bis[(trifluoromethane)sulfonyl]imide | Ref. [1] |

| | | | | |
|---|---|---|---|---|
| 30 | $[C_2C_0Im][NTf_2]$ | 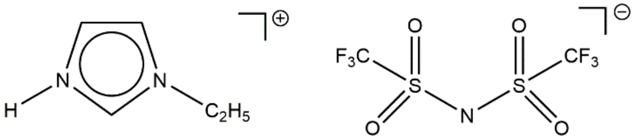 | 1–ethyl–imidazolium<br>bis[(trifluoromethane)sulfonyl]imide | Ref. [1] |
| 31 | $[C_4C_0Im][NTf_2]$ | 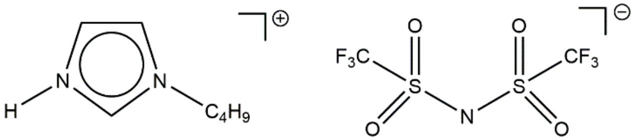 | 1–butyl–imidazolium<br>bis[(trifluoromethane)sulfonyl]imide | Ref. [1] |
| 32 | $[N_{4,1,1,1}][NTf_2]$ | 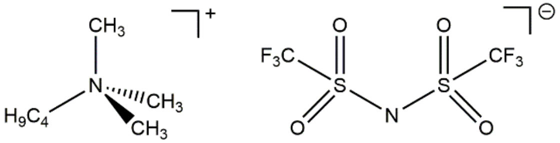 | butyl(trimethyl)ammonium<br>bis[(trifluoromethane)sulfonyl]imide | Ref. [1] |
| 33 | $[N_{3,2,1,1}][NTf_2]$ | 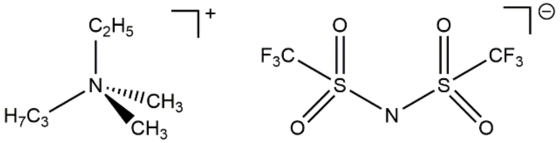 | propyl(ethyl)(dimethyl)ammonium<br>bis[(trifluoromethane)sulfonyl]imide | Ref. [1] |
| 34 | $[N_{8,8,8,1}][NTf_2]$ | 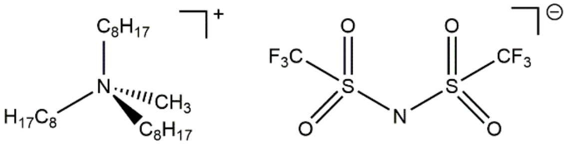 | trioctyl(methyl)ammonium<br>bis[(trifluoromethane)sulfonyl]imide | Ref. [1] |
| 35 | $[S_{2,2,1}][NTf_2]$ | 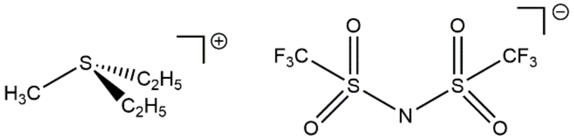 | diethyl(methyl)sulfonium<br>bis[(trifluoromethane)sulfonyl]imide | Ref. [1] |
| 36 | $[S_{2,2,2}][NTf_2]$ | 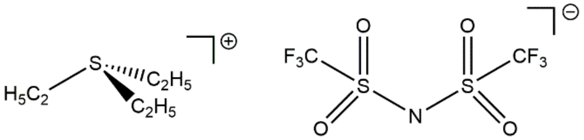 | triethylsulfonium<br>bis[(trifluoromethane)sulfonyl]imide | Ref. [1] |
| 37 | $[P_{6,6,6,14}][NTf_2]$ | 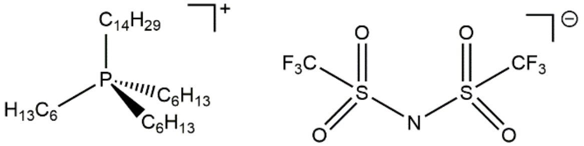 | hexadecyl(trihexyl)phosphonium<br>bis[(trifluoromethane)sulfonyl]imide | Ref. [1] |

|  |  |  |  |  |
|---|---|---|---|---|
| 38 | $[C_4C_1Pyrr][NTf_2]$ | 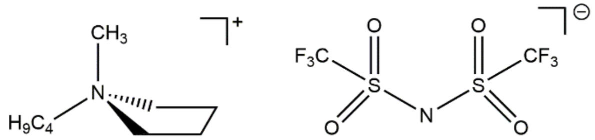 | 1-butyl-1-methylpyrridinium bis[(trifluoromethane)sulfonyl]imide | Ref. [2] |
| 39 | $[C_4Py][NTf_2]$ | 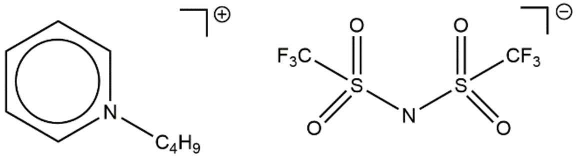 | 1-butylpyridinium bis[(trifluoromethane)sulfonyl]imide | Purchased from Iolitec |
| 41 | $[C_8Py][BF_4]$ | 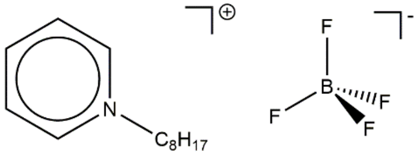 | 1-octylpyridinium tetrafluoroborate | Ref. [3] |
| 42 | $[C_4C_1Im][PF_6]$ | 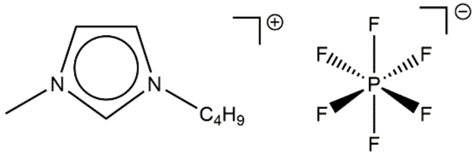 | 1-butyl-3-methylimidazolium hexafluorophosphate | Ref. [4] |
| 43 | $[C_2C_1Im][FAP]$ | 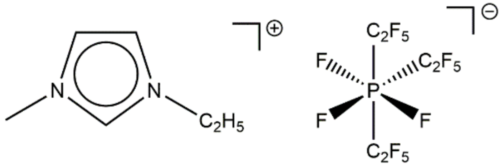 | 1-ethyl-3-methylimidazolium tris(pentafluoroethyl)trifluorophosphate [a] | Purchased from Sigma-Aldrich |
| 44 | $[C_8C_1Im][SbF_6]$ | 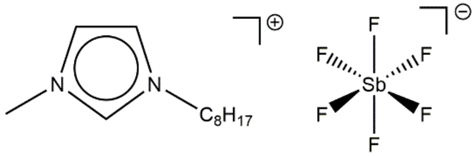 | 1-octyl-3-methylimidazolium hexafluoroantimonate | Ref. [5] |
| 45 | $[C_8C_1Im][I_3]$ | 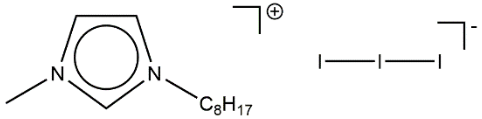 | 1-octyl-3-methylimidazolium triiodide | Ref. [6] |

|  |  |  |  |  |  |
|---|---|---|---|---|---|
| 46 | $[C_8C_1Im]_2[ZnCl_4]$ | 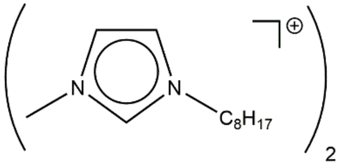 | 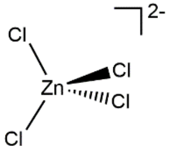 | bis(1-octyl-3-methylimidazolium) tetrachlorozincate | Ref. [7] |
| 47 | $[C_8C_1Im]_2[Zn_2Cl_6]$ | 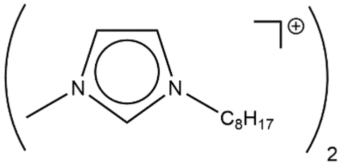 | 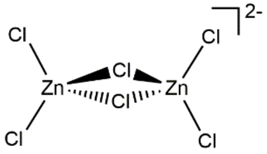 | bis(1-octyl-3-methylimidazolium) hexachlorodizincate | Ref. [7] |
| 48 | $[C_8C_1Im]_2[Zn_4Cl_{10}]$ | 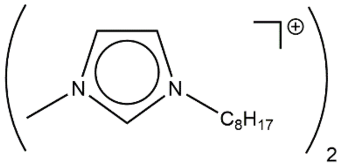 | 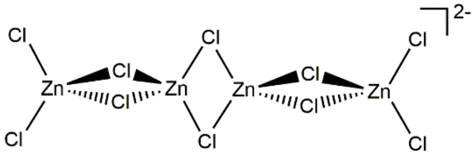 | bis(1-octyl-3-methylimidazolium) decachlorotetrazincate [b] | Ref. [7] |
| 49 | $[C_8C_1Im]_2[ZnCl_2Br_2]$ | 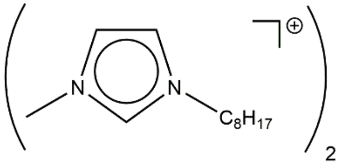 | 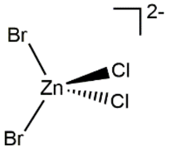 | bis(1-octyl-3-methylimidazolium) dichlorodibromozincate | This work |
| 50 | $[C_8C_1Im]_2[ZnBr_4]$ | 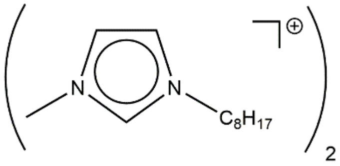 | 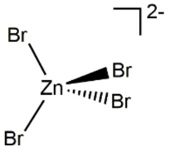 | bis(1-octyl-3-methylimidazolium) tetrabromozincate | Ref. [7] |
| 51 | $[C_8C_1Im]_2[Zn_2Br_6]$ | 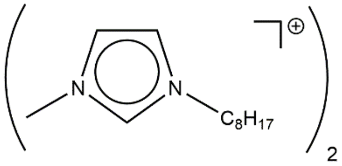 | 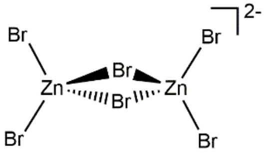 | bis(1-octyl-3-methylimidazolium) hexabromodizincate | Ref. [7] |

| | | | | |
|---|---|---|---|---|
| 52 | $[C_8C_1Im]_2[Zn_3Br_8]$ | 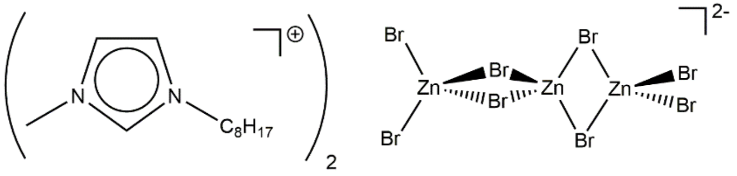 | bis(1-octyl-3-methylimidazolium) octabromotrizincate | This work |
| 53 | $[C_8C_1Im]_2[Zn_4Br_{10}]$ | 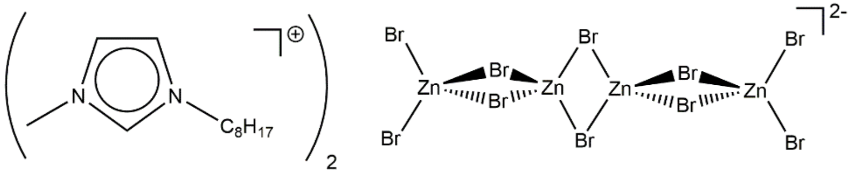 | bis(1-octyl-3-methylimidazolium) decabromotetrazincate | Ref. [7] |
| 54 | $[P_{6,6,6,14}]_2[ZnCl_4]$ | 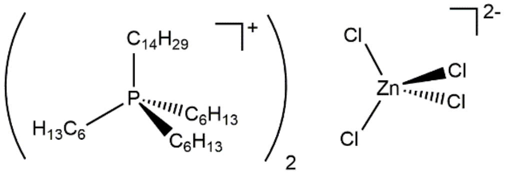 | hexadecyl(trihexyl)phosphonium tetrachlorozincate | Ref. [7] |
| 54 | $[C_8C_1Im][InCl_4]$ | 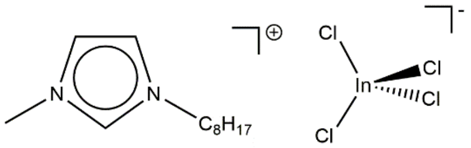 | 1-octyl-3-methylimidazolium tetrachloroindate | Ref. [8] |
| 55 | $[C_8C_1Im][SnCl_3]$ | 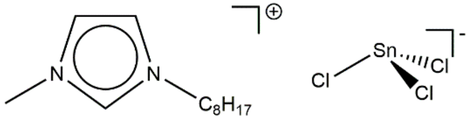 | 1-octyl-3-methylimidazolium trichlorostannate | Ref. [8] |
| 56 | $[C_8C_1Im]_2[FeCl_4]$ | 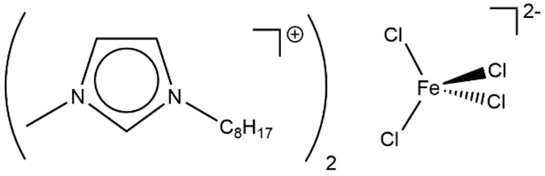 | bis(1-octyl-3-methylimidazolium) tetrachloroferrate | This work |
| 57 | $[C_8C_1Im]_2[CoCl_4]$ | 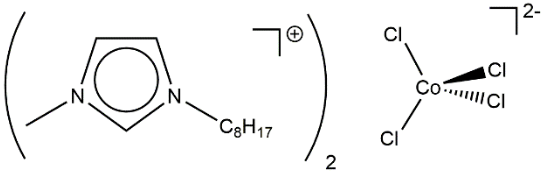 | bis(1-octyl-3-methylimidazolium) tetrachlorocobaltate | This work |

| | | | | |
|---|---|---|---|---|
| 58 | $[C_8C_1Im]_2[CoBr_4]$ | 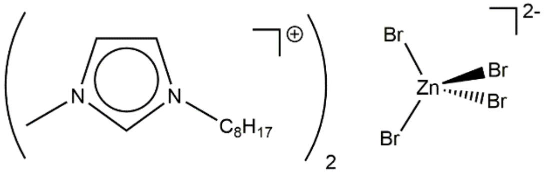 | bis(1-octyl-3-methylimidazolium)<br>tetrabromocobaltate | This work |
| 59 | $[C_8C_1Im]_2[NiCl_4]$ | 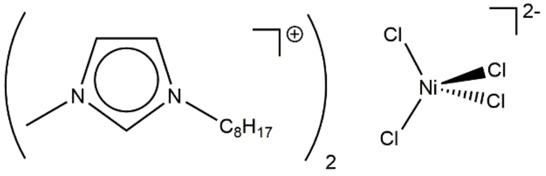 | bis(1-octyl-3-methylimidazolium)<br>tetrachloronickelate | This work |
| 60 | $[C_8C_1Im]_2[Co(NTf_2)_4]$ | 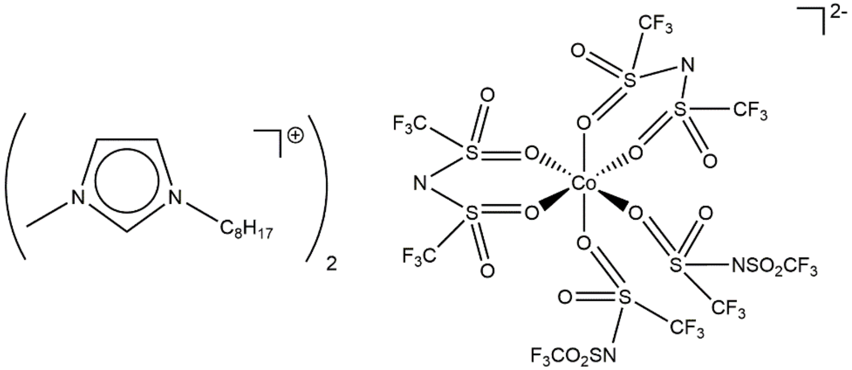 | bis(1-octyl-3-methylimidazolium)<br>tetra(bis(trifluoromethylsulfonyl)imide)cobaltate [c] | This work |

[a] $[FAP]^-$ drawn as meridional isomer, although facial isomer also expected to be present in the IL[9]

[b] $[Zn_4Cl_{10}]^{2-}$ and $[Zn_4Br_{10}]^{2-}$ drawn as linear, but ring could also be present

[c] $[Co(NTf_2)_4]^{2-}$ drawn with two bidentate anions and two monodentate anions; other combinations are possible

**Table S2.** Metal salts used to make halometallate ILs

| Salt | Formula | Purity | Purchased from |
|---|---|---|---|
| iron(II) chloride | $FeCl_2$ | anhydrous, 99.5% | VWR International Ltd. |
| cobalt(II) chloride | $CoCl_2$ | 97% | Sigma-Aldrich |
| cobalt(II) bromide | $CoBr_2$ | 99% | Sigma-Aldrich |
| cobalt(II) bis[(trifluoromethane)sulfonyl]imide | $Co[(CF_3SO_2)_2N]_2 = Co[NTf_2]_2$ | 99.5% | Solvionic |
| nickel(II) chloride | $NiCl_2$ | 99.995% metals basis | Fisher Scientific Ltd. |
| zinc(II) chloride | $ZnCl_2$ | 99.999% metals basis | Sigma-Aldrich |
| zinc(II) bromide | $ZnBr_2$ | 99.999% metals basis | Sigma-Aldrich |

**Table S3.** Techniques used for each IL in this work.

| IL no. | Abbreviation | Variable $h\nu$ XPS | RAES/RXPS | Lab-based XPS | Published |
|---|---|---|---|---|---|
| 1 | $[C_8C_1Im]Cl$ | Ref. [1] | N 1s in ref. [1] | UCL (Kα)[1] and UCL (Theta Probe) | Ref. [1] |
| 2 | $[C_8C_1Im]Br$ | | | Imperial (Kα)[1] and UCL (Theta Probe) | Ref. [1] |
| 3 | $[C_6C_1Im]I$ | | | UCL (Kα)[1] | Ref. [1] |
| 4 | $[P_{6,6,6,14}]Cl$ | | | UCL (Kα)[1] | Ref. [1] |
| 5 | $[P_{6,6,6,14}]Br$ | | | UCL (Kα)[1] | Ref. [1] |
| 6 | $[C_4C_1Im][SCN]$ | Ref. [1] | N 1s; C 1s in ref. [1] | UCL (Kα)[1] | Ref. [1] |
| 7 | $[C_8C_1Im][SCN]$ | | | Imperial[1] | Ref. [1] |
| 8 | $[C_4C_1Im][N(CN)_2]$ | | | UCL (Kα)[1] | Ref. [1] |
| 9 | $[P_{6,6,6,14}][N(CN)_2]$ | | | UCL (Kα)[1] | Ref. [1] |
| 10 | $[C_8C_1Im][C(CN)_3]$ | | N 1s; C 1s in ref. [1] | UCL (Kα)[1] | Ref. [1] |
| 11 | $[C_6C_1Im][B(CN)_4]$ | | | UCL (Kα)[1] | Ref. [1] |
| 12 | $[C_8C_1Im][BF_4]$ | | N 1s on B07 | UCL (Kα)[1] | Ref. [1] |
| 13 | $[P_{6,6,6,14}][NO_3]$ | Ref. [1] | C 1s; N 1s; O 1s in ref. [1] | UCL (Kα)[1] | Ref. [1] |
| 14 | $[C_4C_1Im][HSO_4]$ | | | UCL (Kα)[1] | Ref. [1] |
| 15 | $[C_8C_1Im][HSO_4]$ | | | UCL (Kα)[1] | Ref. [1] |
| 16 | $[C_4C_0Im][HSO_4]$ | | | UCL (Kα)[1] | Ref. [1] |
| 17 | $[N_{4,1,1,0}][HSO_4]$ | Ref. [1] | C 1s; N 1s; O 1s in ref. [1] | UCL (Kα)[1] | Ref. [1] |
| 18 | $[N_{8,1,1,0}][HSO_4]$ | | | UCL (Kα)[1] | Ref. [1] |
| 19 | $[C_4C_1Im][MeSO_4]$ | | | UCL (Kα)[1] | Ref. [1] |
| 20 | $[C_4C_1Im][OcSO_4]$ | | | UCL (Kα)[1] | Ref. [1] |
| 21 | $[C_2C_1Im][MeSO_3]$ | | | UCL (Kα)[1] | Ref. [1] |
| 22 | $[C_4C_1Im][Me_2PO_4]$ | | | UCL (Kα)[1] | Ref. [1] |
| 23 | $[C_4C_1Im][TfO]$ | | | UCL (Kα)[1] | Ref. [1] |
| 24 | $[C_8C_1Im][TfO]$ | | | UCL (Kα)[1] | Ref. [1] |
| 25 | $[N_{2,2,1,0}][TfO]$ | Ref. [1] | C 1s; N 1s; O 1s in ref. [1] | UCL (Kα)[1] | Ref. [1] |
| 26 | $[N_{2OH,2OH,2OH,1}][TfO]$ | | | UCL (Kα)[1] | Ref. [1] |
| 27 | $[C_4C_1Im][NTf_2]$ | | | UCL (Kα)[1] | Ref. [1] |
| 28 | $[C_6C_1Im][NTf_2]$ | | | UCL (Kα)[1] | Ref. [1] |
| 29 | $[C_8C_1Im][NTf_2]$ | Ref. [1] | C 1s; N 1s; O 1s in ref. [1] | UCL (Kα)[1] and UCL (Theta Probe) | Ref. [1] |
| 30 | $[C_2C_0Im][NTf_2]$ | | | UCL (Kα)[1] | Ref. [1] |
| 31 | $[C_4C_0Im][NTf_2]$ | | | UCL (Kα)[1] | Ref. [1] |
| 32 | $[N_{4,1,1,1}][NTf_2]$ | | | UCL (Kα)[1] | Ref. [1] |
| 33 | $[N_{3,2,1,1}][NTf_2]$ | | | UCL (Kα)[1] | Ref. [1] |
| 34 | $[N_{8,8,8,1}][NTf_2]$ | | | UCL (Kα)[1] | Ref. [1] |
| 35 | $[S_{2,2,1}][NTf_2]$ | | | UCL (Kα)[1] | Ref. [1] |
| 36 | $[S_{2,2,2}][NTf_2]$ | | | UCL (Kα)[1] | Ref. [1] |
| 37 | $[P_{6,6,6,14}][NTf_2]$ | | | UCL (Kα)[1] | Ref. [1] |

|  |  |  |  |  |
|---|---|---|---|---|
| 38 | $[C_4C_1Pyrr][NTf_2]$ |  | Kratos Axis Ultra (Nottingham) | Core levels in ref. [2]. Valence levels in this work |
| 39 | $[C_4Py][NTf_2]$ | N 1s on B07 | UCL ($K\alpha$) | This work |
| 41 | $[C_8Py][BF_4]$ |  | Kratos Axis Ultra (Nottingham) | This work |
| 42 | $[C_4C_1Im][PF_6]$ |  | UCL ($K\alpha$) | This work |
| 43 | $[C_2C_1Im][FAP]$ | N 1s on B07 | Kratos Axis Ultra (Harwell) | This work |
| 44 | $[C_8C_1Im][SbF_6]$ |  | Kratos Axis Ultra (Nottingham) | Core levels in ref. [5]. Valence levels in this work |
| 45 | $[C_8C_1Im][I_3]$ |  | Kratos Axis Ultra (Nottingham) | Core levels in ref. [6]. Valence levels in this work |
| 46 | $[C_8C_1Im]_2[ZnCl_4]$ | N 1 on B07 | UCL (Theta Probe) | This work |
| 47 | $[C_8C_1Im]_2[Zn_2Cl_6]$ |  | UCL (Theta Probe) | This work |
| 48 | $[C_8C_1Im]_2[Zn_4Cl_{10}]$ | N 1s on B07 | UCL (Theta Probe) | This work |
| 49 | $[C_8C_1Im]_2[ZnCl_2Br_2]$ |  | UCL (Theta Probe) | This work |
| 50 | $[C_8C_1Im]_2[ZnBr_4]$ |  | UCL (Theta Probe) | This work |
| 51 | $[C_8C_1Im]_2[Zn_2Br_6]$ |  | UCL (Theta Probe) | This work |
| 52 | $[C_8C_1Im]_2[Zn_3Br_8]$ |  | UCL (Theta Probe) | This work |
| 53 | $[C_8C_1Im]_2[Zn_4Br_{10}]$ | N 1s on B07 | UCL (Theta Probe) | This work |
| 54 | $[P_{6,6,6,14}]_2[ZnCl_4]$ |  | UCL (Theta Probe) | This work |
| 54 | $[C_8C_1Im][InCl_4]$ | N 1s on B07 | UCL (Theta Probe) | This work |
| 55 | $[C_8C_1Im][SnCl_3]$ | N 1s on I09 | UCL (Theta Probe) | This work |
| 56 | $[C_8C_1Im]_2[FeCl_4]$ | N 1s on B07 | UCL (Theta Probe) | This work |
| 57 | $[C_8C_1Im]_2[CoCl_4]$ | N 1s on B07 | UCL (Theta Probe) | This work |
| 58 | $[C_8C_1Im]_2[CoBr_4]$ |  | UCL (Theta Probe) | This work |
| 59 | $[C_8C_1Im]_2[NiCl_4]$ | N 1s on B07 | UCL (Theta Probe) | This work |
| 60 | $[C_8C_1Im]_2[Co(NTf_2)_4]$ | C 1s on B07 | UCL (Theta Probe) | This work |

## 2. Data analysis. Synchrotron XPS: sample charging

In reference [1] we noted that the greater flux of synchrotrons, relative to lab XPS apparatus, can give significant damage/charging. To overcome these challenges, we either used a static sample with greatly reduced flux (I09 and the B07 T-pot sample holder, all ILs studied at the synchrotron apart from one) or rastered the sample (the B07 T-pot sample holder for one IL only, $[C_8C_1Im]_2[Co(NTf_2)_4]$). Both of these strategies were successful.

## 3. Data analysis. Peak fitting core level XP spectra

Peak fitting core level XP spectra is important for demonstrating purity (ESI Section 6), but for this work it is just as important for charge referencing. In ESI Table S4, the core orbital used for charge referencing is given, along with any constraints used. The constraints used were all explained in the ESI of reference [1], apart from for $[C_8Py][BF_4]$ which was explained in reference [3].

**Table S4.** Experimental X-ray photoelectron spectroscopy (XPS) details on the charge correction applied for each ionic liquid, and any fitting constraints needed to fit the core orbital used for charge referencing

| IL no. | Abbreviation | Charge referencing method used | Core orbital used for charge referencing | Fitting constraints used | $E_B$ for core orbital used for charge referencing / eV | Rationale for choosing core orbital used for charge referencing | $E_B$ value shifted for valence XP spectrum / eV |
|---|---|---|---|---|---|---|---|
| 1 | $[C_8C_1Im]Cl$ | i | $C_{alkyl}$ 1s | 1:4:7 for $C^2$:$C_{hetero}$:$C_{alkyl}$ | 285.0 | Long alkyl chain | -0.23 |
| 2 | $[C_8C_1Im]Br$ | i | $C_{alkyl}$ 1s | 1:4:7 for $C^2$:$C_{hetero}$:$C_{alkyl}$ | 285.0 | Long alkyl chain | 0.09 |
| 3 | $[C_6C_1Im]I$ | ii | $N_{cation}$ 1s | None | 401.9 | $N_{cation}$ 1s for $[C_8C_1Im]I$ [10] | 0.05 |
| 4 | $[P_{6,6,6,14}]Cl$ | i | $C_{alkyl}$ 1s | 4:28 for $C_{hetero}$:$C_{alkyl}$<br>FWHM($C_{hetero}$) = FWHM($C_{alkyl}$) | 285.0 | Long alkyl chain | -0.19 |
| 5 | $[P_{6,6,6,14}]Br$ | i | $C_{alkyl}$ 1s | 4:28 for $C_{hetero}$:$C_{alkyl}$<br>FWHM($C_{hetero}$) = FWHM($C_{alkyl}$) | 285.0 | Long alkyl chain | -0.42 |
| 6 | $[C_4C_1Im][SCN]$ | ii | $N_{cation}$ 1s | None | 401.9 | $N_{cation}$ 1s for $[C_8C_1Im][SCN]$ | 0.10 |
| 7 | $[C_8C_1Im][SCN]$ | i | $C_{alkyl}$ 1s | 1:4:7 for $C^2$:$C_{hetero}$:$C_{alkyl}$ | 285.0 | Long alkyl chain | -0.13 |
| 8 | $[C_4C_1Im][N(CN)_2]$ | ii | $N_{cation}$ 1s | None | 402.0 | $N_{cation}$ 1s for $[C_8C_1Im][N(CN)_2]$ [10] | 0.04 |
| 9 | $[P_{6,6,6,14}][N(CN)_2]$ | i | $C_{alkyl}$ 1s | 4:28 for $C_{hetero}$:$C_{alkyl}$<br>FWHM($C_{hetero}$) = FWHM($C_{alkyl}$) | 285.0 | Long alkyl chain | 0.22 |
| 10 | $[C_8C_1Im][C(CN)_3]$ | i | $C_{alkyl}$ 1s | 1:4:7 for $C^2$:$C_{hetero}$:$C_{alkyl}$ | 285.0 | Long alkyl chain | 0.01 |
| 11 | $[C_6C_1Im][B(CN)_4]$ | i | $C_{alkyl}$ 1s | 1:4:5 for $C^2$:$C_{hetero}$:$C_{alkyl}$ | 285.0 | Long alkyl chain | -0.24 |
| 12 | $[C_8C_1Im][BF_4]$ | i | $C_{alkyl}$ 1s | 1:4:7 for $C^2$:$C_{hetero}$:$C_{alkyl}$ | 285.0 | Long alkyl chain | -0.10 |
| 13 | $[P_{6,6,6,14}][NO_3]$ | i | $C_{alkyl}$ 1s | 4:28 for $C_{hetero}$:$C_{alkyl}$<br>FWHM($C_{hetero}$) = FWHM($C_{alkyl}$) | 285.0 | Long alkyl chain | -0.10 |
| 14 | $[C_4C_1Im][HSO_4]$ | ii | $N_{cation}$ 1s | None | 401.8 | $N_{cation}$ 1s for $[C_8C_1Im][HSO_4]$ | -0.38 |
| 15 | $[C_8C_1Im][HSO_4]$ | i | $C_{alkyl}$ 1s | 1:4:7 for $C^2$:$C_{hetero}$:$C_{alkyl}$ | 285.0 | Long alkyl chain | -0.39 |
| 16 | $[C_4C_0Im][HSO_4]$ | iv | $C_{alkyl}$ 1s | 1:4:3 for $C^2$:$C_{hetero}$:$C_{alkyl}$ | 285.0 | $C_{alkyl}$ 1s for $[C_4C_1Im][HSO_4]$ | -0.21 |
| 17 | $[N_{4,1,1,0}][HSO_4]$ | ii | $S_{anion}$ $2p_{3/2}$ | 3:3 for $C_{hetero}$:$C_{alkyl}$ | 168.7 | $S_{anion}$ $2p_{3/2}$ for $[N_{8,1,1,0}][HSO_4]$ | -0.28 |
| 18 | $[N_{8,1,1,0}][HSO_4]$ | i | $C_{alkyl}$ 1s | 3:7 for $C_{hetero}$:$C_{alkyl}$ | 285.0 | Long alkyl chain | 0.11 |
| 19 | $[C_4C_1Im][MeSO_4]$ | iii | $N_{cation}$ 1s | None | 401.7 | $N_{cation}$ 1s for $[C_4C_1Im][OcSO_4]$ | -0.26 |
| 20 | $[C_4C_1Im][OcSO_4]$ | i | $C_{alkyl}$ 1s | 1:5:10 for $C^2$:$C_{hetero}$:$C_{alkyl}$ | 285.0 | Long alkyl chain | 0.02 |
| 21 | $[C_2C_1Im][MeSO_3]$ | vi | $N_{cation}$ 1s | None | 401.9 | Average $N_{cation}$ 1s for $[C_8C_1Im][A]$ [10] | 0.12 |
| 22 | $[C_4C_1Im][Me_2PO_4]$ | vi | $N_{cation}$ 1s | None | 401.9 | Average $N_{cation}$ 1s for $[C_8C_1Im][A]$ [10] | -0.17 |
| 23 | $[C_4C_1Im][TfO]$ | ii | $N_{cation}$ 1s | None | 402.0 | $N_{cation}$ 1s for $[C_8C_1Im][TfO]$ | -0.83 |
| 24 | $[C_8C_1Im][TfO]$ | i | $C_{alkyl}$ 1s | 1:4:7 for $C^2$:$C_{hetero}$:$C_{alkyl}$ | 285.0 | Long alkyl chain | -0.46 |

| | | | | | | | |
|---|---|---|---|---|---|---|---|
| 25 | [N$_{2,2,1,0}$][TfO] | v | F$_{\mathrm{anion}}$ 1s | None | 688.4 | F$_{\mathrm{anion}}$ 1s for [C$_8$C$_1$Im][TfO] | -0.49 |
| 26 | [N$_{2\mathrm{OH},2\mathrm{OH},2\mathrm{OH},1}$][TfO] | v | F$_{\mathrm{anion}}$ 1s | None | 688.4 | F$_{\mathrm{anion}}$ 1s for [C$_8$C$_1$Im][TfO] | -0.44 |
| 27 | [C$_4$C$_1$Im][NTf$_2$] | ii | N$_{\mathrm{cation}}$ 1s | None | 402.1 | N$_{\mathrm{cation}}$ 1s for [C$_8$C$_1$Im][NTf$_2$] | 0.04 |
| 28 | [C$_6$C$_1$Im][NTf$_2$] | ii | N$_{\mathrm{cation}}$ 1s | None | 402.1 | N$_{\mathrm{cation}}$ 1s for [C$_8$C$_1$Im][NTf$_2$] | 0.04 |
| 29 | [C$_8$C$_1$Im][NTf$_2$] | i | C$_{\mathrm{alkyl}}$ 1s | 1:4:7 for C$^2$:C$_{\mathrm{hetero}}$:C$_{\mathrm{alkyl}}$ | 285.0 | Long alkyl chain | 0.21 |
| 30 | [C$_2$C$_0$Im][NTf$_2$] | ii | F$_{\mathrm{anion}}$ 1s | None | 688.8 | F$_{\mathrm{anion}}$ 1s for [N$_{8,8,8,1}$][NTf$_2$] | -0.01 |
| 31 | [C$_4$C$_0$Im][NTf$_2$] | ii | F$_{\mathrm{anion}}$ 1s | None | 688.8 | F$_{\mathrm{anion}}$ 1s for [N$_{8,8,8,1}$][NTf$_2$] | 0.07 |
| 32 | [N$_{4,1,1,1}$][NTf$_2$] | ii | F$_{\mathrm{anion}}$ 1s | None | 688.8 | F$_{\mathrm{anion}}$ 1s for [N$_{8,8,8,1}$][NTf$_2$] | -0.30 |
| 33 | [N$_{3,2,1,1}$][NTf$_2$] | ii | F$_{\mathrm{anion}}$ 1s | None | 688.8 | F$_{\mathrm{anion}}$ 1s for [N$_{8,8,8,1}$][NTf$_2$] | -0.07 |
| 34 | [N$_{8,8,8,1}$][NTf$_2$] | i | C$_{\mathrm{alkyl}}$ 1s | 4:3:18 for C$_{\mathrm{hetero}}$:C$_{\mathrm{inter}}$:C$_{\mathrm{alkyl}}$ | 285.0 | Long alkyl chain | 0.03 |
| 35 | [S$_{2,2,1}$][NTf$_2$] | v | F$_{\mathrm{anion}}$ 1s | None | 688.8 | F$_{\mathrm{anion}}$ 1s for [N$_{8,8,8,1}$][NTf$_2$] | -0.36 |
| 36 | [S$_{2,2,2}$][NTf$_2$] | v | F$_{\mathrm{anion}}$ 1s | None | 688.8 | F$_{\mathrm{anion}}$ 1s for [N$_{8,8,8,1}$][NTf$_2$] | -0.10 |
| 37 | [P$_{6,6,6,14}$][NTf$_2$] | i | C$_{\mathrm{alkyl}}$ 1s | 4:28 for C$_{\mathrm{hetero}}$:C$_{\mathrm{alkyl}}$<br>FWHM(C$_{\mathrm{hetero}}$) = FWHM(C$_{\mathrm{alkyl}}$) | 285.0 | Long alkyl chain | 0.01 |
| 38 | [C$_4$C$_1$Pyrr][NTf$_2$] | ii | N$_{\mathrm{cation}}$ 1s | None | 402.7 | N$_{\mathrm{cation}}$ 1s for [C$_8$C$_1$Pyrr][NTf$_2$] | -0.13 |
| 39 | [C$_4$Py][NTf$_2$] | ii | CF$_3$ C 1s | None | 292.9 | CF$_3$ C 1s for [C$_8$Py][NTf$_2$] | -0.05 |
| 41 | [C$_8$Py][BF$_4$] | i | C$_{\mathrm{alkyl}}$ 1s | 2.8:2.7:7 for C$_{\mathrm{hetero}}$:C$_{\mathrm{inter}}$:C$_{\mathrm{alkyl}}$<br>FWHM(C$_{\mathrm{hetero}}$) = FWHM(C$_{\mathrm{inter}}$)<br>FWHM(C$_{\mathrm{alkyl}}$) = FWHM(C$_{\mathrm{hetero}}$) × 1.08<br>(taken from reference [3]) | 285.0 | Long alkyl chain | -0.01 |
| 42 | [C$_4$C$_1$Im][PF$_6$] | ii | N$_{\mathrm{cation}}$ 1s | None | 402.1 | N$_{\mathrm{cation}}$ 1s for [C$_8$C$_1$Im][PF$_6$] | 0.33 |
| 43 | [C$_2$C$_1$Im][FAP] | ii | CF$_3$ C 1s | None | 293.14 | N$_{\mathrm{cation}}$ 1s for [C$_8$C$_1$Im][FAP] [11] | 1.01 |
| 44 | [C$_8$C$_1$Im][SbF$_6$] | i | C$_{\mathrm{alkyl}}$ 1s | 1:4:7 for C$^2$:C$_{\mathrm{hetero}}$:C$_{\mathrm{alkyl}}$ | 285.0 | Long alkyl chain | -0.41 |
| 45 | [C$_8$C$_1$Im][I$_3$] | i | C$_{\mathrm{alkyl}}$ 1s | 1:4:7 for C$^2$:C$_{\mathrm{hetero}}$:C$_{\mathrm{alkyl}}$ | 285.0 | Long alkyl chain | 0.39 |
| 46 | [C$_8$C$_1$Im]$_2$[ZnCl$_4$] | i | C$_{\mathrm{alkyl}}$ 1s | 1:4:7 for C$^2$:C$_{\mathrm{hetero}}$:C$_{\mathrm{alkyl}}$ | 285.0 | Long alkyl chain | 0.57 |
| 47 | [C$_8$C$_1$Im]$_2$[Zn$_2$Cl$_6$] | i | C$_{\mathrm{alkyl}}$ 1s | 1:4:7 for C$^2$:C$_{\mathrm{hetero}}$:C$_{\mathrm{alkyl}}$ | 285.0 | Long alkyl chain | 0.28 |
| 48 | [C$_8$C$_1$Im]$_2$[Zn$_4$Cl$_{10}$] | i | C$_{\mathrm{alkyl}}$ 1s | 1:4:7 for C$^2$:C$_{\mathrm{hetero}}$:C$_{\mathrm{alkyl}}$ | 285.0 | Long alkyl chain | 0.56 |
| 49 | [C$_8$C$_1$Im]$_2$[ZnCl$_2$Br$_2$] | i | C$_{\mathrm{alkyl}}$ 1s | 1:4:7 for C$^2$:C$_{\mathrm{hetero}}$:C$_{\mathrm{alkyl}}$ | 285.0 | Long alkyl chain | 0.44 |
| 50 | [C$_8$C$_1$Im]$_2$[ZnBr$_4$] | i | C$_{\mathrm{alkyl}}$ 1s | 1:4:7 for C$^2$:C$_{\mathrm{hetero}}$:C$_{\mathrm{alkyl}}$ | 285.0 | Long alkyl chain | 0.53 |
| 51 | [C$_8$C$_1$Im]$_2$[Zn$_2$Br$_6$] | i | C$_{\mathrm{alkyl}}$ 1s | 1:4:7 for C$^2$:C$_{\mathrm{hetero}}$:C$_{\mathrm{alkyl}}$ | 285.0 | Long alkyl chain | 0.60 |
| 52 | [C$_8$C$_1$Im]$_2$[Zn$_3$Br$_8$] | i | C$_{\mathrm{alkyl}}$ 1s | 1:4:7 for C$^2$:C$_{\mathrm{hetero}}$:C$_{\mathrm{alkyl}}$ | 285.0 | Long alkyl chain | 0.44 |
| 53 | [C$_8$C$_1$Im]$_2$[Zn$_4$Br$_{10}$] | i | C$_{\mathrm{alkyl}}$ 1s | 1:4:7 for C$^2$:C$_{\mathrm{hetero}}$:C$_{\mathrm{alkyl}}$ | 285.0 | Long alkyl chain | 0.67 |
| 54 | [P$_{6,6,6,14}$]$_2$[ZnCl$_4$] | i | C$_{\mathrm{alkyl}}$ 1s | 4:28 for C$_{\mathrm{hetero}}$:C$_{\mathrm{alkyl}}$<br>FWHM(C$_{\mathrm{hetero}}$) = FWHM(C$_{\mathrm{alkyl}}$) | 285.0 | Long alkyl chain | 0.07 |
| 54 | [C$_8$C$_1$Im][InCl$_4$] | i | C$_{\mathrm{alkyl}}$ 1s | 1:4:7 for C$^2$:C$_{\mathrm{hetero}}$:C$_{\mathrm{alkyl}}$ | 285.0 | Long alkyl chain | 0.06 |
| 55 | [C$_8$C$_1$Im][SnCl$_3$] | i | C$_{\mathrm{alkyl}}$ 1s | 1:4:7 for C$^2$:C$_{\mathrm{hetero}}$:C$_{\mathrm{alkyl}}$ | 285.0 | Long alkyl chain | 0.15 |
| 56 | [C$_8$C$_1$Im]$_2$[FeCl$_4$] | i | C$_{\mathrm{alkyl}}$ 1s | 1:4:7 for C$^2$:C$_{\mathrm{hetero}}$:C$_{\mathrm{alkyl}}$ | 285.0 | Long alkyl chain | -0.09 |
| 57 | [C$_8$C$_1$Im]$_2$[CoCl$_4$] | i | C$_{\mathrm{alkyl}}$ 1s | 1:4:7 for C$^2$:C$_{\mathrm{hetero}}$:C$_{\mathrm{alkyl}}$ | 285.0 | Long alkyl chain | 0.38 |
| 58 | [C$_8$C$_1$Im]$_2$[CoBr$_4$] | i | C$_{\mathrm{alkyl}}$ 1s | 1:4:7 for C$^2$:C$_{\mathrm{hetero}}$:C$_{\mathrm{alkyl}}$ | 285.0 | Long alkyl chain | -1.47 [a] |
| 59 | [C$_8$C$_1$Im]$_2$[NiCl$_4$] | i | C$_{\mathrm{alkyl}}$ 1s | 1:4:7 for C$^2$:C$_{\mathrm{hetero}}$:C$_{\mathrm{alkyl}}$ | 285.0 | Long alkyl chain | 0.43 |

| | | | | | | | |
|---|---|---|---|---|---|---|---|
| 60 | $[C_8C_1Im]_2[Co(NTf_2)_4]$ | i | $C_{alkyl}$ 1s | 1:4:7 for $C^2$:$C_{hetero}$:$C_{alkyl}$ | 285.0 | Long alkyl chain | 0.16 |

[a] $[C_8C_1Im]_2[CoBr_4]$ was the only sample that was mounted on a non-conducting glass substrate; this different sample mounting explains the very different $E_B$ shift value needed to charge corrected the valence XP spectrum for $[C_8C_1Im]_2[CoBr_4]$

## 4. Data analysis. Peak fitting valence level XP spectra

Peak fitting procedures were needed for non-resonant valence XP spectra recorded in the laboratory at $h\nu$ = 1486.6 eV to obtain $E_B$(cation HOFO) and $E_B$(anion HOFO) values. In general, the only constraint used was for the full width at half maximum (FWHM), which was generally constrained to be constant for any components that were likely to be important for obtaining $E_B$(cation HOFO) and $E_B$(anion HOFO) values.

To fit the non-resonant valence XP spectra recorded at $h\nu$ = 1486.6 eV for $[C_8C_1Im][SnCl_3]$, $[C_8C_1Im][InCl_4]$ and halozincate dianions, full width at half maximum (FWHM) values for peaks due to Sn 4d, In 4d and Zn 3d were used to obtain estimates of the FWHM for one valence state; the FWHM values were ~1.0 eV.[8] This knowledge was then used to aid determination of the number of components in the non-resonant valence XP spectra recorded at $h\nu$ = 1486.6 eV, *e.g*. Figure S1 for $[C_8C_1Im]_2[ZnCl_4]$ and for $[C_8C_1Im]_2[FeCl_4]$. Cation contributions were so small that they could be ignored when fitting the non-resonant valence XP spectra recorded at $h\nu$ = 1486.6 eV. Using this approach, $E_B$(anion HOFO) was determined for each metal complex-containing IL, $[C_2C_1Im][FAP]$ and $[C_4C_1Im][PF_6]$ (ESI Figure S9 to ESI Figure S31).

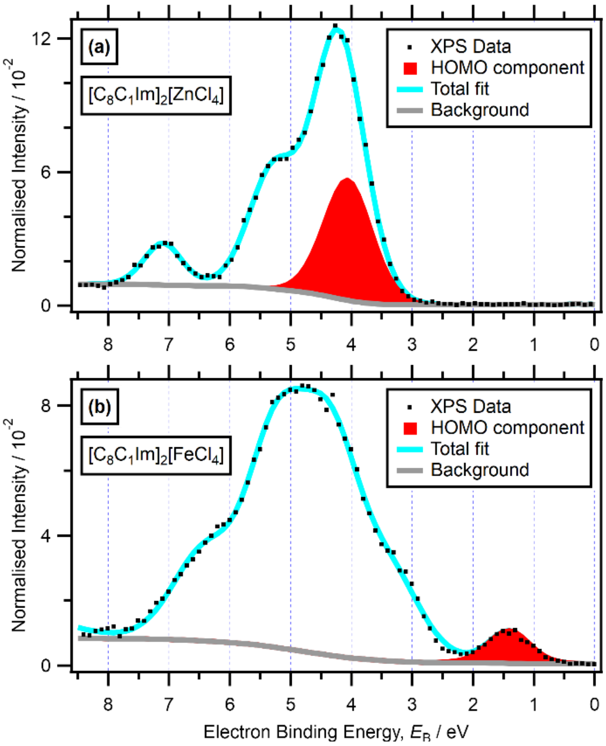

**Figure S1.** Non-resonant laboratory valence XPS at $h\nu$ = 1486.6 eV (including the HOMO fitted component, the total fit and the background for the fitting) for: (a) $[C_8C_1Im]_2[ZnCl_4]$ and (b) $[C_8C_1Im]_2[FeCl_4]$. All electron spectra were charge referenced using methods outlined in Section 2.5.

The FWHM for the fitted peak due to the HOMO for six ILs was ~0.9 eV, *i.e*. FWHM(total) ~0.9 eV. The apparatus contribution (from the light source and the detector) was FWHM(apparatus) ~0.45 eV;[12] the contribution from HOMO core-hole lifetime was negligible (0 eV used here).[13] Using Equation 1 (ESI Section 10),[14, 15] the sample contribution to the FWHM was estimated as 0.8 eV. This variability in $E_B$(HOMO) and $E_i$(IL) is predicted to be applicable to all ILs studied here, and gives a guide to the challenge of formally assigning the HOMO to either the cation or the anion for some ILs.

## 5. Data analysis. Charge referencing methods

Charge referencing methods were needed for both non-resonant valence XP spectra recorded in the laboratory at $h\nu$ = 1486.6 eV and resonant XP spectra recorded at the synchrotron. For non-resonant valence XP spectra recorded in the laboratory, the peak used for each IL is given in Table S4, along with the $E_B$ shift used for each IL. Figure 5 in the manuscript gives a visual demonstration of charge referencing using $E_B$($C_{alkyl}$ 1s) for $[C_8C_1Im]_2[ZnCl_4]$ and $[P_{6,6,6,14}]_2[ZnCl_4]$.

For synchrotron XPS, the method used for charge referencing resonant XP spectra was the same as outlined in reference [1]. Non-resonant valence XP spectra recorded in the lab at $h\nu$ = 1486.6 eV that had been charge referenced already were used as the starting point. Non-resonant valence XP spectra recorded at the synchrotron just before/after the resonant valence XP spectrum was recorded were then used to determine the $E_B$ shift required to successfully charge reference the resonant valence XP spectrum in question. The $E_B$ shift was determined by a visual comparison of the non-resonant valence XP spectrum recorded in the lab at $h\nu$ = 1486.6 eV and the non-resonant valence XP spectrum recorded at the synchrotron; the visual comparison is given in ESI Figure S2 to Figure S4. The synchrotron non-resonant XP spectra recorded to demonstrate IL purity were charge referenced by shifting to match the laboratory non-resonant XP spectra that had already been charge referenced.

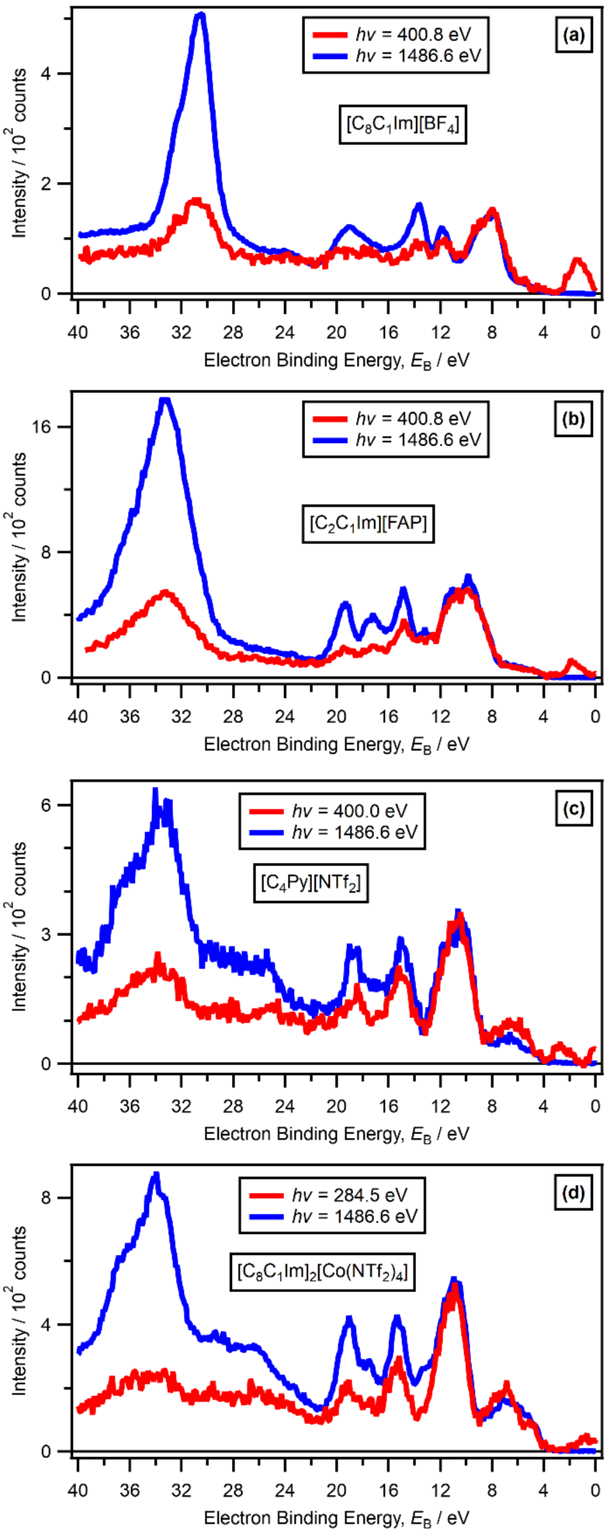

**Figure S2.** Non-resonant XP spectra recorded on laboratory–based XPS recorded at $h\nu$ = 1486.6 eV (charge referenced using data in Table S4) and synchrotron–based XPS (charge referenced by visually matching to the laboratory–based XP spectrum) for: (a) $[C_8C_1Im][BF_4]$, (b) $[C_2C_1Im][FAP]$, (c) $[C_4Py][NTf_2]$, (d) $[C_8C_1Im]_2[Co(NTf_2)_4]$. The $E_B$ shift determined for the synchrotron–based XPS for each IL was used to charge reference resonant XP spectra.

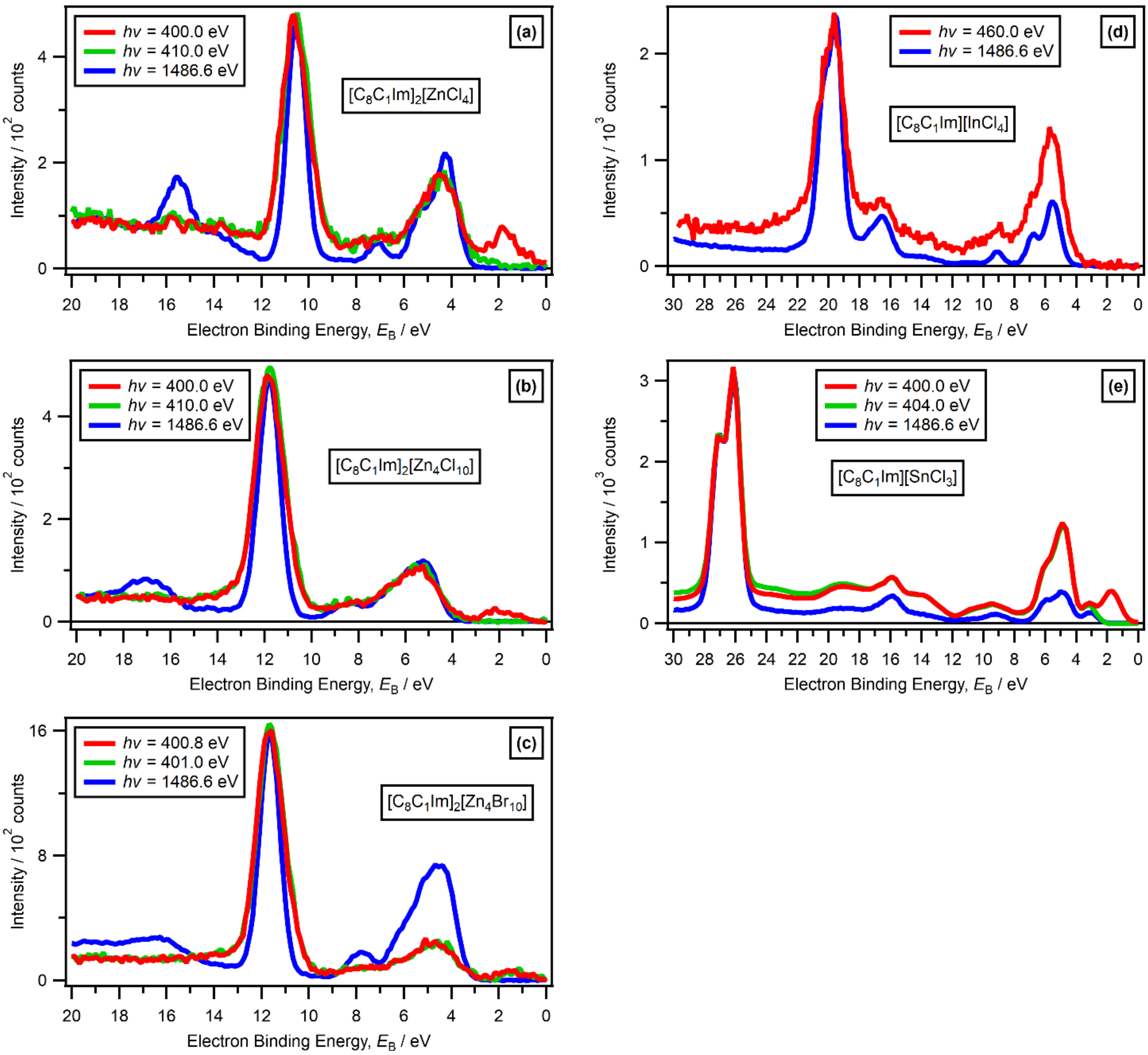

**Figure S3.** Non-resonant XP spectra recorded on laboratory–based XPS recorded at $h\nu$ = 1486.6 eV (charge referenced using data in Table S4) and synchrotron–based XPS (charge referenced by visually matching to the laboratory–based XP spectrum) for: (a) $[C_8C_1Im]_2[ZnCl_4]$, (b) $[C_8C_1Im]_2[Zn_4Cl_{10}]$, (c) $[C_8C_1Im]_2[Zn_4Br_{10}]$, (d) $[C_8C_1Im][InCl_4]$, (e) $[C_8C_1Im]_2[SnCl_3]$. The $E_B$ shift determined for the synchrotron–based XPS for each IL was used to charge reference resonant XP spectra.

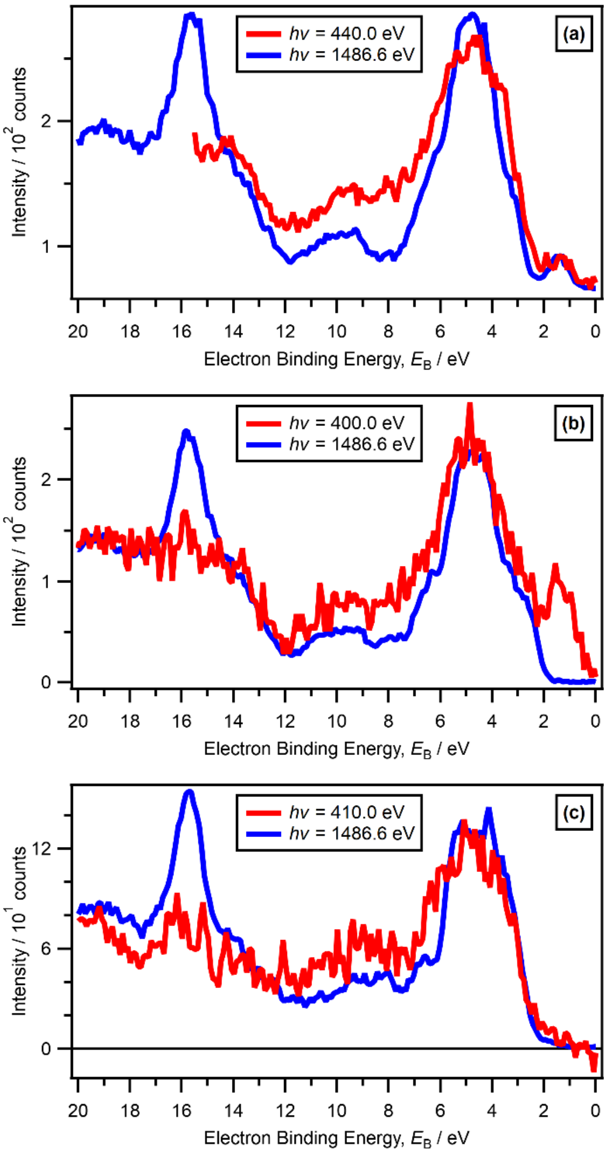

**Figure S4.** Non-resonant XP spectra recorded on laboratory–based XPS recorded at $h\nu$ = 1486.6 eV (charge referenced using data in Table S4) and synchrotron–based XPS (charge referenced by visually matching to the laboratory–based XP spectrum) for: (a) $[C_8C_1Im]_2[FeCl_4]$, (b) $[C_8C_1Im]_2[CoCl_4]$, (c) $[C_8C_1Im]_2[NiCl_4]$. The $E_B$ shift determined for the synchrotron–based XPS for each IL was used to charge reference resonant XP spectra.

## 6. Data analysis. Obtaining $E_B$(ion HOFO) and $E_B$(ion onset)

### 6.1. Obtaining $E_B$(ion HOFO)

Our $E_B$(ion HOFO) values reported here are designed to capture the peak $E_B$ of the lowest $E_B$ anionic and cation contributions. The ideal XP spectrum for obtaining $E_B$(ion HOFO) is one that gives a readily fitted peak for the lowest $E_B$ (anionic or cation) contribution, *e.g.* determining $E_B$(anion HOFO) for [$C_nC_1$Im][SCN]. Furthermore, fitting models have been developed for valence XPS of ILs, as explained in ESI Section 4. For determining some $E_B$(ion HOFO) values, no readily fitted peak occurred. Therefore, a combination of different data sources was used to estimate a peak $E_B$; thus, $E_B$(ion HOFO) was obtained, *e.g.* $E_B$(anion HOFO) for [$N_{4,1,1,0}$][$HSO_4$] was determined using a combination of variable $h\nu$XPS and RAES data. This process of estimating a peak $E_B$ can be challenging for XP spectra that gave a broad feature for the lowest $E_B$ contribution; such features could be potentially be fitted with more than one peak. For such situations, the error given with the value was larger reflecting the greater challenge obtaining $E_B$(ion HOFO) values for such features.

A general observation is that the lowest $E_B$ anionic feature in XP spectra was far more likely to be a sharp peak than the lowest $E_B$ cationic feature in XP spectra. For example, for [$C_4C_1$Im][SCN] and [$C_8C_1$Im]Cl the lowest $E_B$ anionic feature in XP spectra gave a single, relatively intense near-Gaussian shaped peak, whereas the lowest $E_B$ cationic feature in XP spectra for both ILs was a relatively broad feature. This finding was likely the result of a combination of two factors: (i) for anions such as $[SCN]^-$ and $Cl^-$ it is expected that multiple MOs of very similar $E_B$ contribute to the lowest $E_B$ anionic feature, giving rise to a relatively intense peak, (ii) the anions are in general structurally simpler than cations with fewer different atoms potentially contributing to the MOs, meaning that cations have a number of MOs at relatively similar $E_B$ values.

### 6.2. Obtaining $E_B$(ion onset)

$E_B$(ion onset) values represent the experimental HOMO energy. $E_B$(ion onset) was determined by fitting a linear curve to the lowest $E_B$ component in a valence XP spectrum. The x-intercept of this curve is equal to $E_B$(ion onset). The fitting $E_B$ range was chosen by the user to give a good visual fit to the XP spectrum. IAll reported $E_B$(ion onset) values were determined from charge–referenced lab–based valence XP spectra.

## 7. Results. XPS: demonstrating purity

Purity for 37 ILs included in our analysis here has already been demonstrated in reference [1]. Three of these ILs were studied on the Theta Probe XPS apparatus in addition to the K$\alpha$ XPS apparatus used previously; these ILs are presented in ESI Figure S5 to Figure S7. Furthermore, data for $[C_6C_1Im]I$ and $[C_8C_1Im][BF_4]$ presented in reference [1] was re-used with the valence XP spectrum fitted (ESI Figure S8 and ESI Figure S9).

Purity for 23 new ILs is demonstrated here (Figure S10 to Figure S32). For the laboratory XPS, there was a very small N 1s peak due to radiation damage for $[C_4C_1Im][PF_6]$ (ESI Figure S13c), and very small peaks due to silicon-based contamination (small O 1s, Si 2s and Si 2p peaks observed in survey scan, ESI Figure S13a). Also, there was a very small N 1s peak due to radiation damage for $[C_2C_1Im]$[FAP] (ESI Figure S14c), and very small peaks due to silicon-based contamination (small O 1s, Si 2s and Si 2p peaks observed in survey scan, ESI Figure S14a). For the synchrotron XPS, there was a very small N 1s peak due to radiation damage for $[C_8C_1Im]_2[FeCl_4]$ (ESI Figure S40a) and $[C_8C_1Im]_2[CoCl_4]$ (ESI Figure S41a). For the synchrotron data, these non-resonant XP spectra were recorded at $h\nu$ = 700 eV for static samples. The flux at $h\nu$ = 700 eV was significantly larger than at the $h\nu$ where resonant XP spectra were recorded ($h\nu \sim$ 400 eV); therefore, the non-resonant XP spectra were more likely to show radiation damage than the resonant XP spectra.

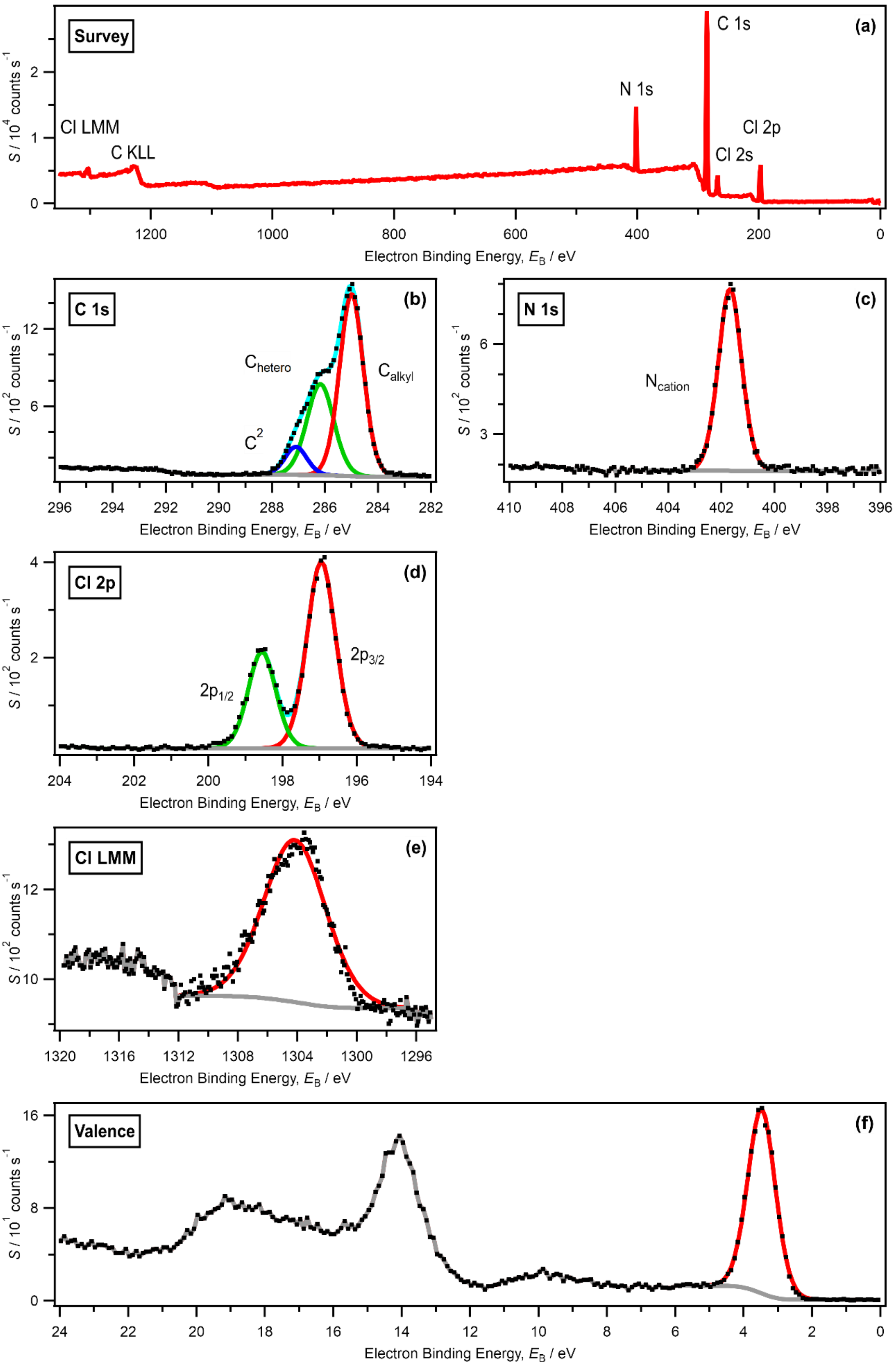

**Figure S5.** (a) Survey, (b-d) core, (e) Auger and (f) valence XP spectra for [$C_8C_1$Im]Cl recorded on laboratory–based XPS apparatus at $h\nu$ = 1486.6 eV. All XP spectra were charge referenced using method 1 outlined in Section 2.5.

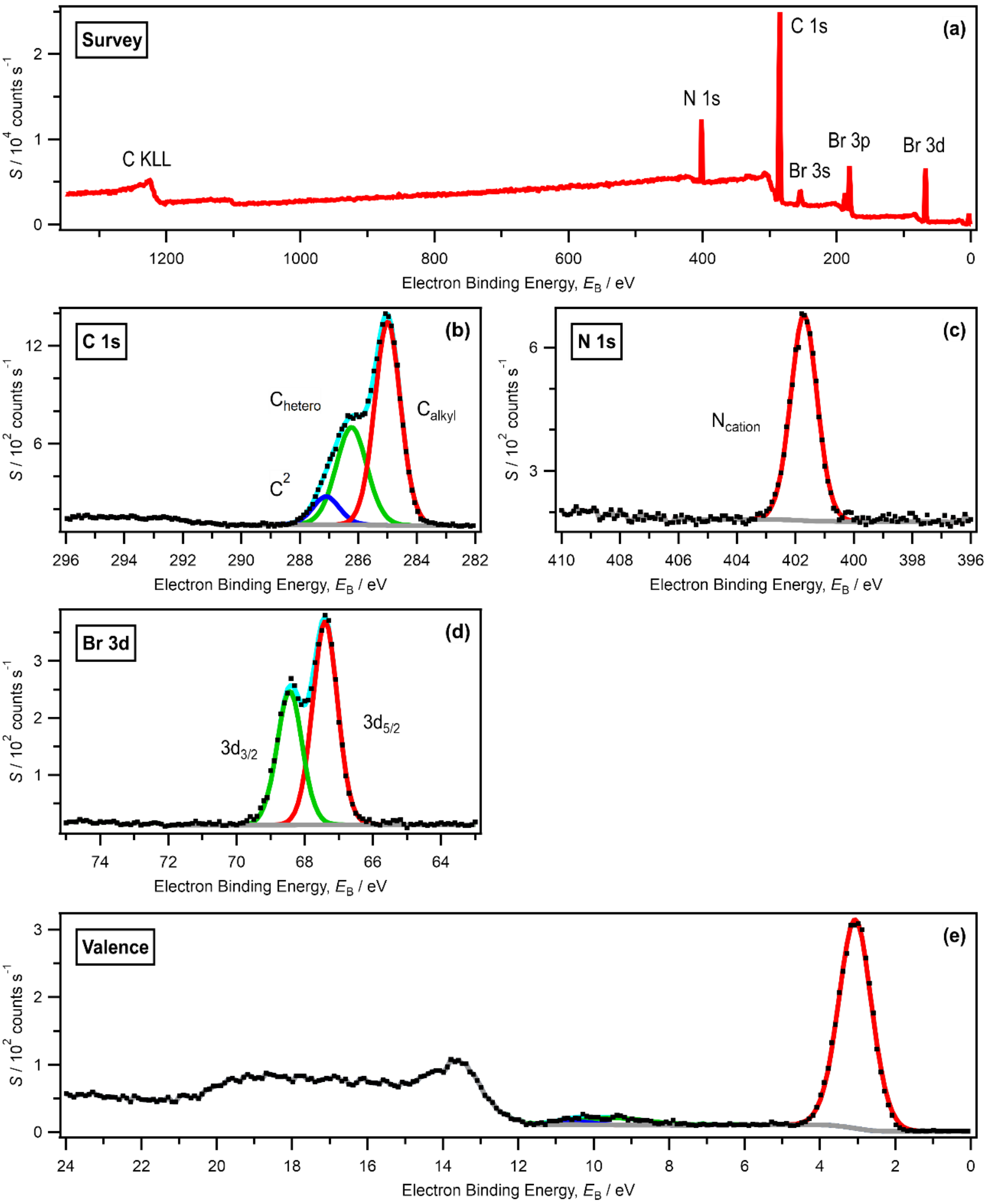

**Figure S6.** (a) Survey, (b-d) core and (e) valence XP spectra for [$C_8C_1$Im]Br recorded on laboratory–based XPS apparatus at $h\nu = 1486.6$ eV. All XP spectra were charge referenced using method i outlined in Section 2.5.

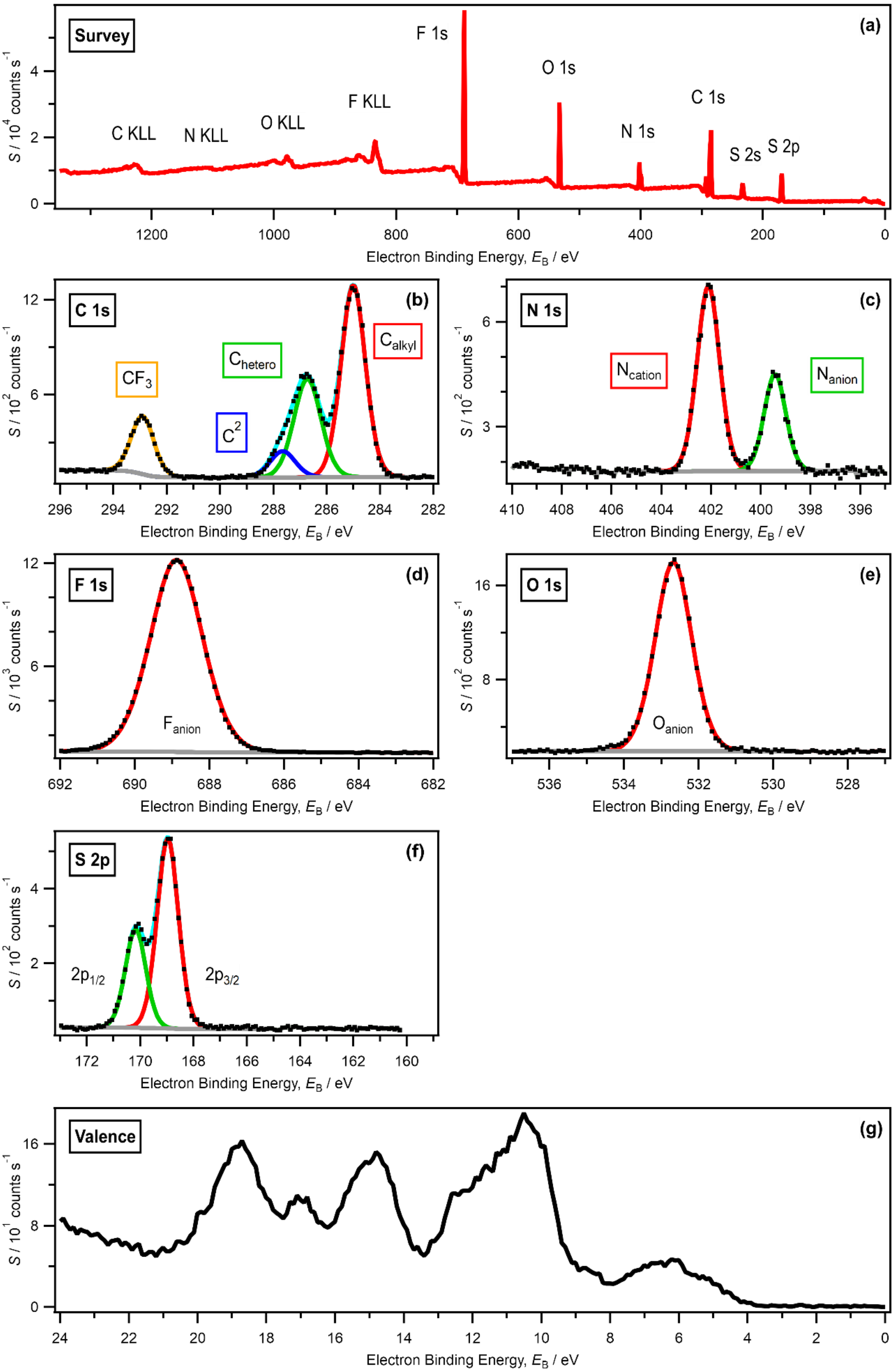

**Figure S7.** (a) Survey, (b-f) core and (g) valence XP spectra for [$C_8C_1Im$][$NTf_2$] recorded on laboratory–based XPS apparatus at *hν* = 1486.6 eV. All XP spectra were charge referenced using method i outlined in Section 2.5.

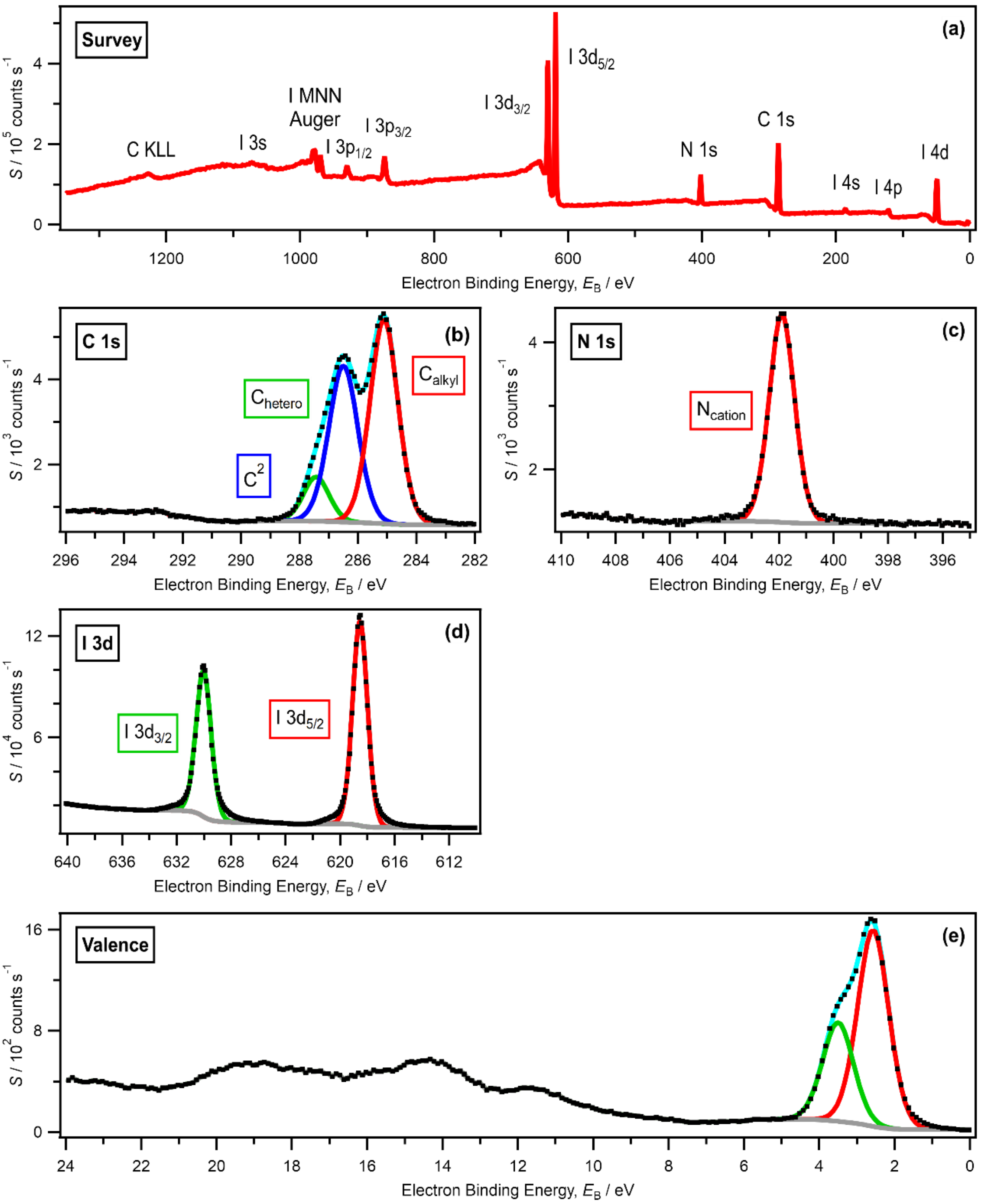

**Figure S8.** (a) Survey, (b-d) core and (e) valence XP spectra for [C$_6$C$_1$Im]I recorded on laboratory–based XPS apparatus at $h\nu$ = 1486.6 eV. All XP spectra were charge referenced using method i outlined in Section 2.5.

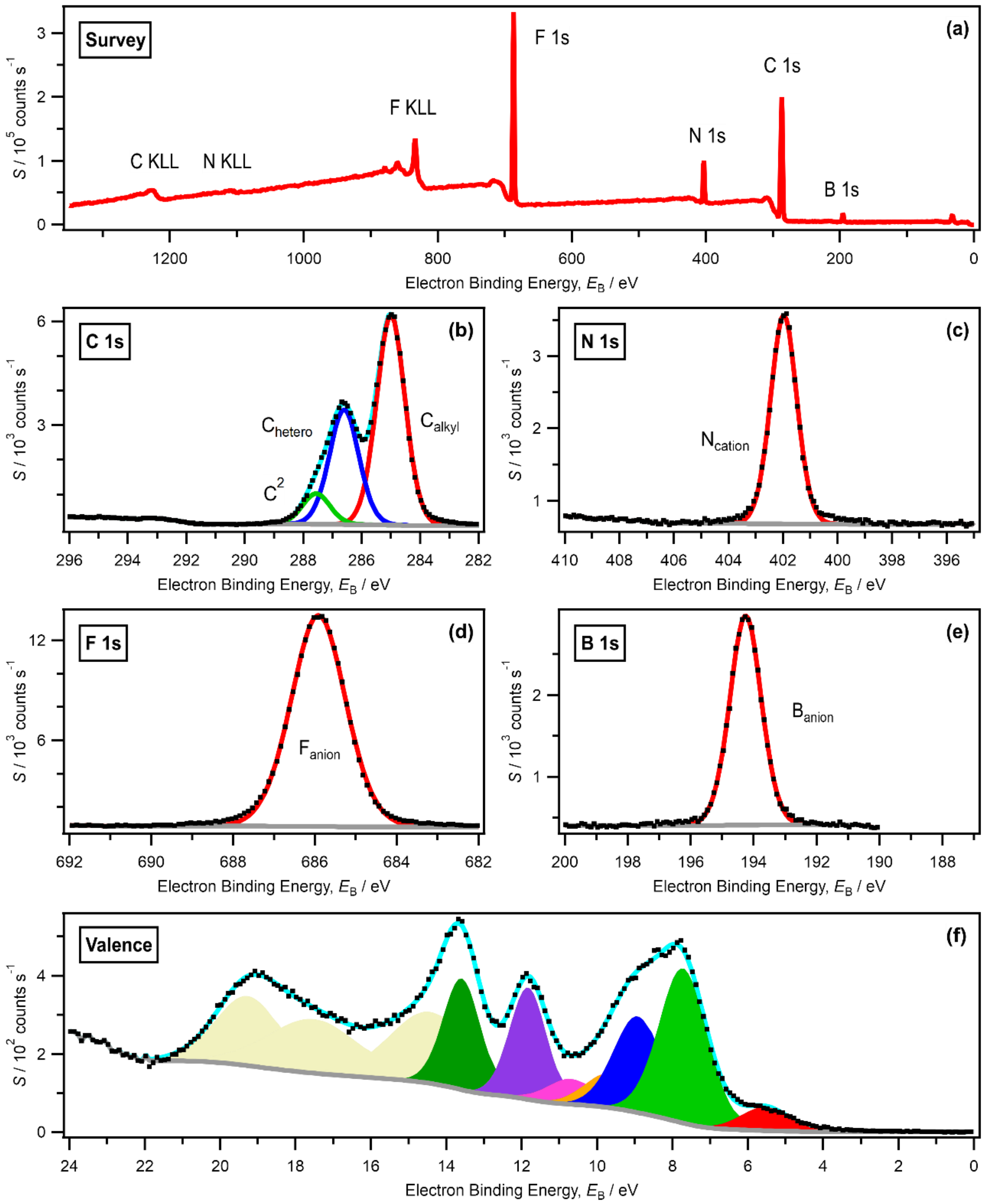

**Figure S9.** (a) Survey, (b-e) core and (f) valence XP spectra for $[C_8C_1Im][BF_4]$ recorded on laboratory–based XPS apparatus at $h\nu$ = 1486.6 eV. All XP spectra were charge referenced using method i outlined in Section 2.5. The component labelled red was principally from the $[C_8C_1Im]^+$ cation.

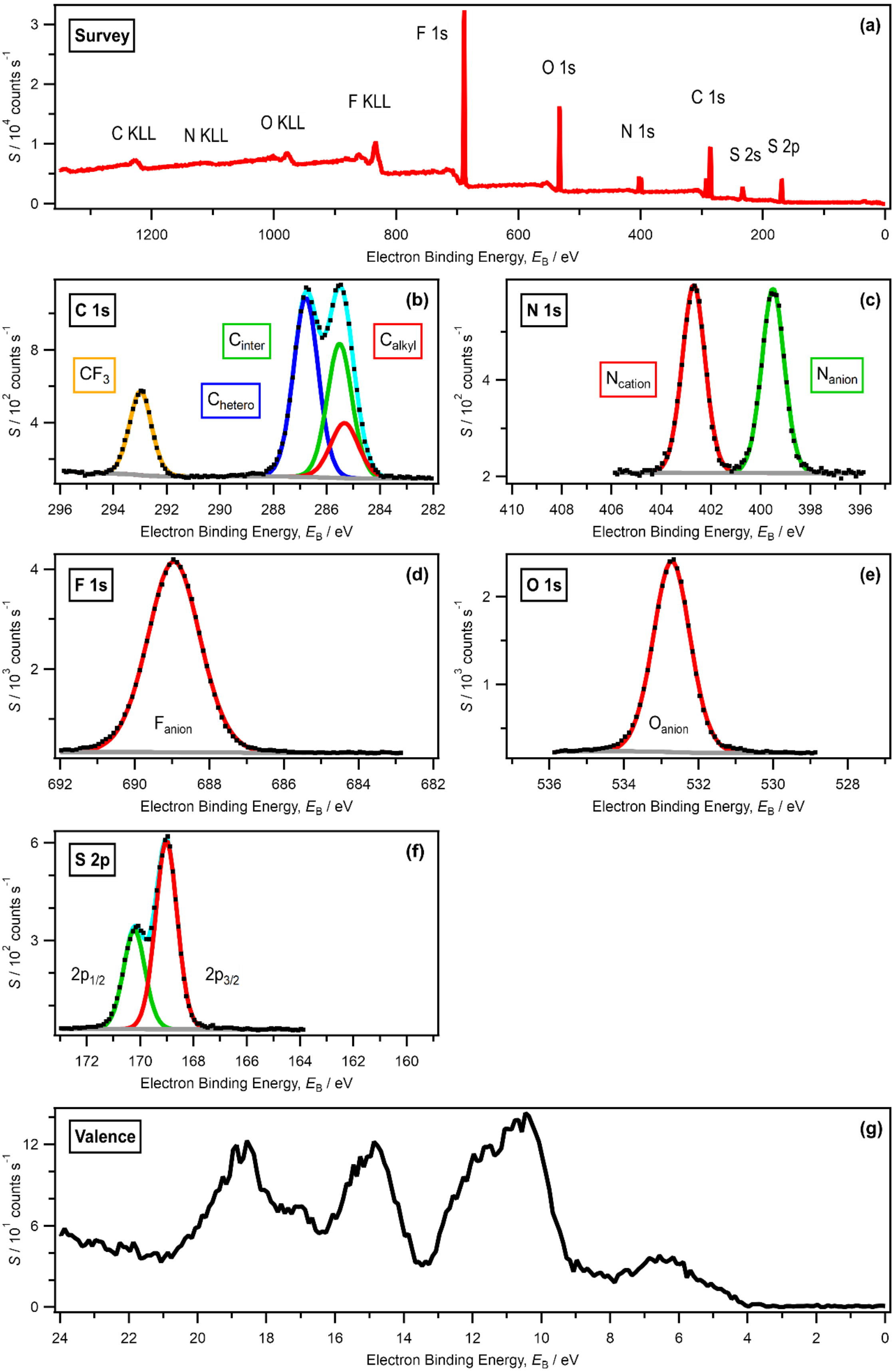

**Figure S10.** (a) Survey, (b-f) core and (g) valence XP spectra for [$C_4C_1$Pyrr][$NTf_2$] recorded on laboratory–based XPS apparatus at *hν* = 1486.6 eV. All XP spectra were charge referenced using method ii outlined in Section 2.5.

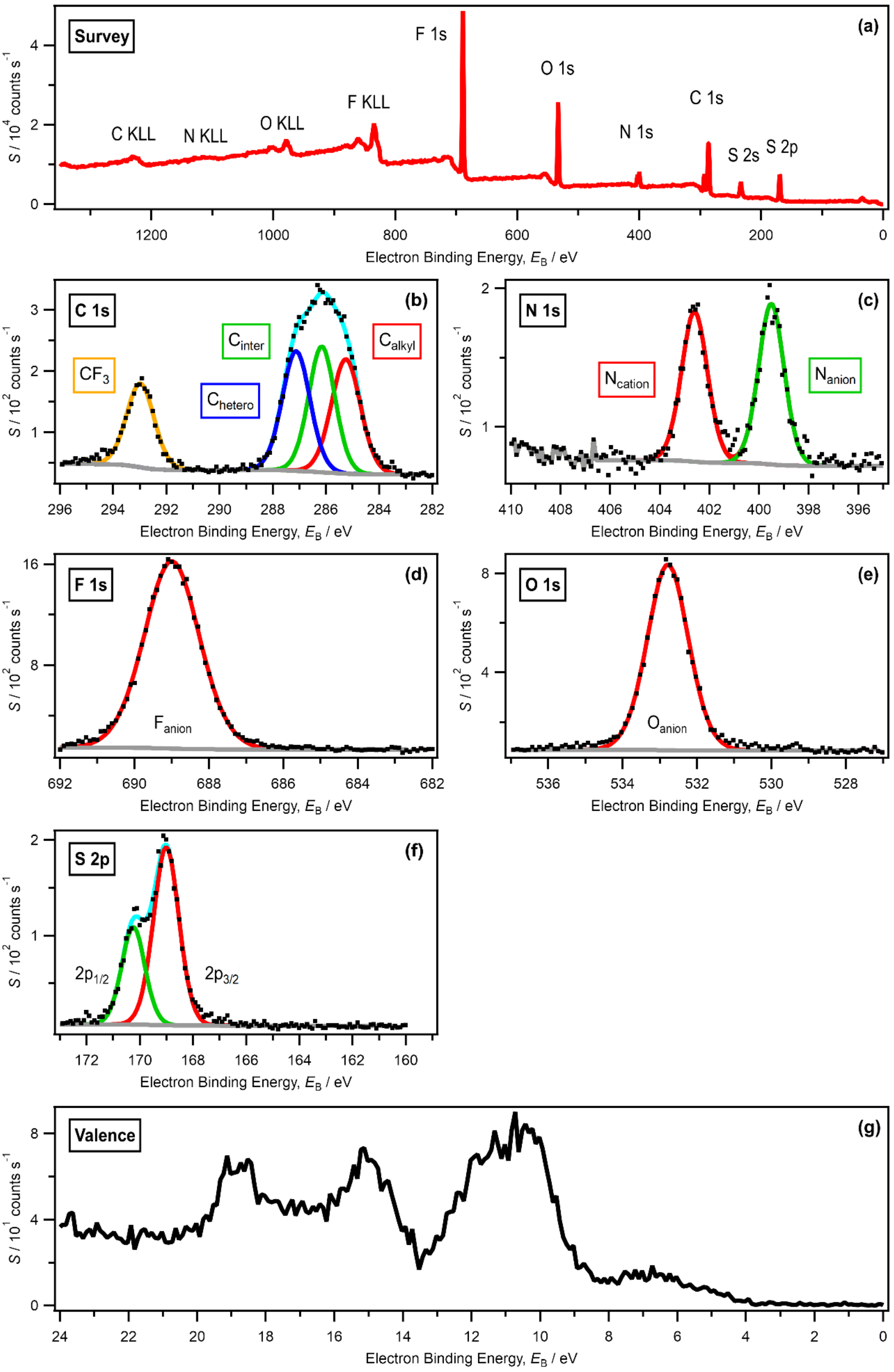

**Figure S11.** (a) Survey, (b-f) core and (g) valence XP spectra for $[C_4Py][NTf_2]$ recorded on laboratory–based XPS apparatus at $h\nu$ = 1486.6 eV. All XP spectra were charge referenced using method ii outlined in Section 2.5.

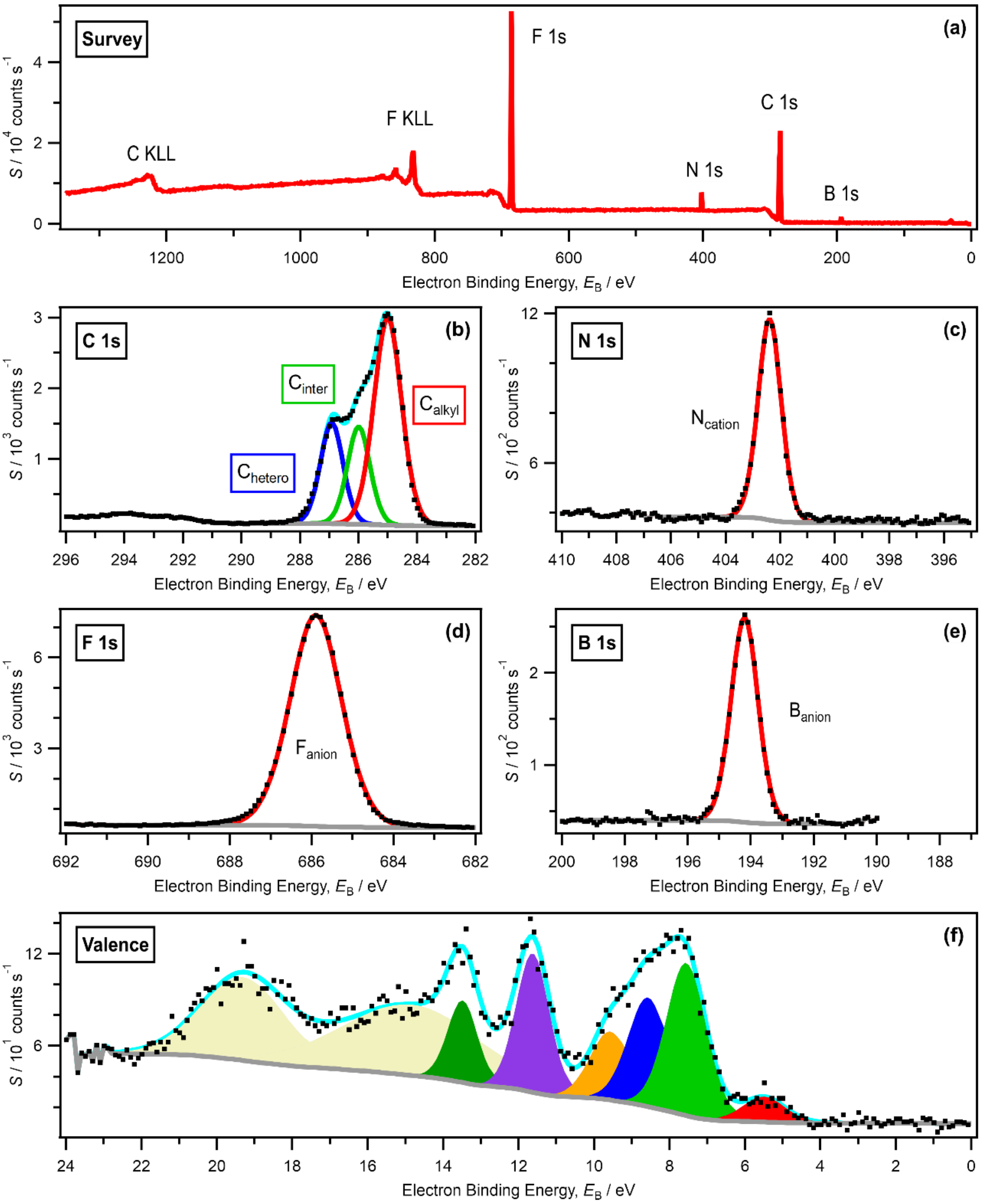

**Figure S12.** (a) Survey, (b-f) core and (g) valence XP spectra for [$C_8$Py][$BF_4$] recorded on laboratory–based XPS apparatus at *hν* = 1486.6 eV. All XP spectra were charge referenced using method i outlined in Section 2.5. The component labelled red was principally from the [$C_8$Py]$^+$ cation.

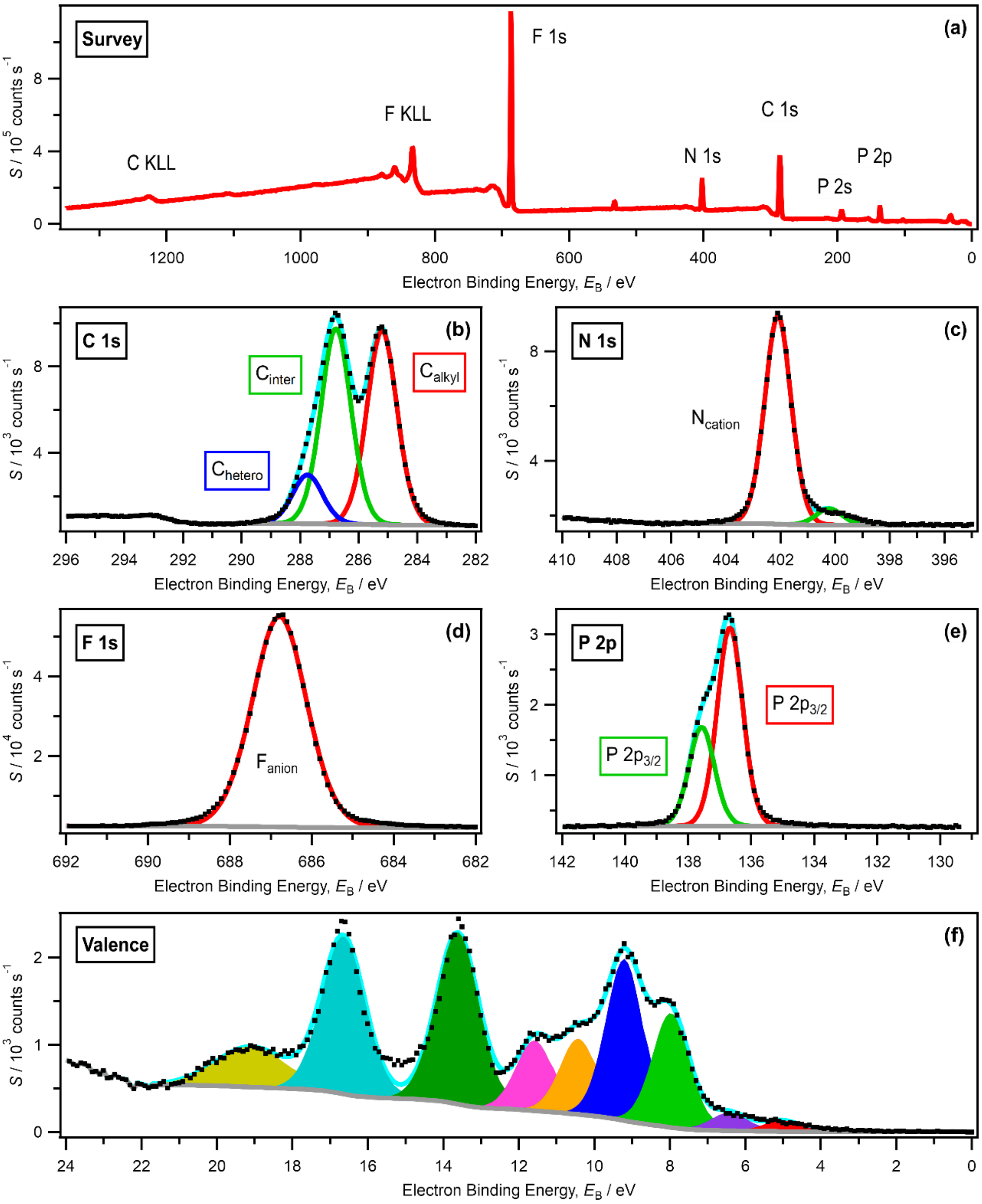

**Figure S13.** (a) Survey, (b-e) core and (f) valence XP spectra for $[C_4C_1Im][PF_6]$ recorded on laboratory–based XPS apparatus at $h\nu$ = 1486.6 eV. All XP spectra were charge referenced using method ii outlined in Section 2.5. The component labelled red was principally from the $[C_4C_1Im]^+$ cation.

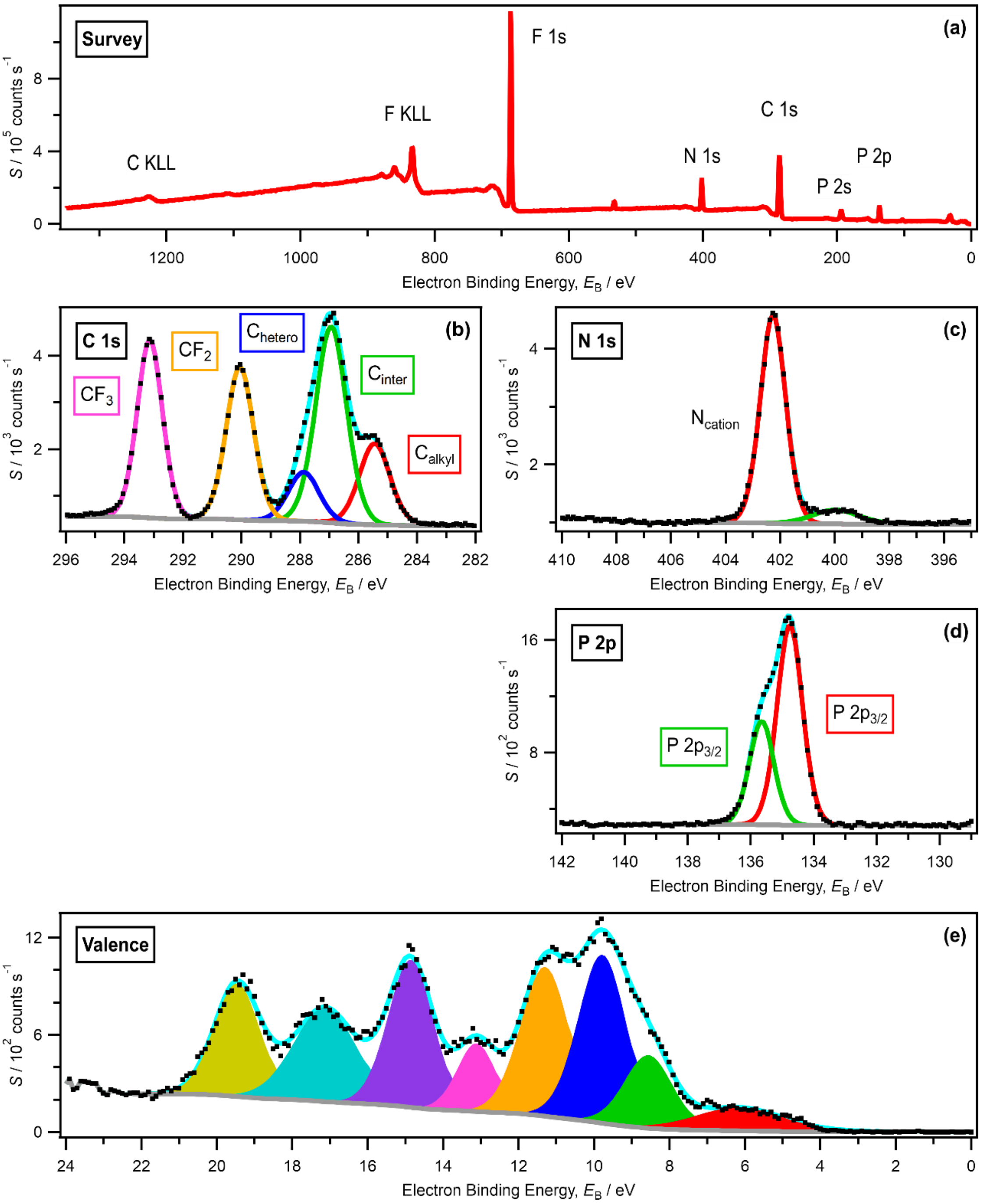

**Figure S14.** (a) Survey, (b-d) core and (e) valence XP spectra for [$C_2C_1$Im][FAP] recorded on laboratory–based XPS apparatus at *hν* = 1486.6 eV. All XP spectra were charge referenced using method ii outlined in Section 2.5. The component labelled red was principally from the [$C_2C_1$Im]$^+$ cation.

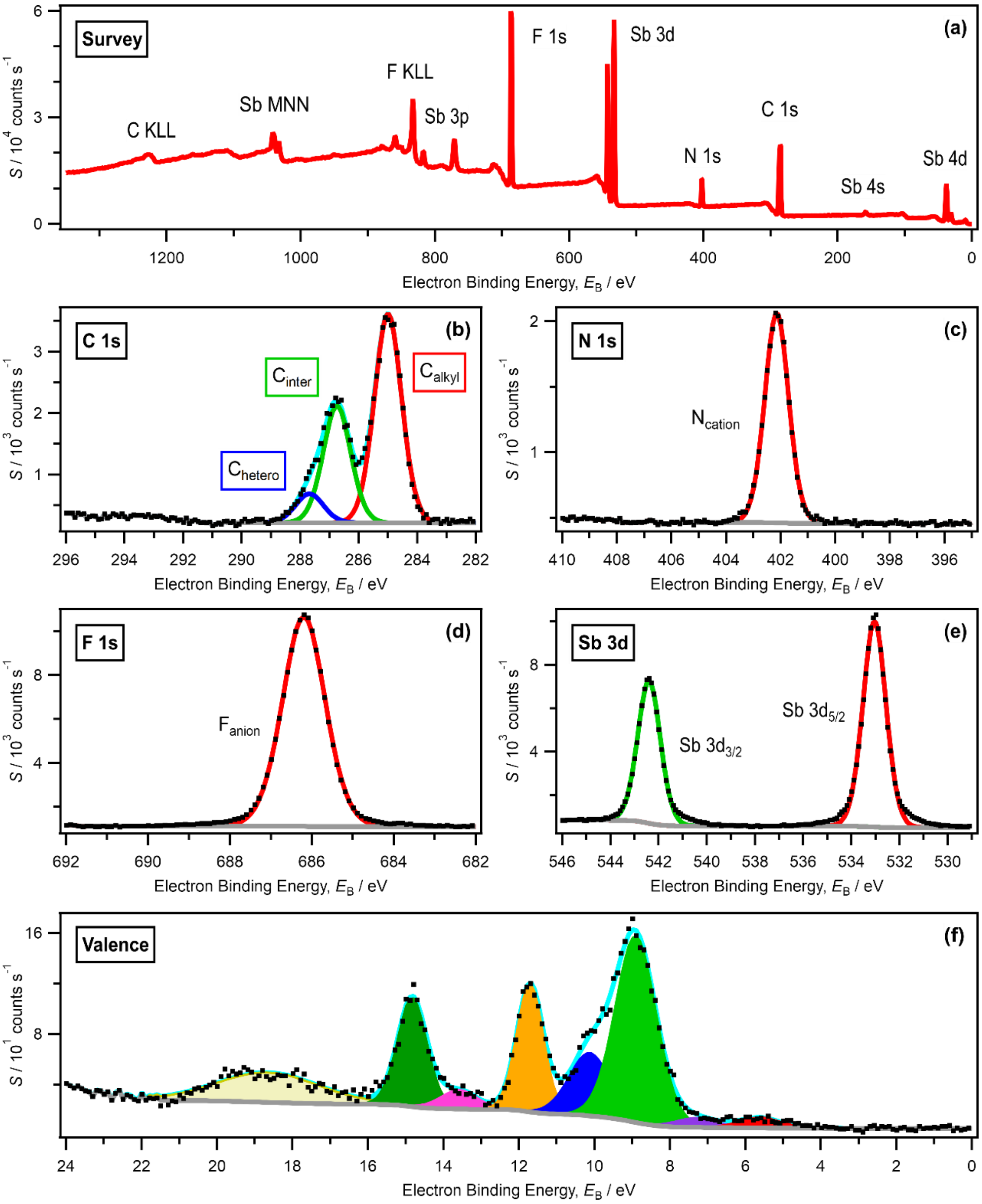

**Figure S15.** (a) Survey, (b-e) core and (f) valence XP spectra for $[C_8C_1Im][SbF_6]$ recorded on laboratory–based XPS apparatus at $h\nu$ = 1486.6 eV. All XP spectra were charge referenced using method i outlined in Section 2.5. The component labelled red was principally from the $[C_4C_1Im]^+$ cation.

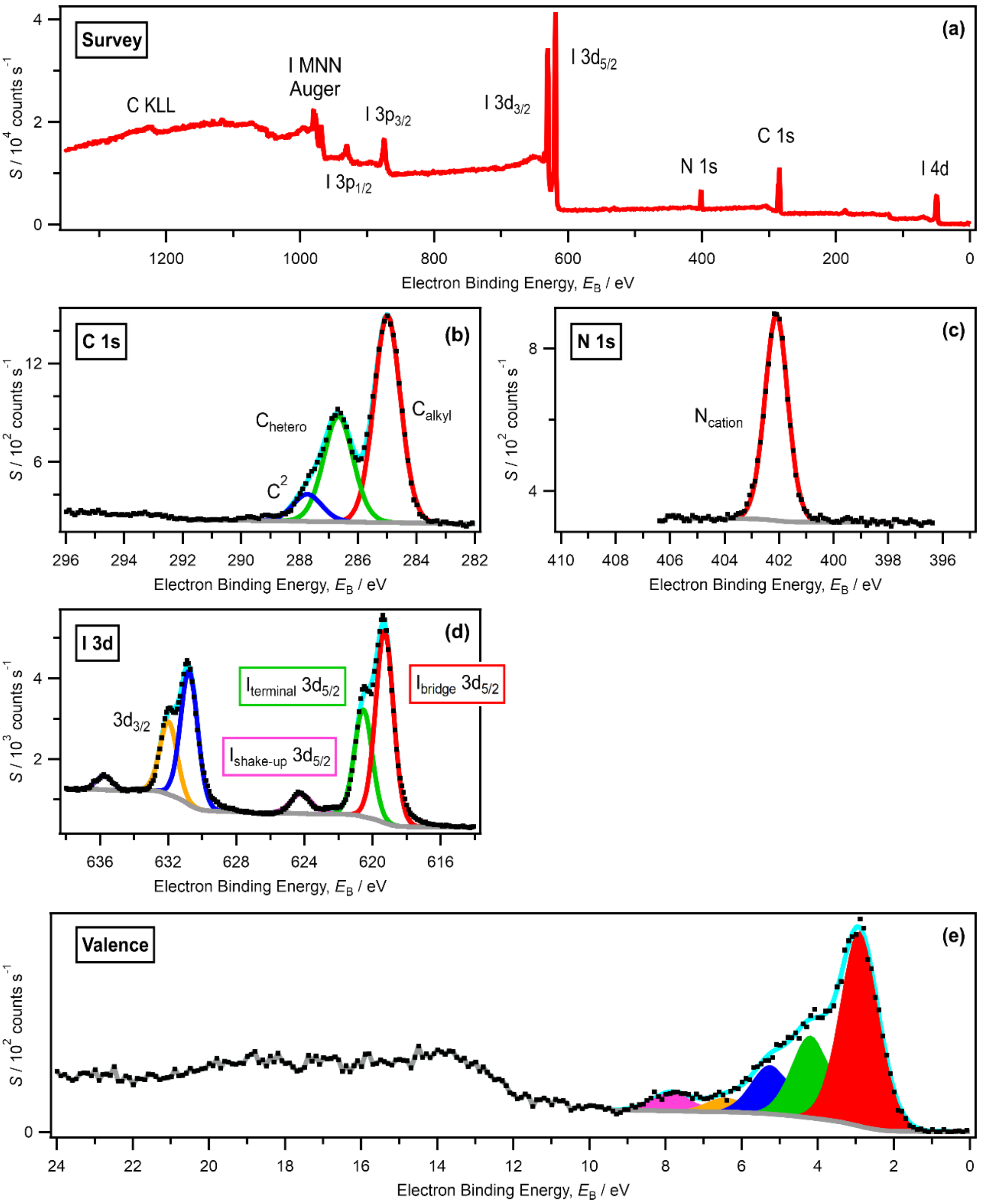

**Figure S16.** (a) Survey, (b-d) core and (e) valence XP spectra for [$C_8C_1Im$][$I_3$] recorded on laboratory–based XPS apparatus at $h\nu$ = 1486.6 eV. All XP spectra were charge referenced using method i outlined in Section 2.5.

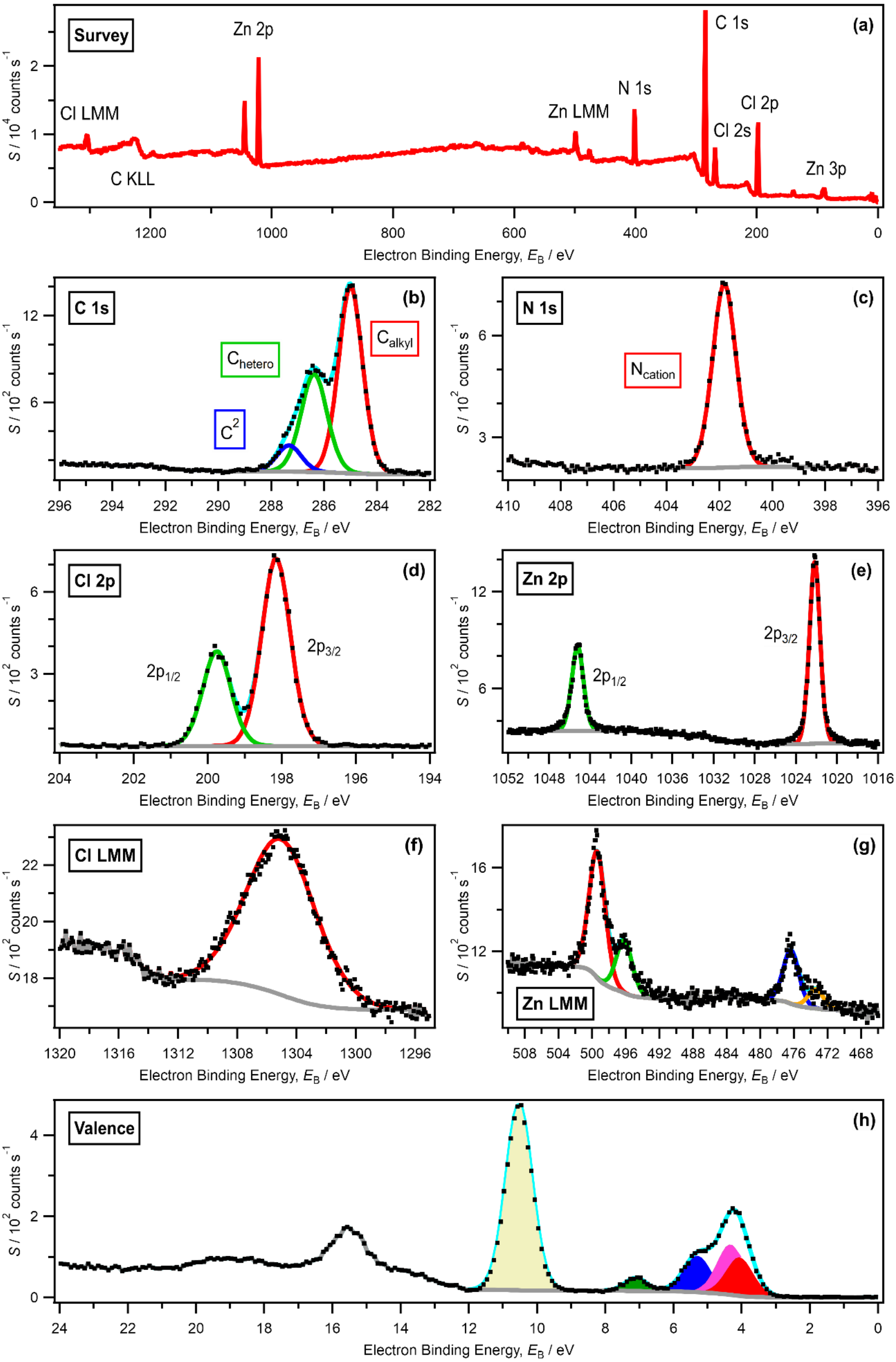

**Figure S17.** (a) Survey, (b-e) core, (f-g) Auger and (h) valence XP spectra for $[C_8C_1Im]_2[ZnCl_4]$ recorded on laboratory–based XPS apparatus at $h\nu$ = 1486.6 eV. All XP spectra were charge referenced using method i outlined in Section 2.5.

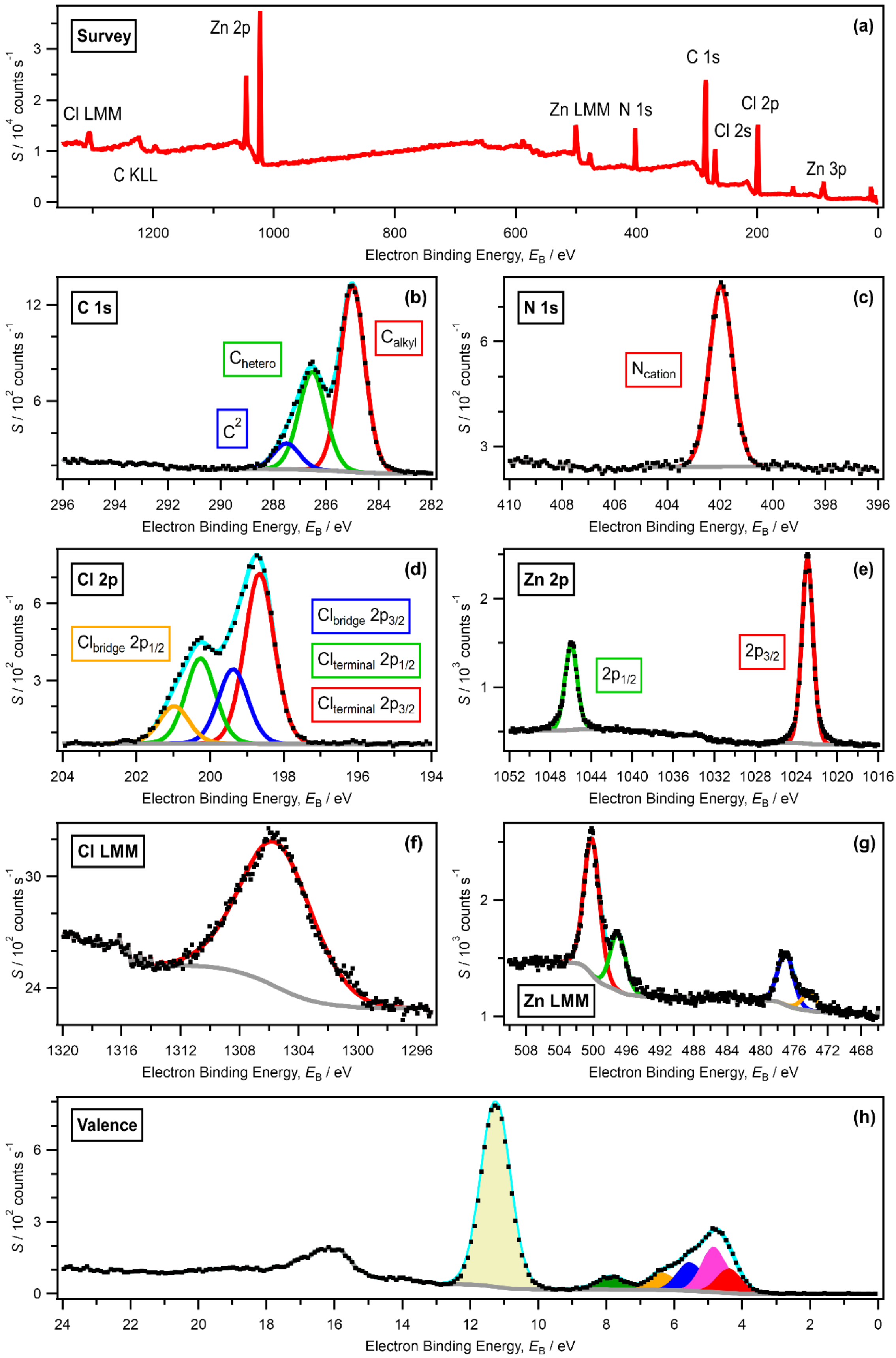

**Figure S18.** (a) Survey, (b-e) core, (f-g) Auger and (h) valence XP spectra for [C$_8$C$_1$Im]$_2$[Zn$_2$Cl$_6$] recorded on laboratory–based XPS apparatus at $h\nu$ = 1486.6 eV. All XP spectra were charge referenced using method i outlined in Section 2.5.

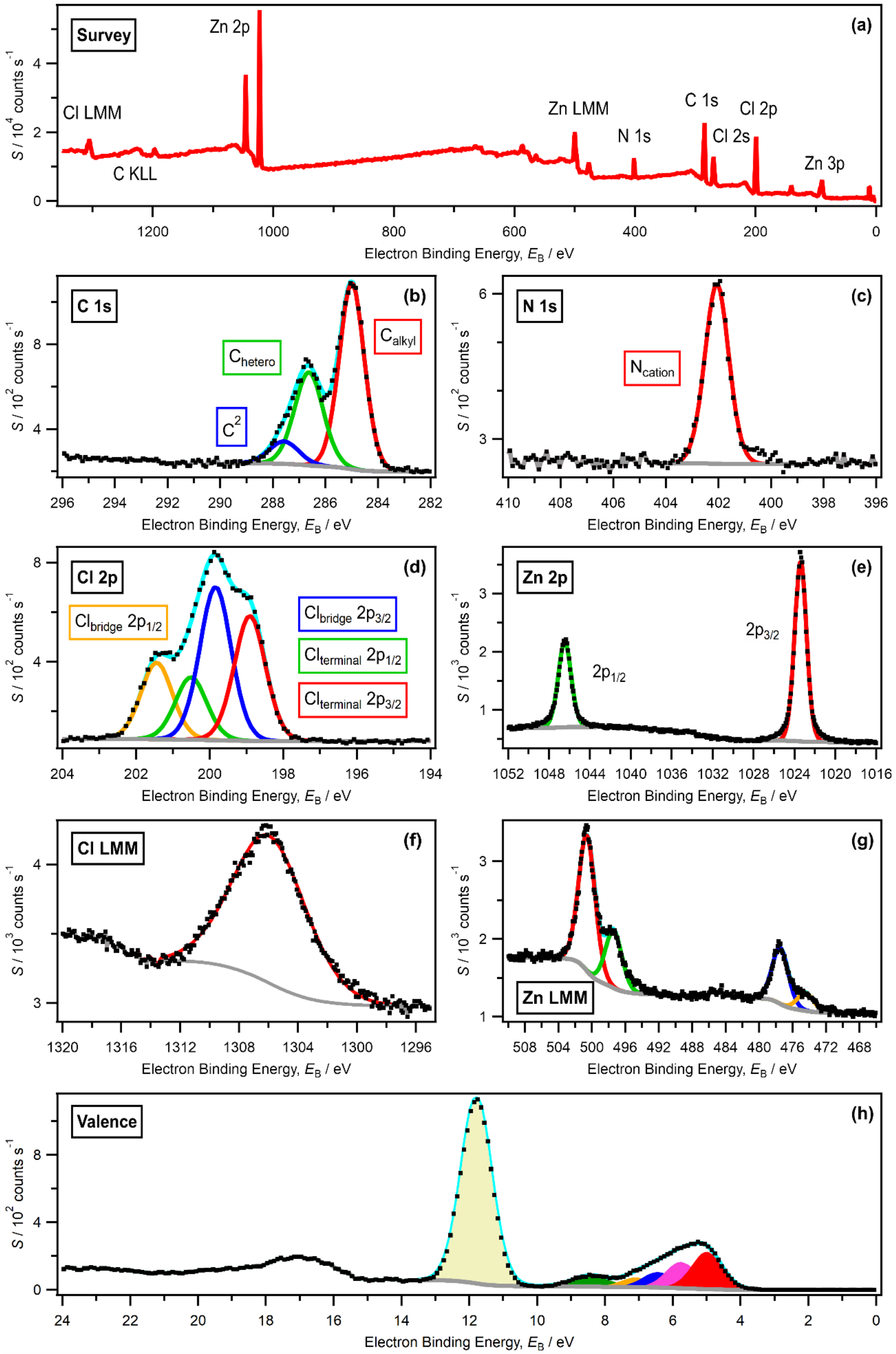

**Figure S19.** (a) Survey, (b-e) core, (f-g) Auger and (h) valence XP spectra for $[C_8C_1Im]_2[Zn_4Cl_{10}]$ recorded on laboratory–based XPS apparatus at $h\nu = 1486.6$ eV. All XP spectra were charge referenced using method i outlined in Section 2.5.

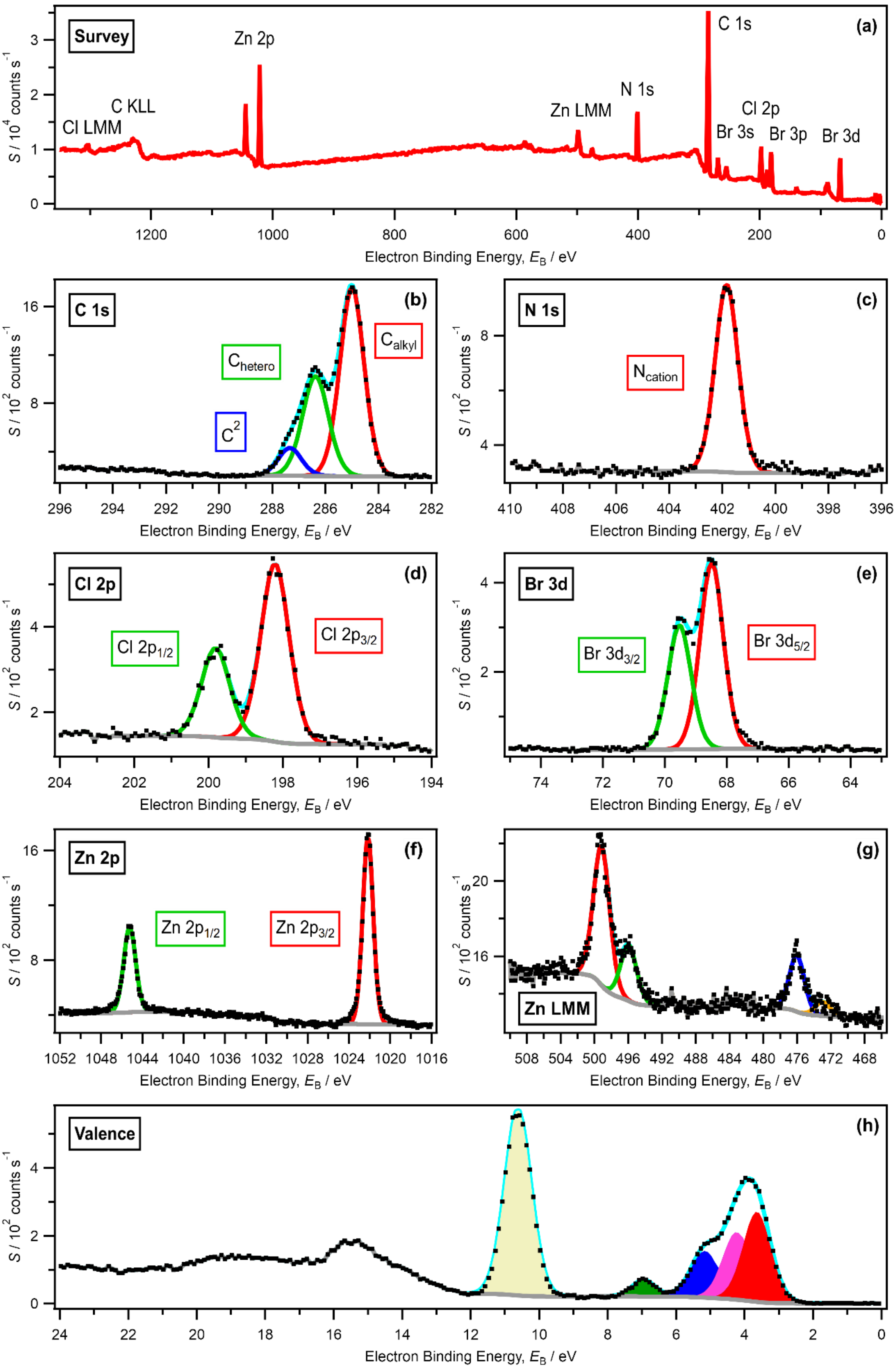

**Figure S20.** (a) Survey, (b-f) core, (g) Auger and (h) valence XP spectra for $[C_8C_1Im]_2[ZnCl_2Br_2]$ recorded on laboratory–based XPS apparatus at $h\nu$ = 1486.6 eV. All XP spectra were charge referenced using method i outlined in Section 2.5.

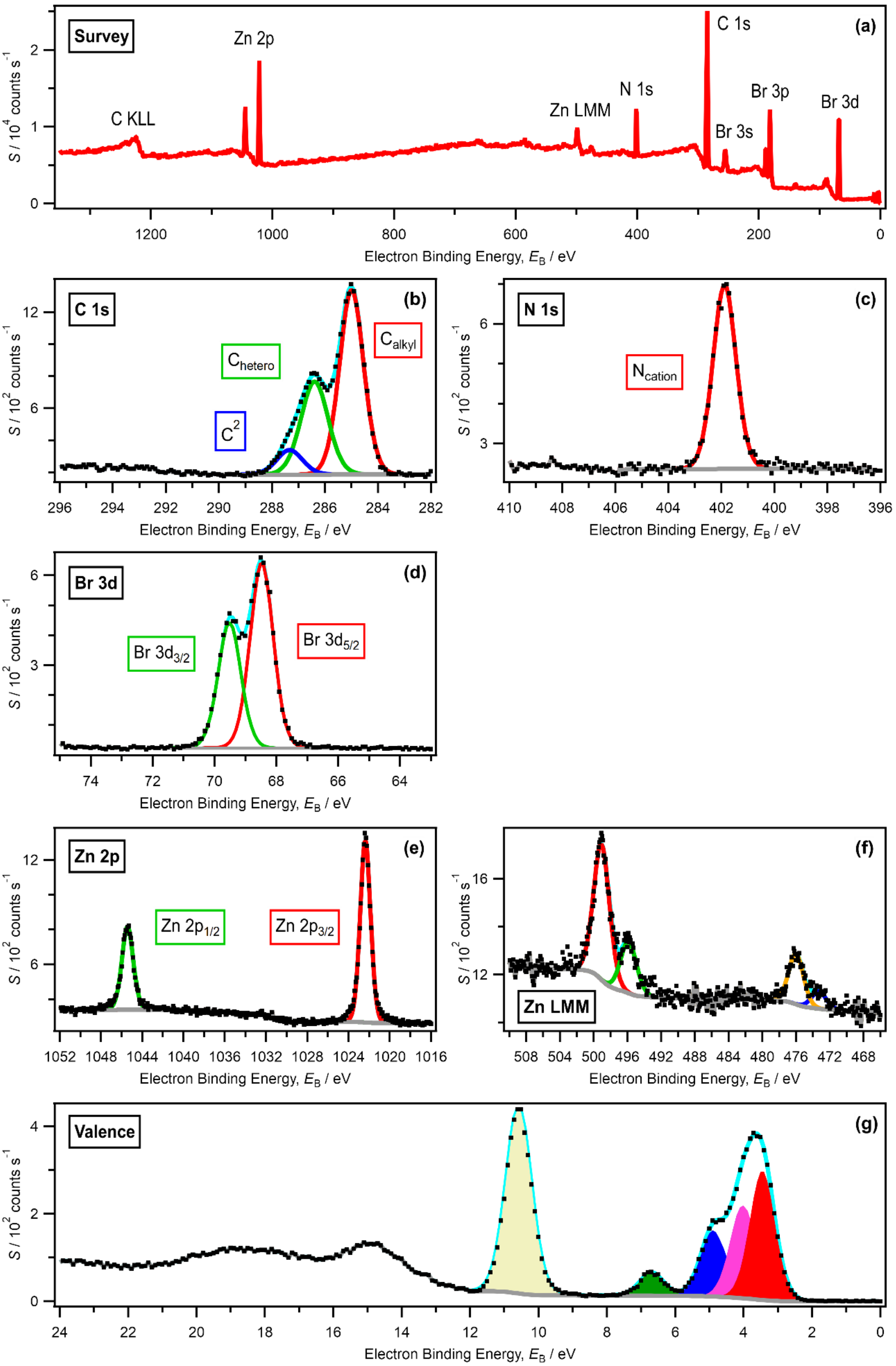

**Figure S21.** (a) Survey, (b-e) core, (f) Auger and (g) valence XP spectra for $[C_8C_1Im]_2[ZnBr_4]$ recorded on laboratory–based XPS apparatus at $h\nu$ = 1486.6 eV. All XP spectra were charge referenced using method i outlined in Section 2.5.

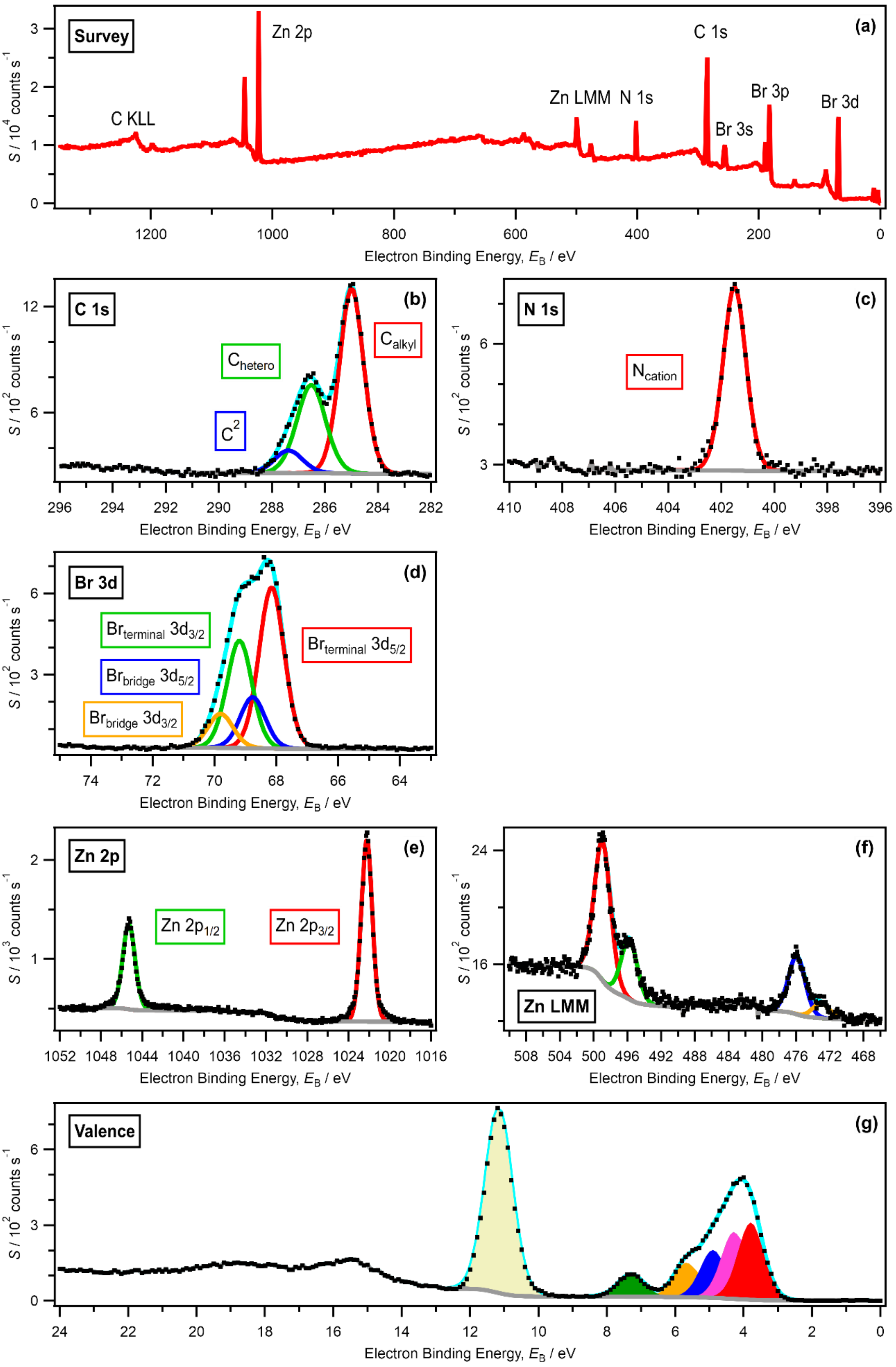

**Figure S22.** (a) Survey, (b-e) core, (f) Auger and (g) valence XP spectra for $[C_8C_1Im]_2[Zn_2Br_6]$ recorded on laboratory–based XPS apparatus at $h\nu$ = 1486.6 eV. All XP spectra were charge referenced using method i outlined in Section 2.5.

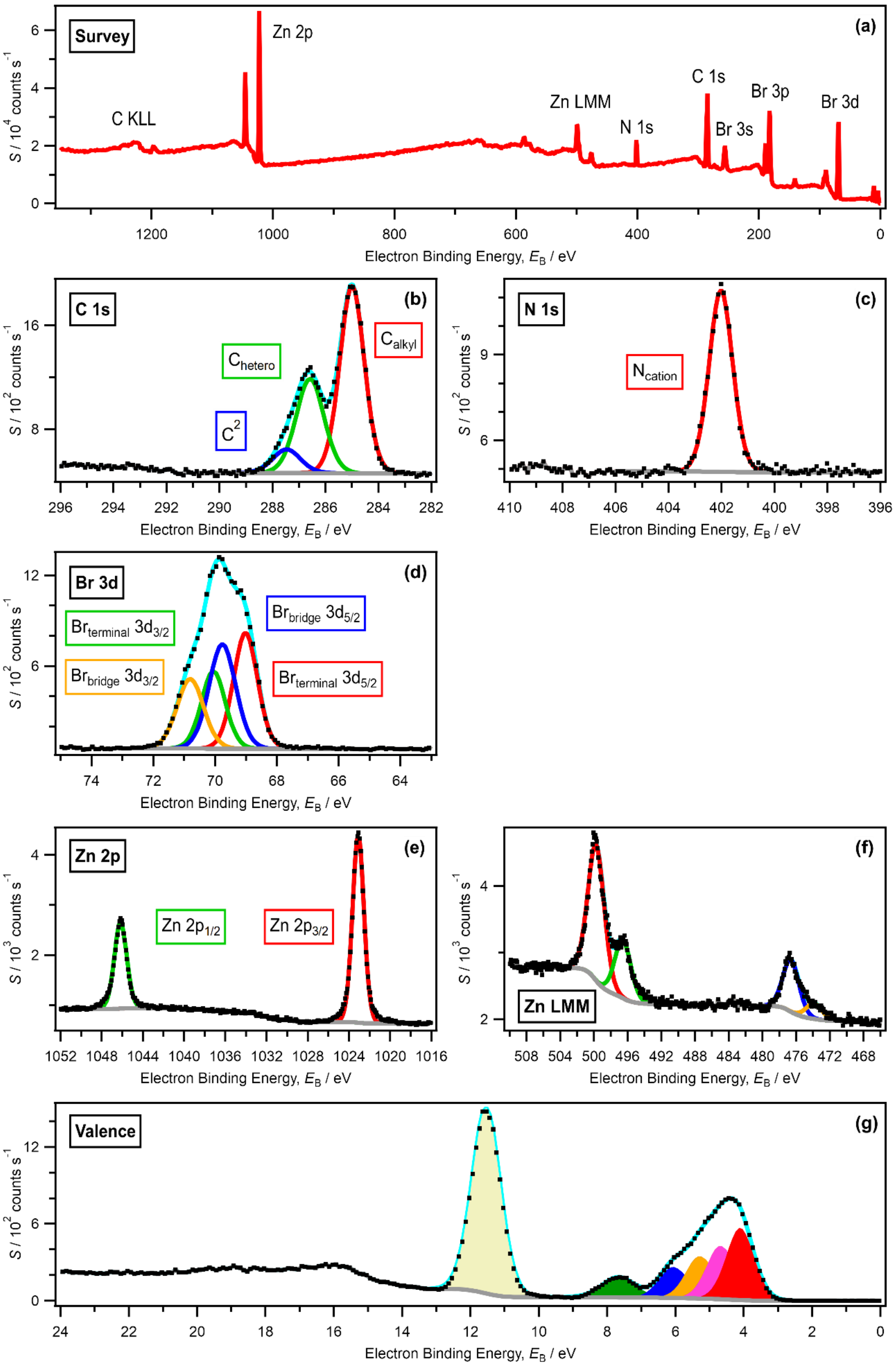

**Figure S23.** (a) Survey, (b-e) core, (f) Auger and (g) valence XP spectra for [$C_8C_1Im$]$_2$[$Zn_3Br_8$] recorded on laboratory–based XPS apparatus at $h\nu$ = 1486.6 eV. All XP spectra were charge referenced using method i outlined in Section 2.5.

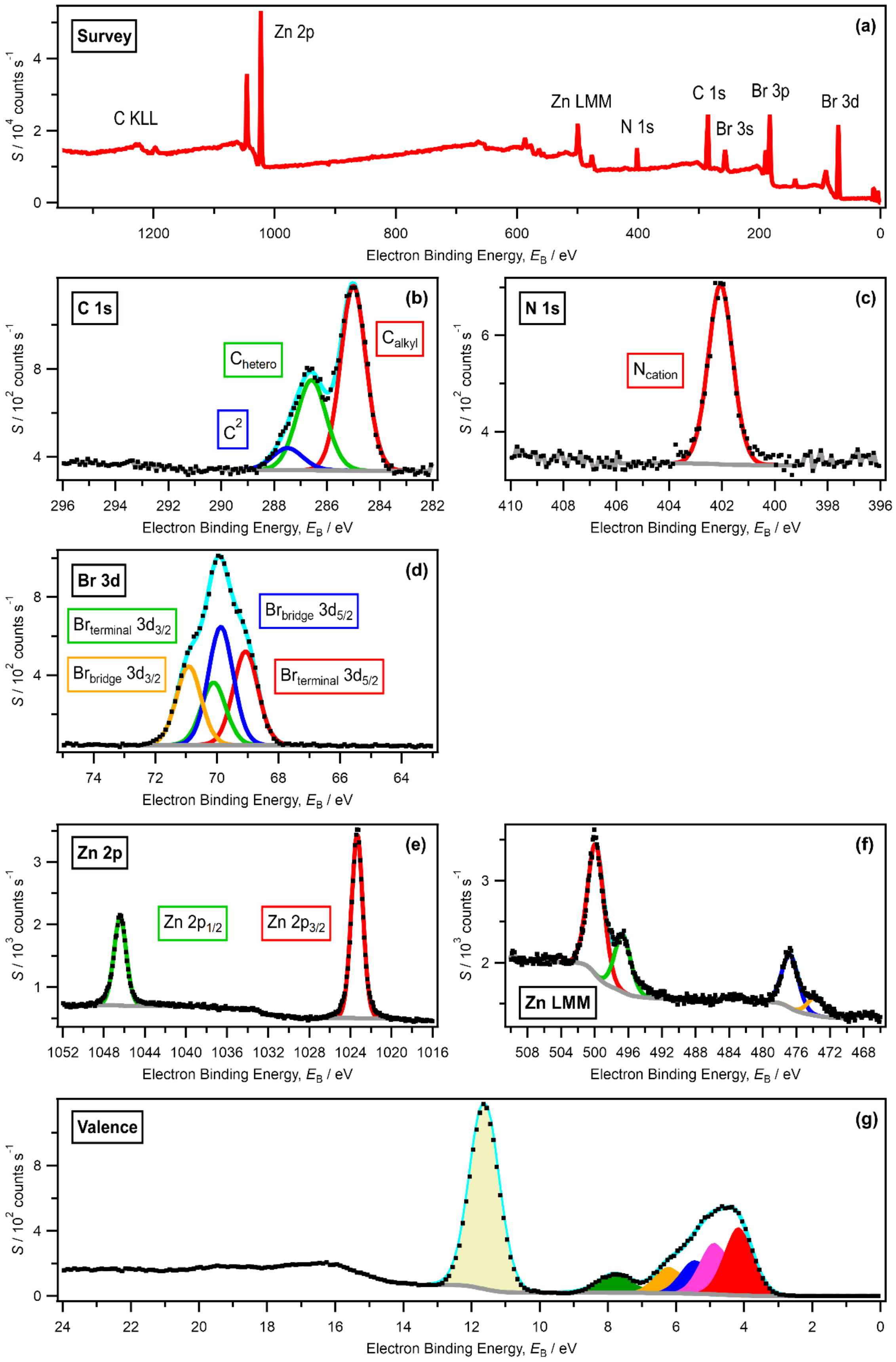

**Figure S24.** (a) Survey, (b-e) core, (f) Auger and (g) valence XP spectra for $[C_8C_1Im]_2[Zn_4Br_{10}]$ recorded on laboratory–based XPS apparatus at $h\nu$ = 1486.6 eV. All XP spectra were charge referenced using method i outlined in Section 2.5.

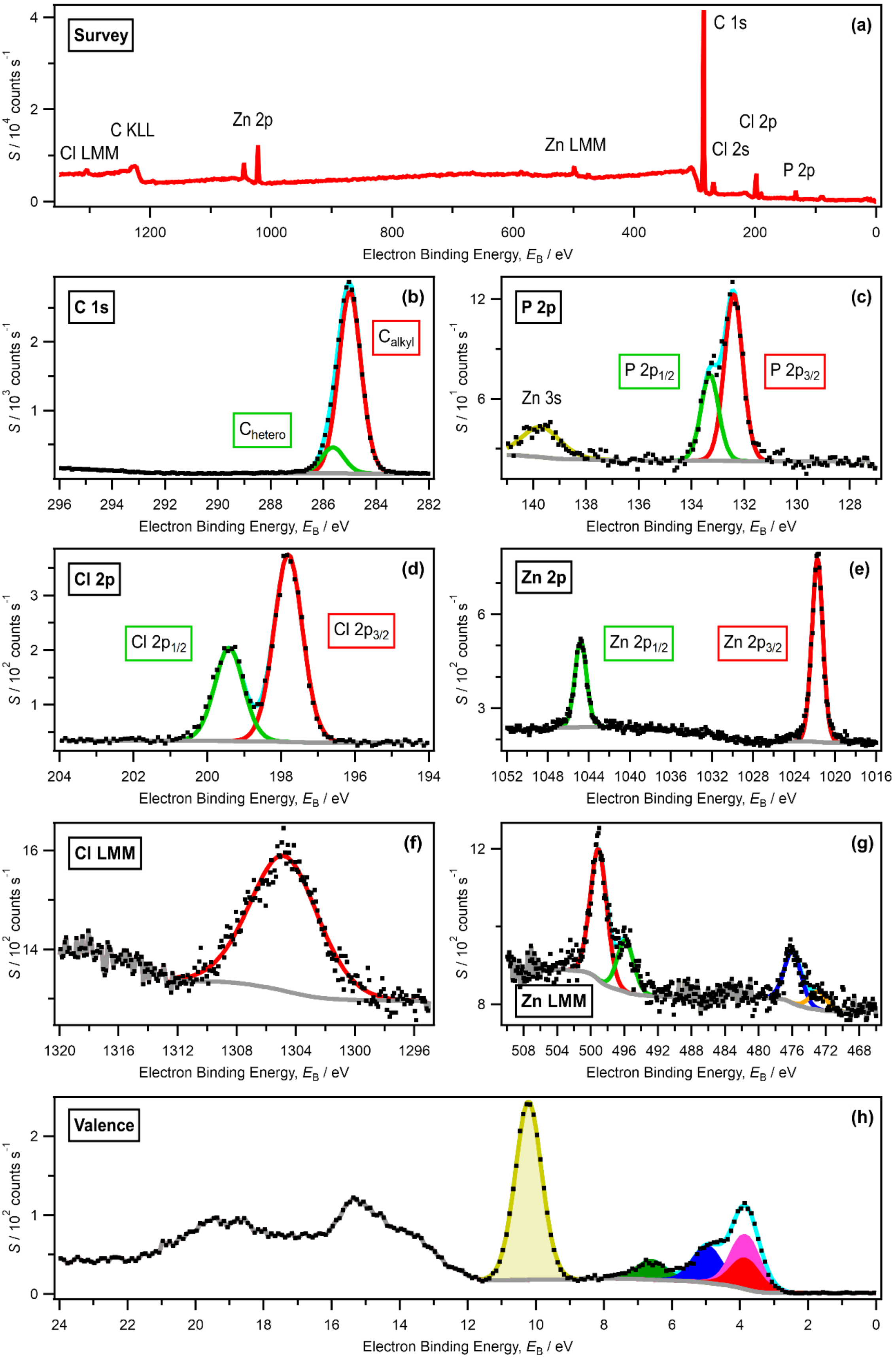

**Figure S25.** (a) Survey, (b-e) core, (f-g) Auger and (h) valence XP spectra for $[P_{6,6,6,14}]_2[ZnCl_4]$ recorded on laboratory–based XPS apparatus at $h\nu$ = 1486.6 eV. All XP spectra were charge referenced using method i outlined in Section 2.5.

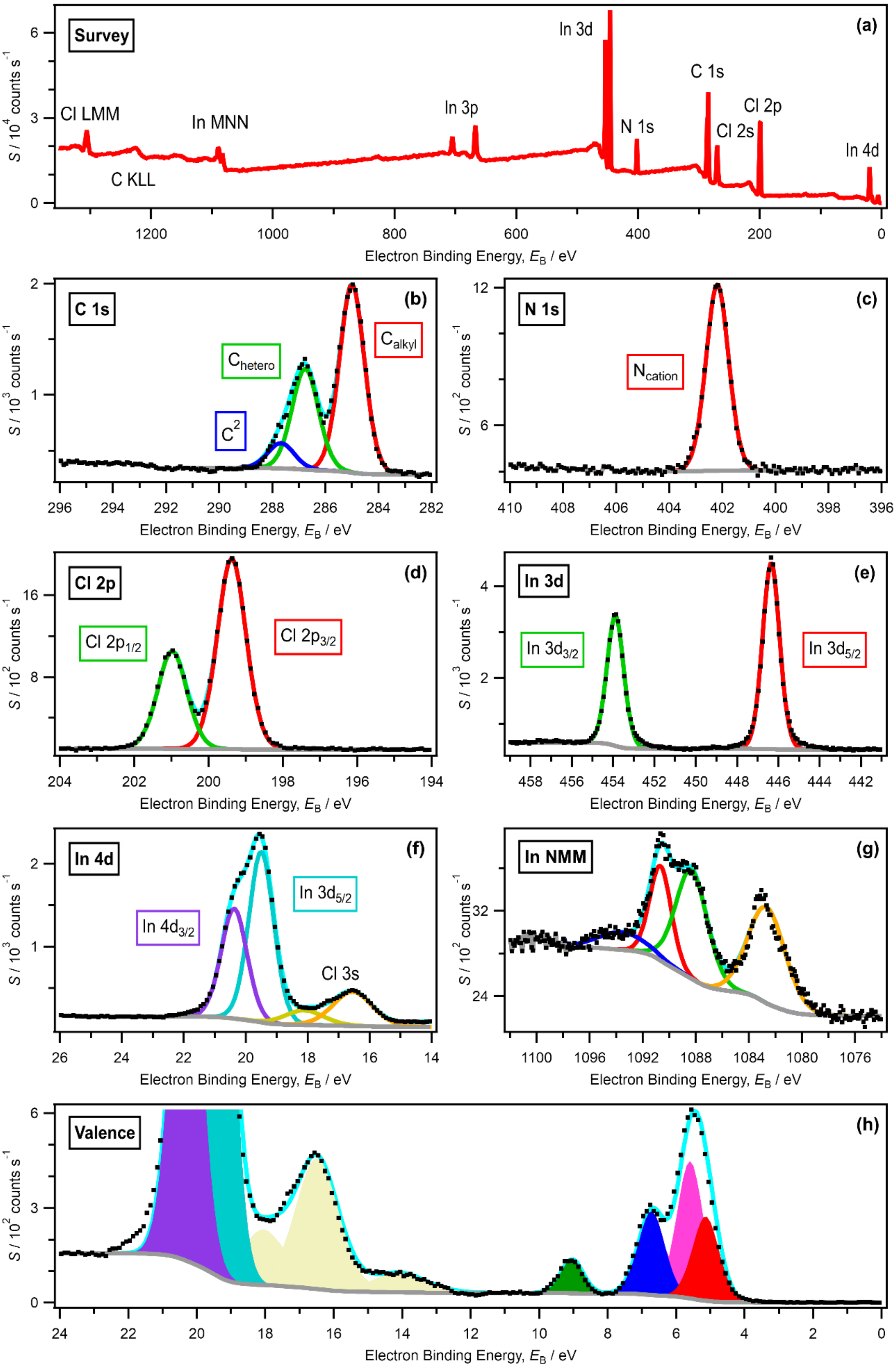

**Figure S26.** (a) Survey, (b-f) core, (g) Auger and (h) valence XP spectra for [$C_8C_1$Im][$InCl_4$] recorded on laboratory–based XPS apparatus at *hν* = 1486.6 eV. All XP spectra were charge referenced using method i outlined in Section 2.5.

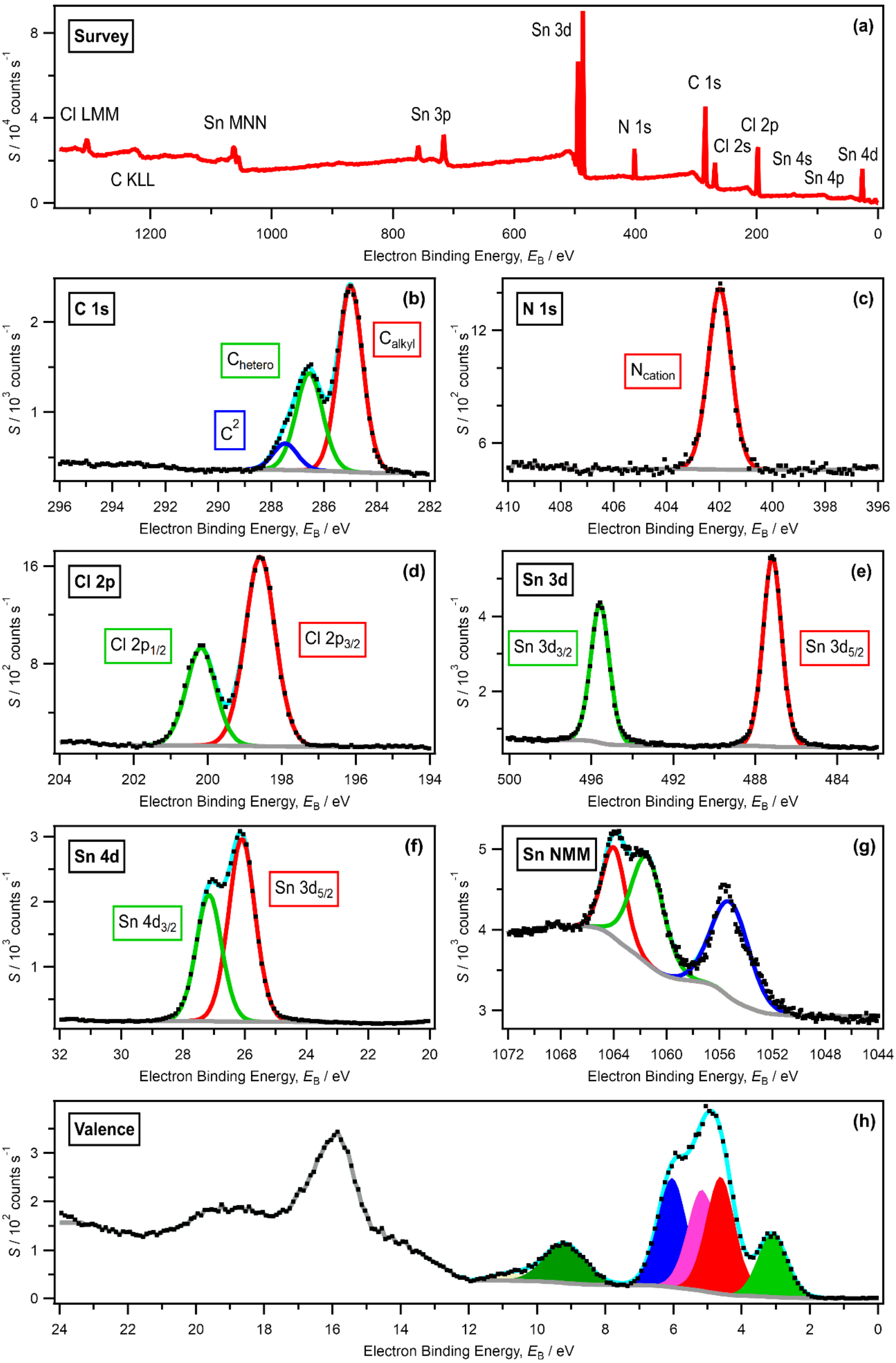

**Figure S27.** (a) Survey, (b-f) core, (g) Auger and (h) valence XP spectra for [$C_8C_1$Im][$SnCl_3$] recorded on laboratory–based XPS apparatus at *hν* = 1486.6 eV. All XP spectra were charge referenced using method i outlined in Section 2.5.

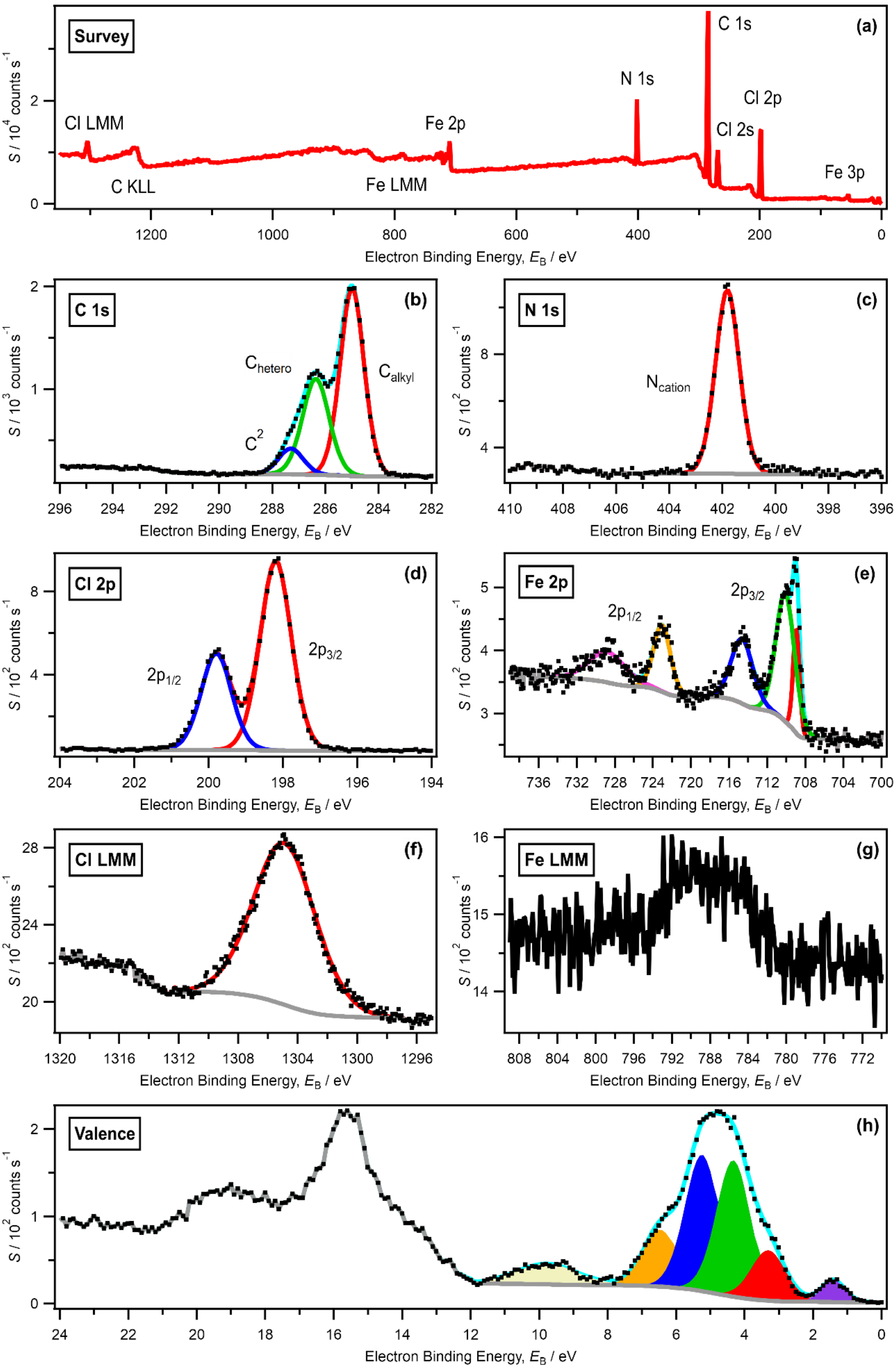

**Figure S28.** (a) Survey, (b-e) core, (f-g) Auger and (h) valence XP spectra for [$C_8C_1Im$]$_2$[$FeCl_4$] recorded on laboratory–based XPS apparatus at *hν* = 1486.6 eV. All XP spectra were charge referenced using method i outlined in Section 2.5.

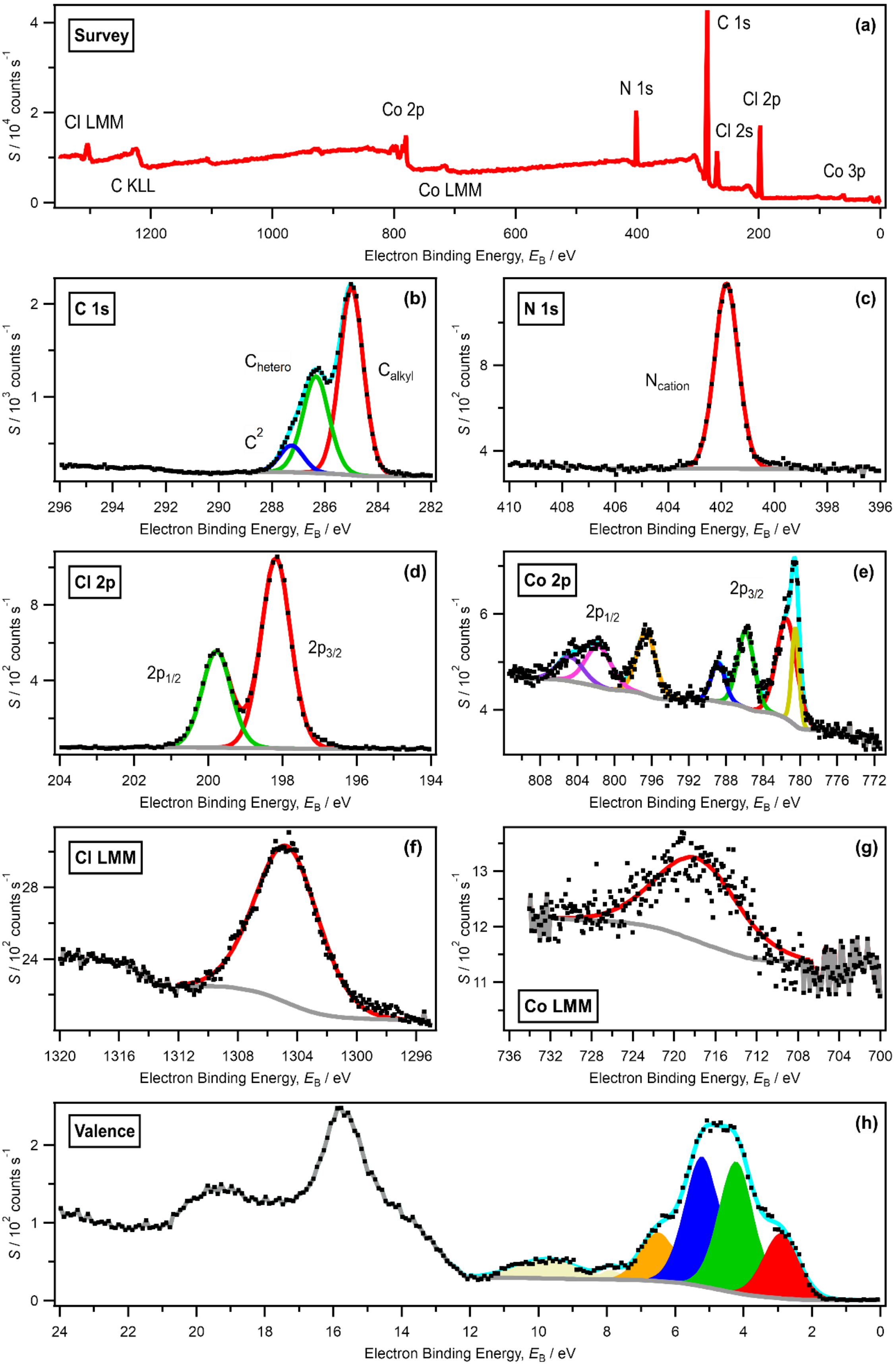

**Figure S29.** (a) Survey, (b-e) core, (f-g) Auger and (h) valence XP spectra for $[C_8C_1Im]_2[CoCl_4]$ recorded on laboratory–based XPS apparatus at *hν* = 1486.6 eV. All XP spectra were charge referenced using method i outlined in Section 2.5.

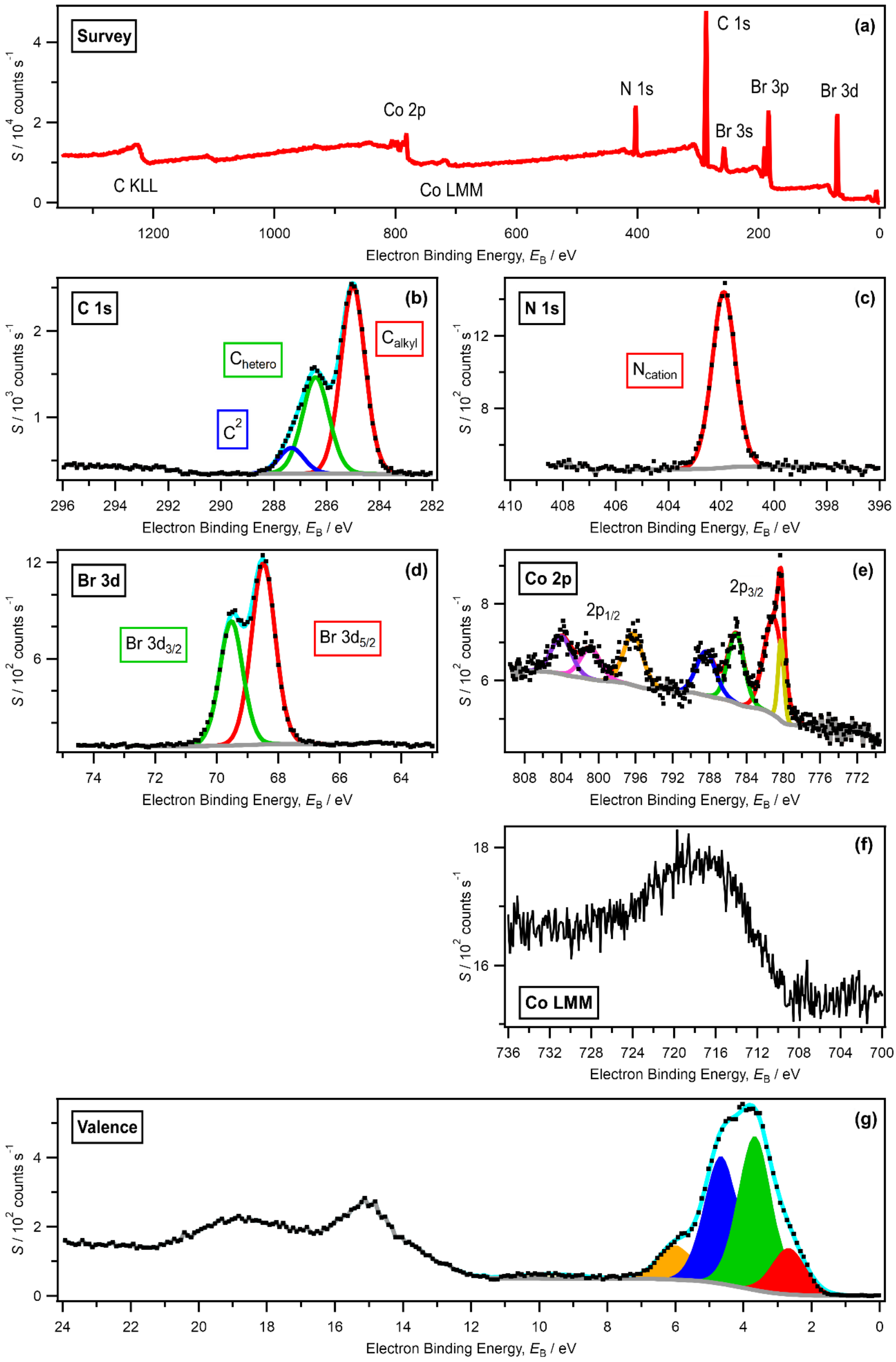

**Figure S30.** (a) Survey, (b-e) core, (f) Auger and (g) valence XP spectra for $[C_8C_1Im]_2[CoBr_4]$ recorded on laboratory–based XPS apparatus at $h\nu = 1486.6$ eV. All XP spectra were charge referenced using method i outlined in Section 2.5.

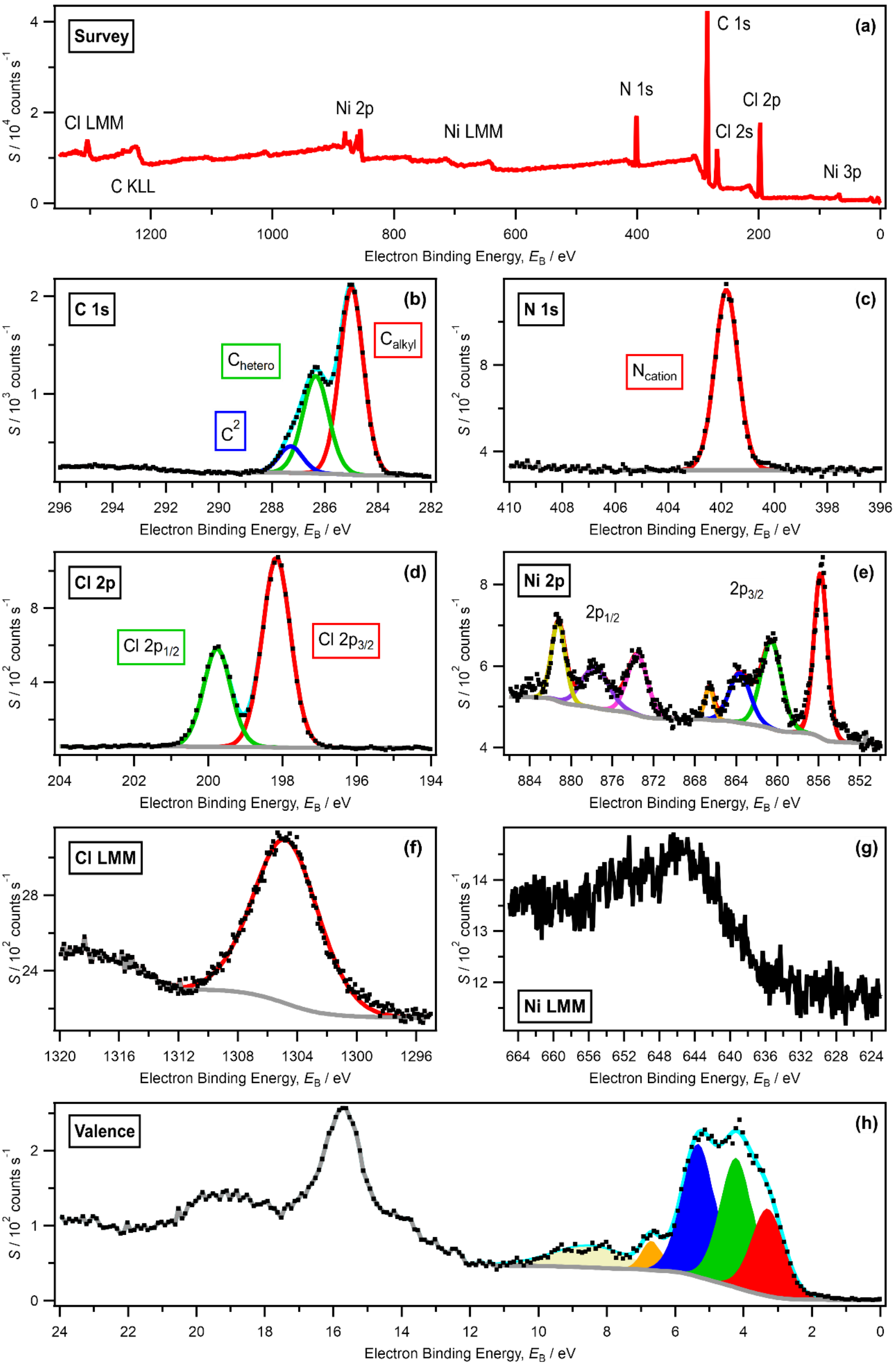

**Figure S31.** (a) Survey, (b-e) core, (f-g) Auger and (h) valence XP spectra for $[C_8C_1Im]_2[NiCl_4]$ recorded on laboratory–based XPS apparatus at $h\nu$ = 1486.6 eV. All XP spectra were charge referenced using method i outlined in Section 2.5.

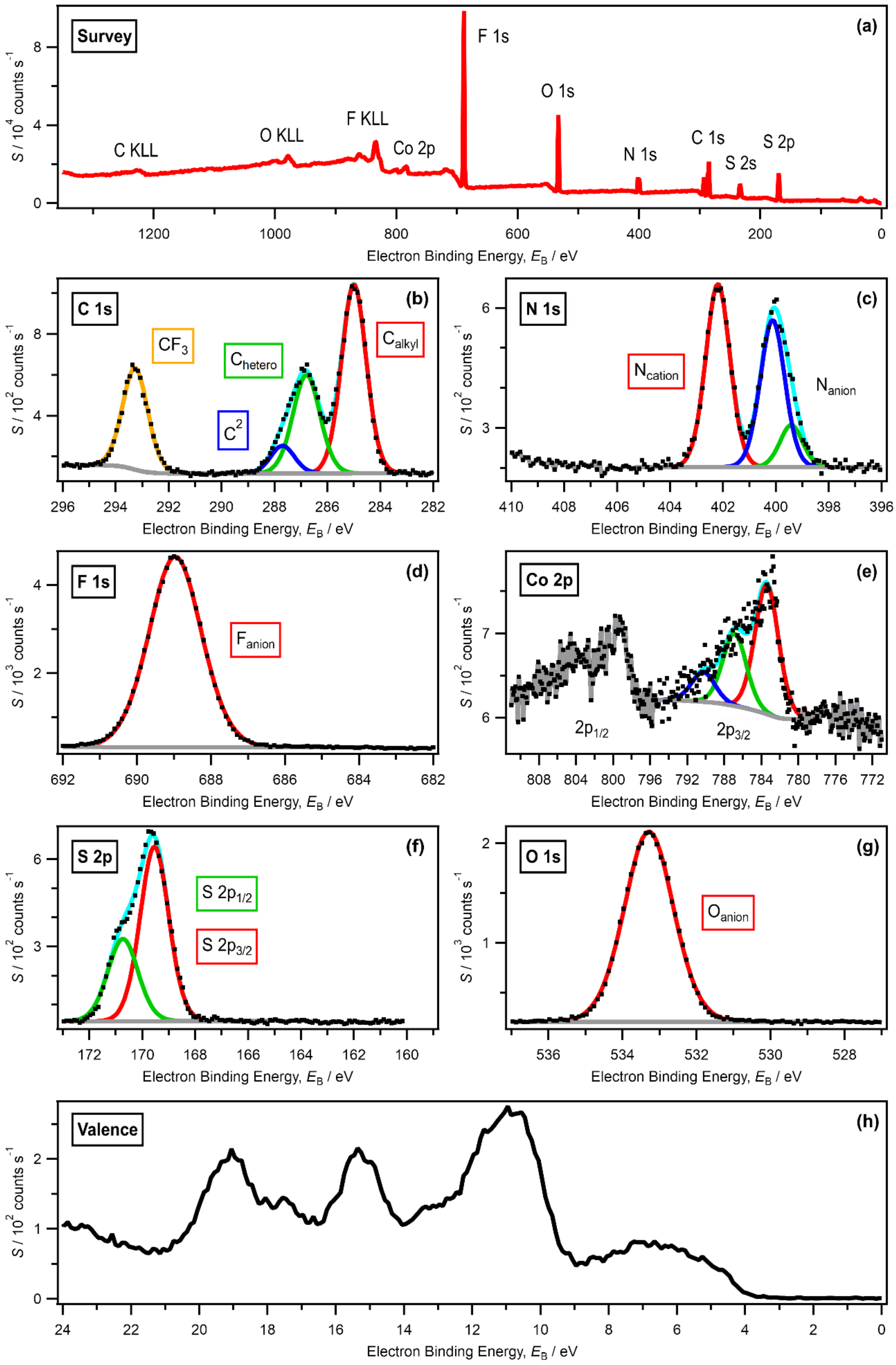

**Figure S32.** (a) Survey, (b-g) core and (h) valence XP spectra for $[C_8C_1Im]_2[Co(NTf_2)_4]$ recorded on laboratory–based XPS apparatus at $h\nu = 1486.6$ eV. All XP spectra were charge referenced using method i outlined in Section 2.5.

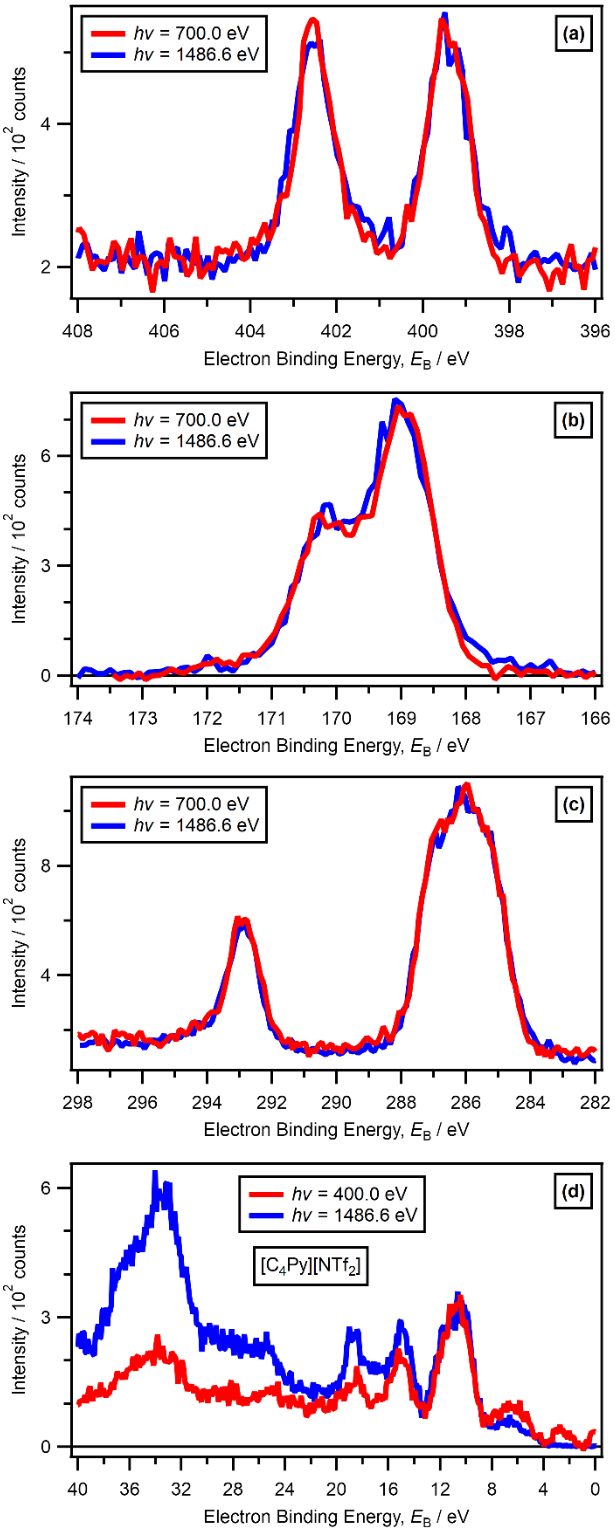

**Figure S33.** (a-c) core and (d) valence XP spectra for [C$_4$Py][NTf$_2$] recorded on laboratory–based apparatus (at $h\nu$ = 1486.6 eV) and synchrotron-based XPS apparatus. All electron spectra were charge referenced using procedures outlined in ESI Section 5.

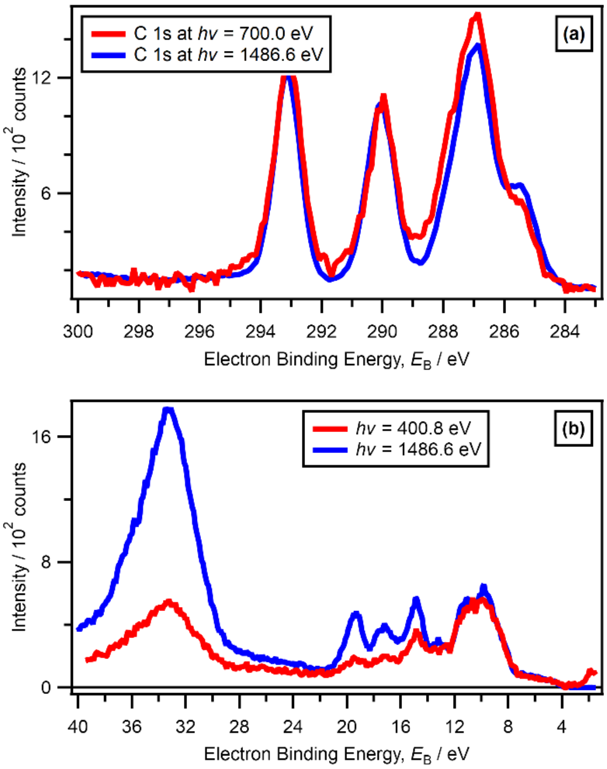

**Figure S34.** (a) core and (b) valence XP spectra for [$C_2C_1$Im][FAP] recorded on laboratory–based apparatus (at $h\nu$ = 1486.6 eV) and synchrotron-based XPS apparatus. All electron spectra were charge referenced using procedures outlined in ESI Section 5.

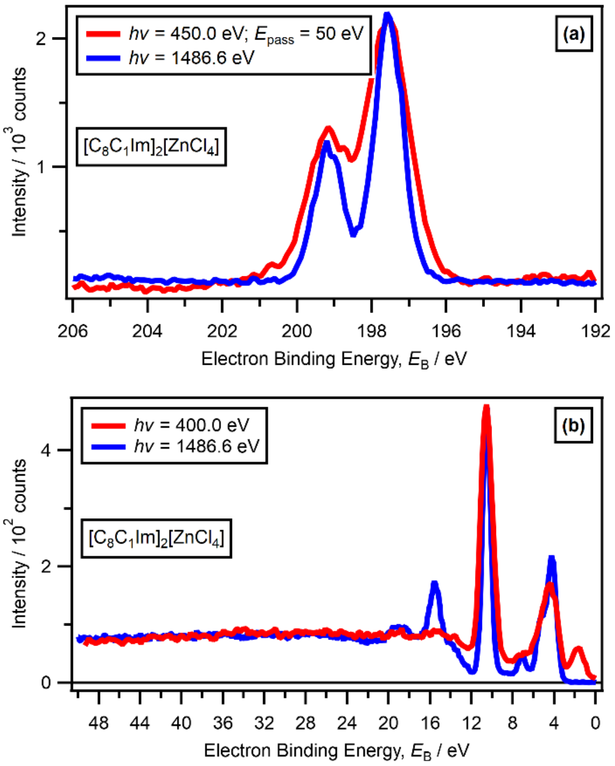

**Figure S35.** (a) core and (b) valence XP spectra for [$C_8C_1$Im]$_2$[$ZnCl_4$] recorded on laboratory–based apparatus (at $h\nu$ = 1486.6 eV) and synchrotron-based XPS apparatus. All electron spectra were charge referenced using procedures outlined in ESI Section 5.

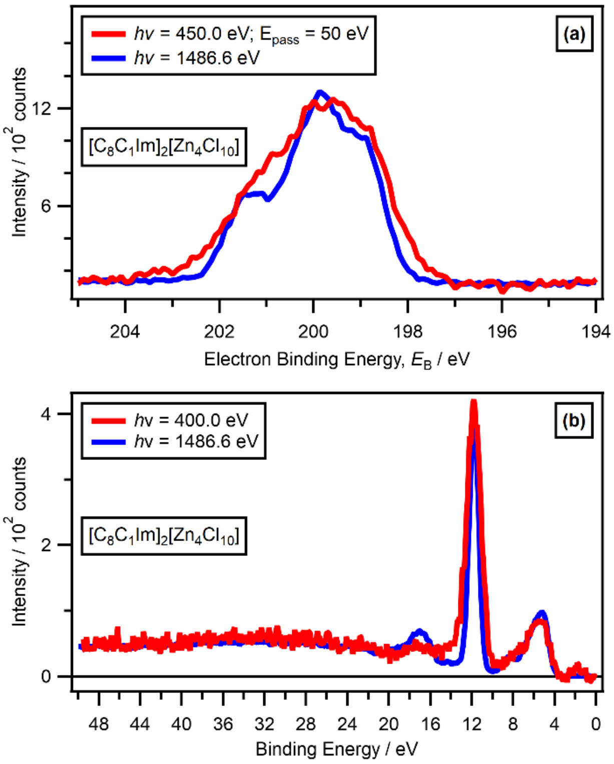

**Figure S36.** (a) core and (b) valence XP spectra for $[C_8C_1Im]_2[Zn_4Cl_{10}]$ recorded on laboratory–based apparatus (at $h\nu$ = 1486.6 eV) and synchrotron-based XPS apparatus. All electron spectra were charge referenced using procedures outlined in ESI Section 5.

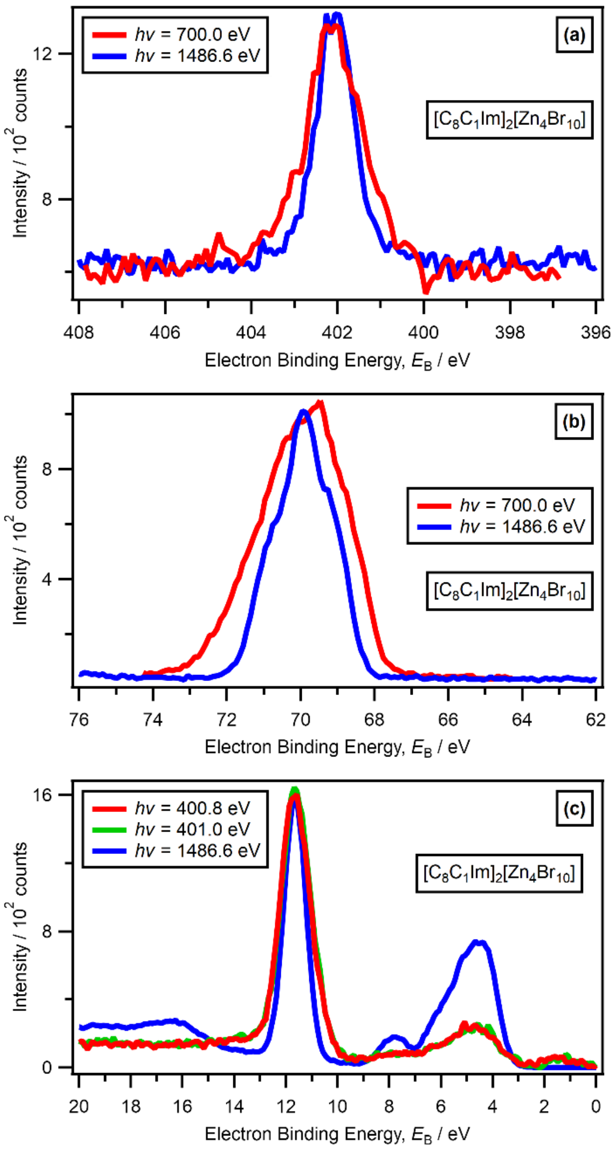

**Figure S37.** (a-b) core and (c) valence XP spectra for $[C_8C_1Im]_2[Zn_4Br_{10}]$ recorded on laboratory–based apparatus (at $h\nu$ = 1486.6 eV) and synchrotron-based XPS apparatus. All electron spectra were charge referenced using procedures outlined in ESI Section 5.

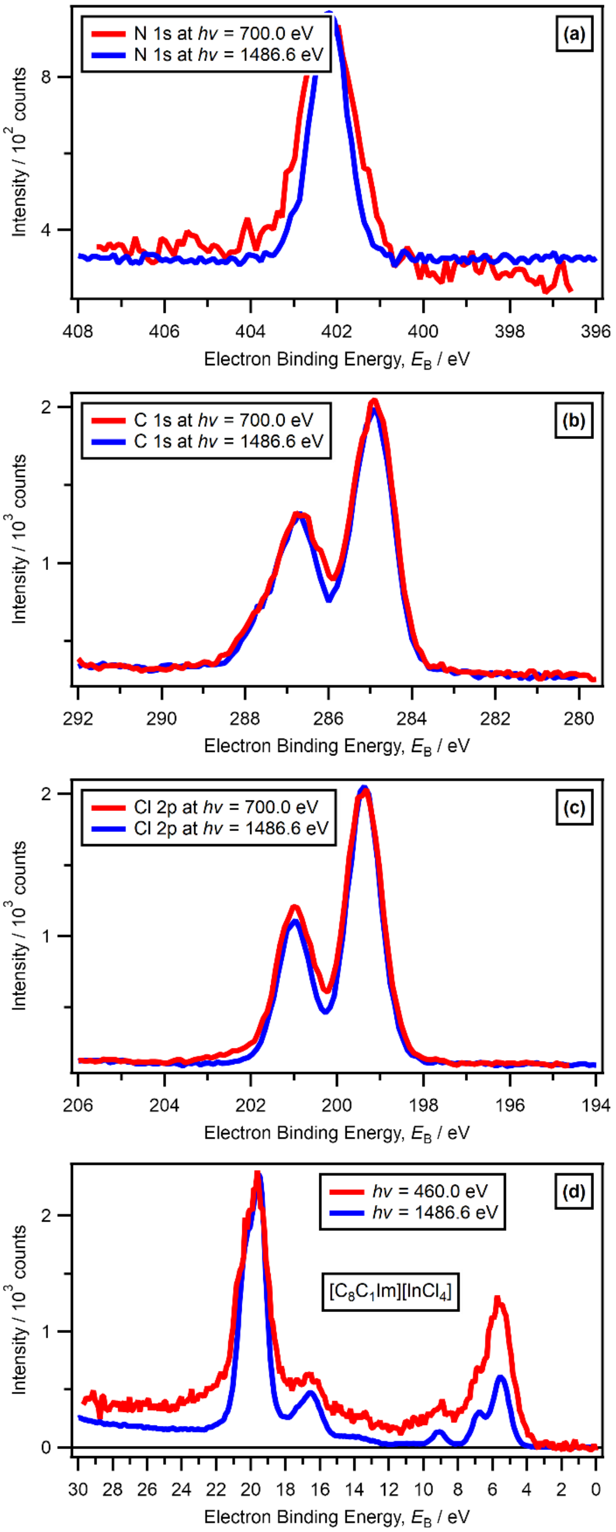

**Figure S38.** (a-c) core and (d) valence XP spectra for [$C_8C_1Im$][$InCl_4$] recorded on laboratory–based apparatus (at *hν* = 1486.6 eV) and synchrotron-based XPS apparatus. All electron spectra were charge referenced using procedures outlined in ESI Section 5.

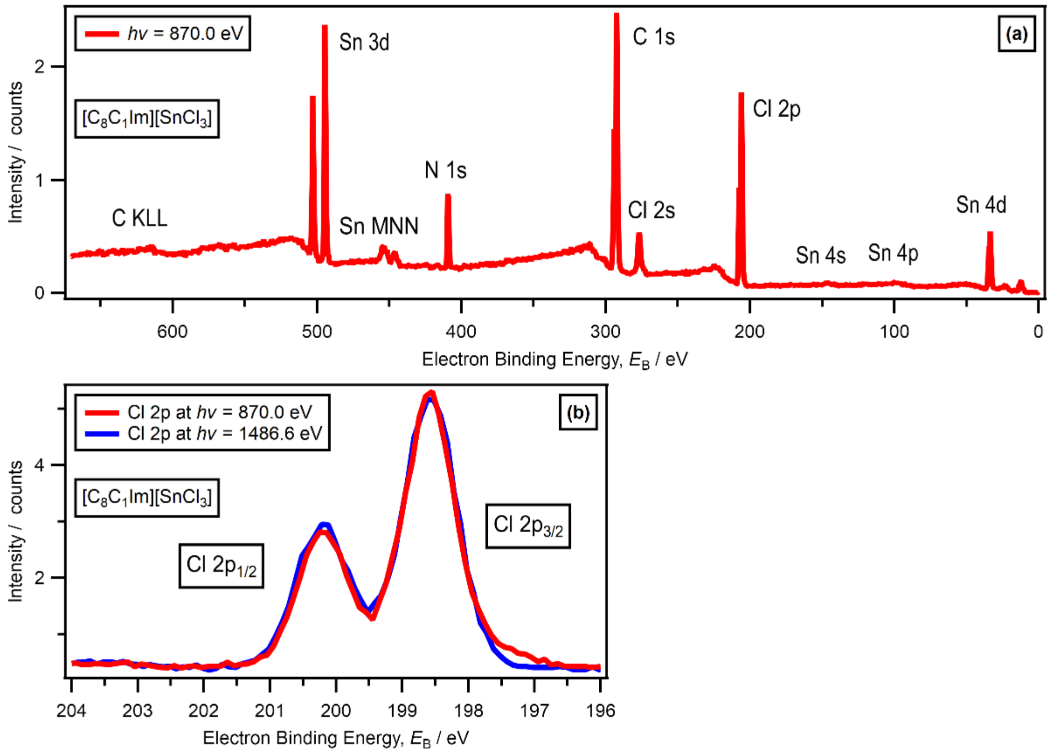

**Figure S39.** (a) survey and (d) core XP spectra for [$C_8C_1$Im]$SnCl_3$] recorded on laboratory–based apparatus (at *hν* = 1486.6 eV) and synchrotron-based XPS apparatus. All electron spectra were charge referenced using procedures outlined in ESI Section 5.

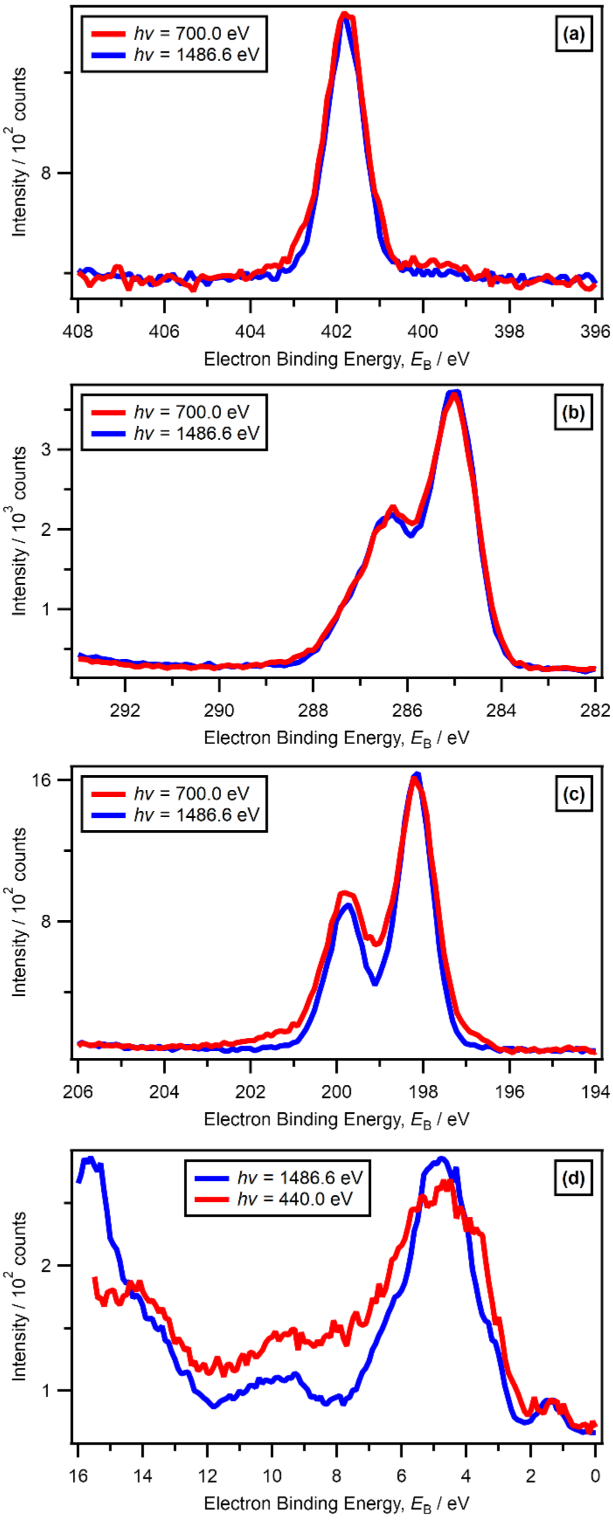

**Figure S40.** (a-c) core and (d) valence XP spectra for $[C_8C_1Im]_2[FeCl_4]$ recorded on laboratory–based apparatus (at $h\nu$ = 1486.6 eV) and synchrotron-based XPS apparatus. All electron spectra were charge referenced using procedures outlined in ESI Section 5.

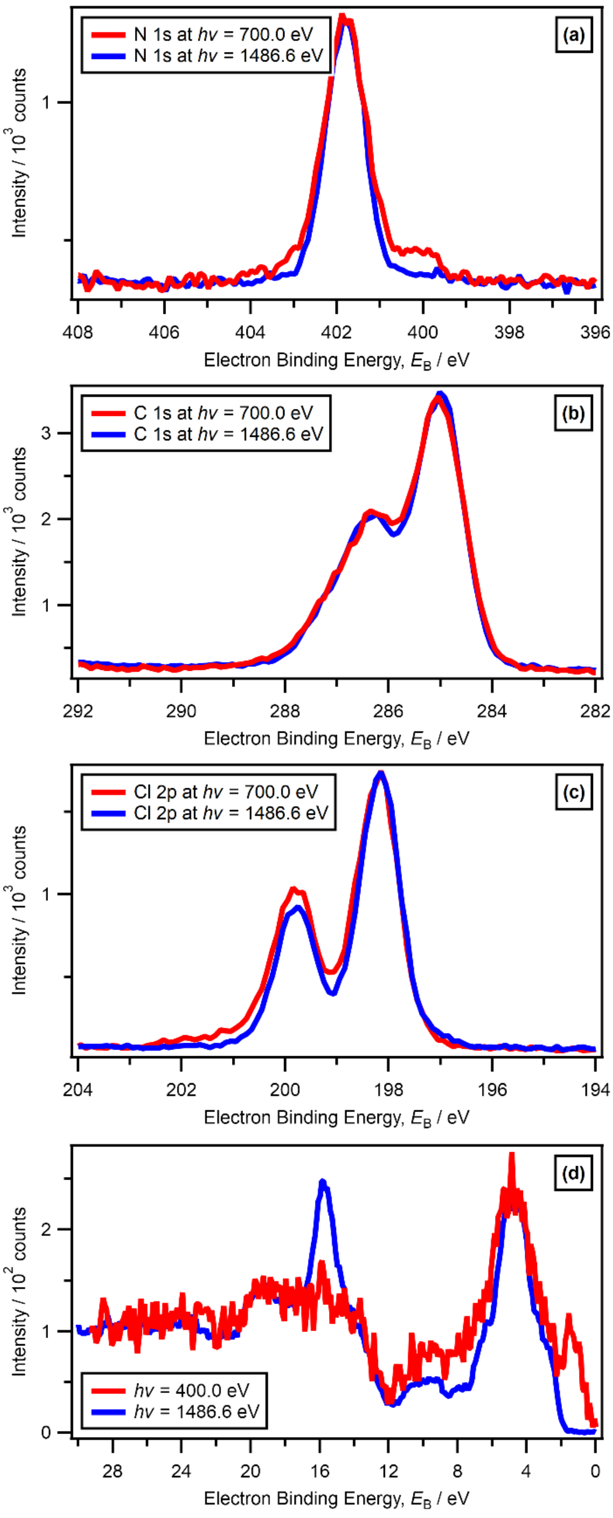

**Figure S41.** (a-c) core and (d) valence XP spectra for $[C_8C_1Im]_2[CoCl_4]$ recorded on laboratory–based apparatus (at $h\nu = 1486.6$ eV) and synchrotron-based XPS apparatus. All electron spectra were charge referenced using procedures outlined in ESI Section 5.

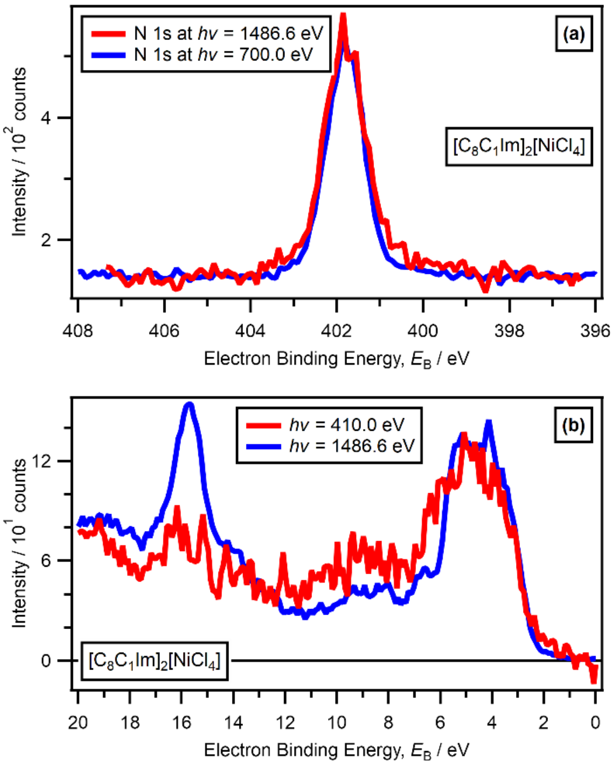

**Figure S42.** (a) core and (b) valence XP spectra for $[C_8C_1Im]_2[NiCl_4]$ recorded on laboratory–based apparatus (at *hν* = 1486.6 eV) and synchrotron-based XPS apparatus. All electron spectra were charge referenced using procedures outlined in ESI Section 5.

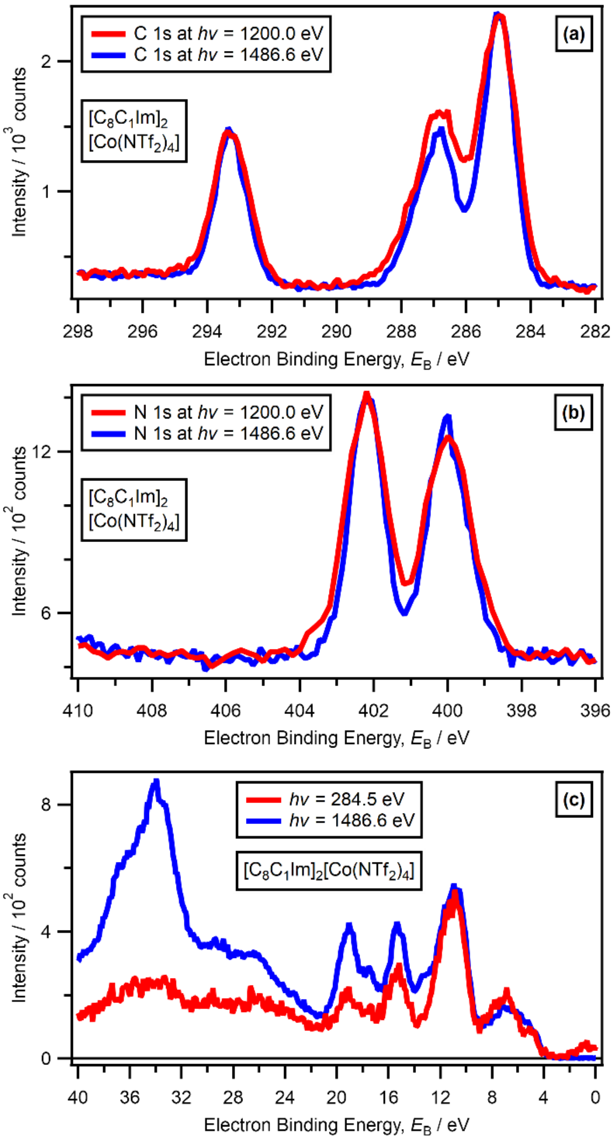

**Figure S43.** (a-b) core and (d) valence XP spectra for $[C_8C_1Im]_2[Co(NTf_2)_4]$ recorded on laboratory–based apparatus (at $h\nu$ = 1486.6 eV) and synchrotron-based XPS apparatus. All electron spectra were charge referenced using procedures outlined in ESI Section 5.

## 8. Results. RXPS data: $E_B$ heat maps

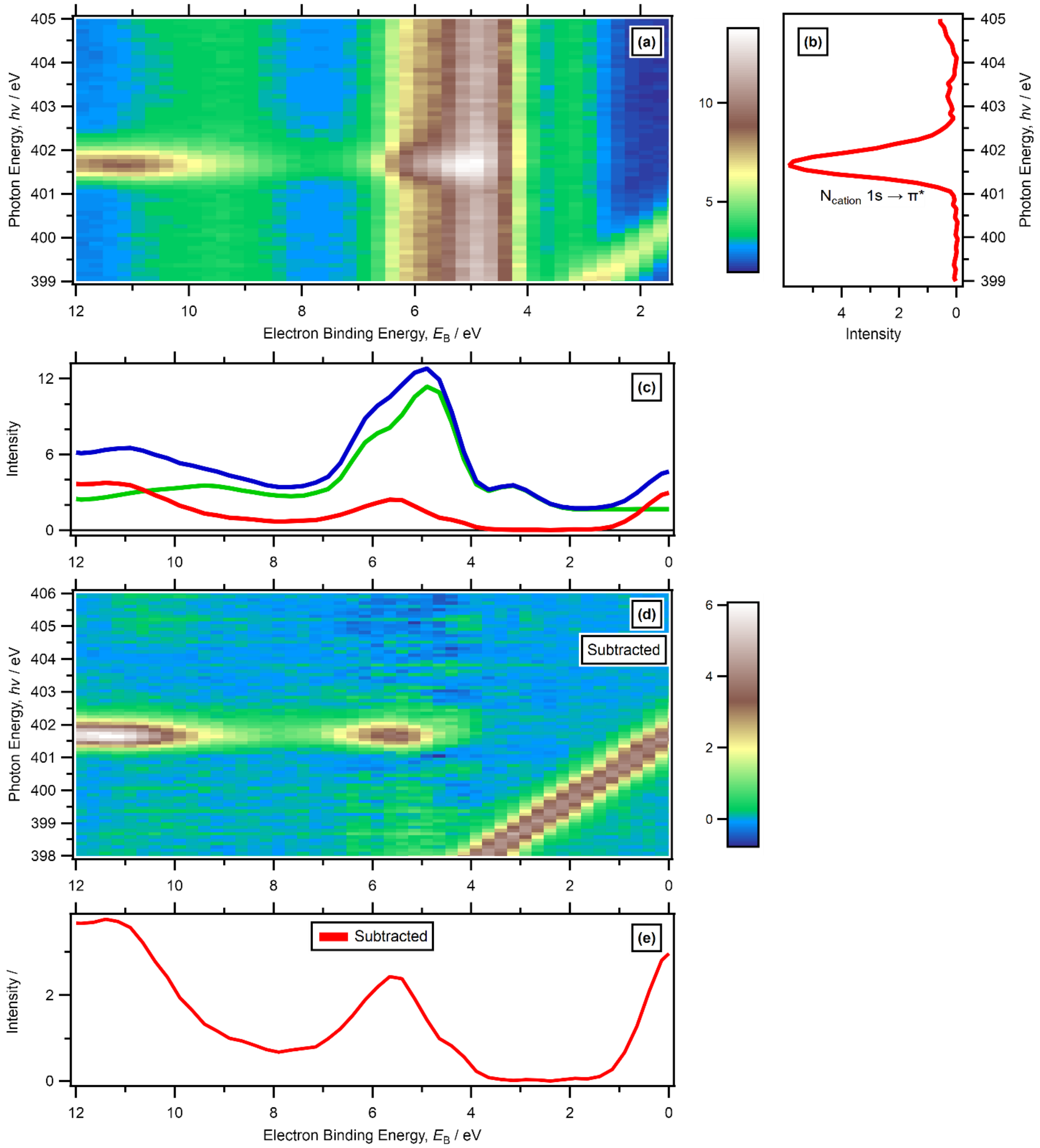

**Figure S44.** RXPS N 1s edge data for [$C_8C_1$Im][$SnCl_3$]. (a) Heat map of $h\nu$ against $E_B$ for the N 1s edge (produced by combining individual electron spectra taken at varying $h\nu$ around N 1s edge). This plot represents the raw data, with no subtraction performed. (b) Partial electron yield NEXAFS spectrum for the N 1s edge. (c) Non-resonant valence XP spectrum above the N 1s absorption edge ($h\nu$ = 404.0 eV) and resonant valence XP spectrum (*i.e.* RXPS trace) at the N 1s absorption edge ($h\nu$ = 401.8 eV). (d) Heat map of $h\nu$ against $E_B$ for the N 1s edge (produced by combining individual electron spectra taken at varying $h\nu$ around N 1s edge). (e) Subtracted $N_{cation}$ resonant Auger electron spectrum ($h\nu$ = 401.8 eV). The heat map in (d) and the RXPS trace in (e) were produced by subtraction of non-resonant XP contributions. All electron spectra were charge referenced as explained in ESI Section 5.

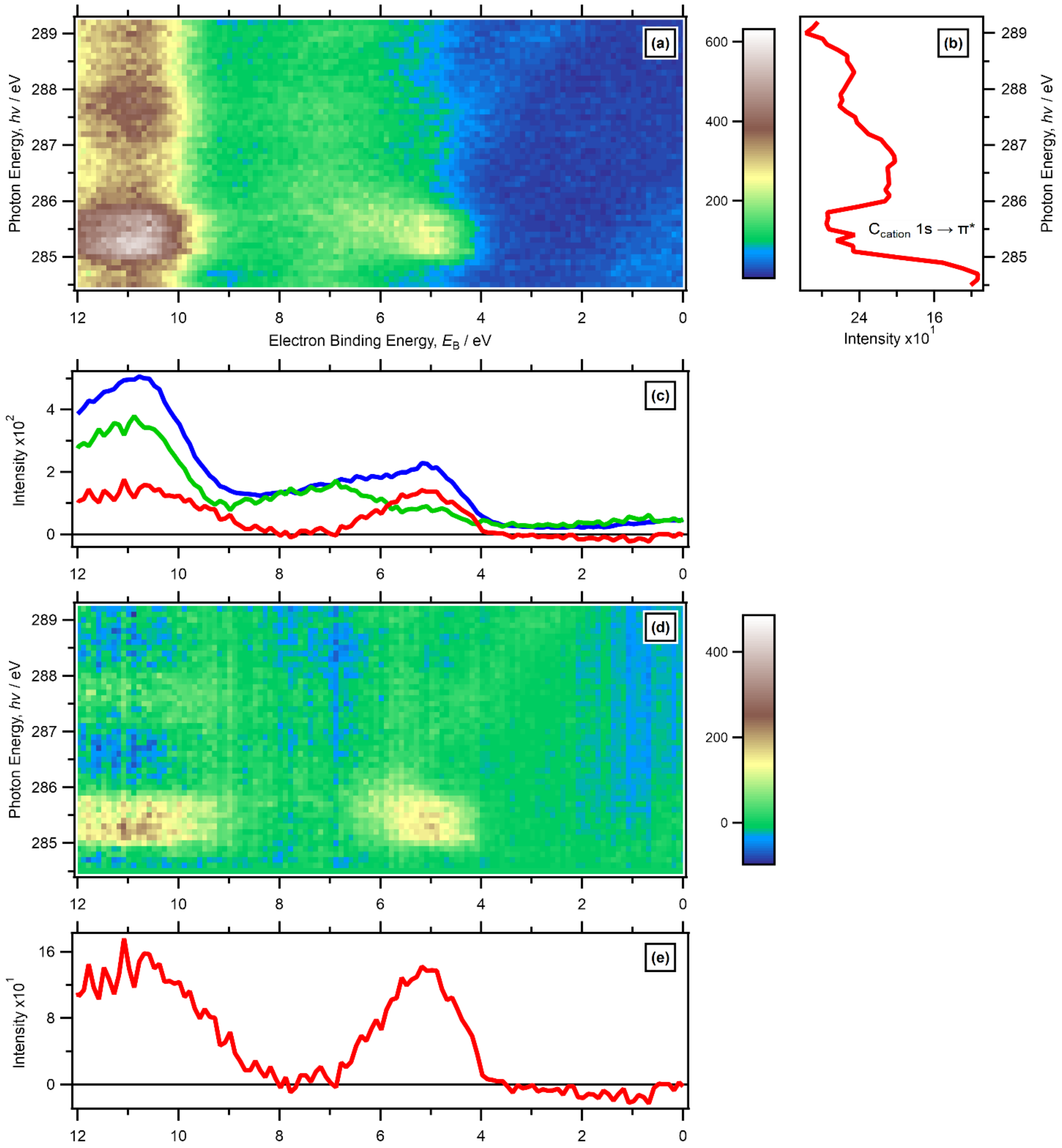

**Figure S45.** RXPS C 1s edge data for [$C_8C_1$Im]$_2$[Co(NTf$_2$)$_4$]. (a) Heat map of $h\nu$ against $E_B$ for the C 1s edge (produced by combining individual electron spectra taken at varying $h\nu$ around C 1s edge). This plot represents the raw data, with no subtraction performed. (b) Partial electron yield NEXAFS spectrum for the C 1s edge. (c) Non-resonant valence XP spectrum below the C 1s absorption edge ($h\nu$ = 284.50 eV) and resonant valence XP spectrum (*i.e.* RXPS trace) at the C 1s absorption edge ($h\nu$ = 285.45 eV). (d) Heat map of $h\nu$ against $E_B$ for the C 1s edge (produced by combining individual electron spectra taken at varying $h\nu$ around C 1s edge). (e) Subtracted $C_{cation}$ resonant Auger electron spectrum ($h\nu$= 285.45 eV). The heat map in (d) and the RXPS trace in (e) were produced by subtraction of non-resonant XP contributions. All electron spectra were charge referenced as explained in ESI Section 5.

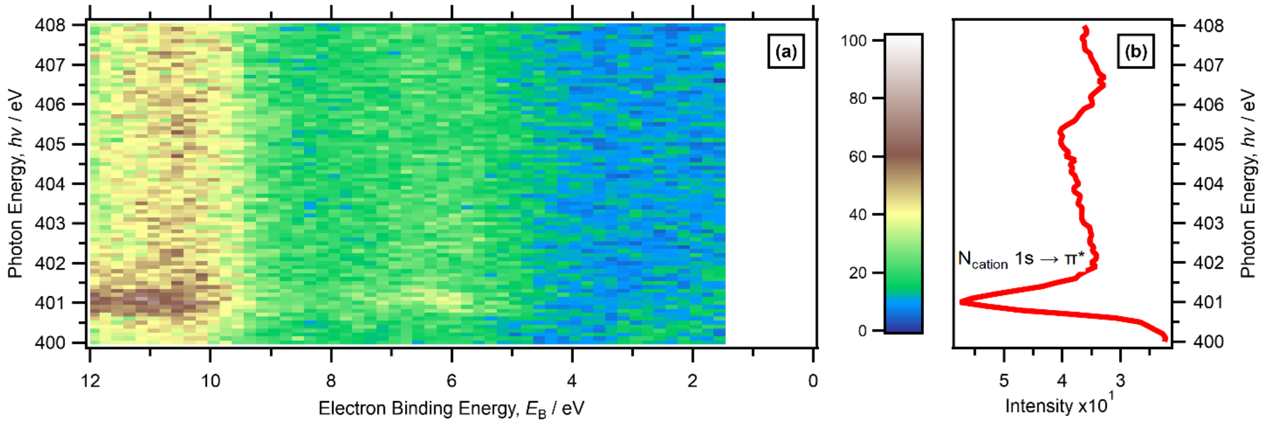

**Figure S46.** RXPS N 1s edge data for [$C_4$Py][$NTf_2$]. (a) Heat map of *hν* against $E_B$ for the N 1s edge (produced by combining individual electron spectra taken at varying *hν* around N 1s edge). This plot represents the raw data, with no subtraction performed. (b) Partial electron yield NEXAFS spectrum for the N 1s edge. All electron spectra were charge referenced as explained in ESI Section 5.

The $C_{cation}$ RXPS feature for [$C_8C_1$Im]$_2$[Co($NTf_2$)$_4$] recorded at *hν* = 285.45 eV, which was from the imidazolium carbon and not from the $CF_3$ carbon,[1, 16] showed a feature at 4 eV < $E_B$ < 7 eV. The $E_B$ separation between the $N_{cation}$ RXPS feature for [$C_8C_1$Im][$NTf_2$] ($N_{anion}$ did not give an RXPS feature for [$NTf_2$]$^-$)[1] and the $C_{cation}$ RXPS feature for [$C_8C_1$Im]$_2$[Co($NTf_2$)$_4$], $\Delta E_B$(imidazolium RXPS) = $E_B$($N_{cation}$ RXPS) - $E_B$($C_{cation}$ RXPS), was ~0.9 eV (ESI Figure S47). The ILs [$C_8C_1$Im][$NTf_2$] and [$C_8C_1$Im]$_2$[Co($NTf_2$)$_4$] gave very similar $E_B$($N_{cation}$ 1s) values (within 0.1 eV, Table 1), so a comparison of $N_{cation}$ RXPS and $C_{cation}$ RXPS for these two ILs is valid. Overall, the $C_{cation}$ RXPS feature matched to the imidazolium cation HOFO, whereas the $N_{cation}$ RXPS feature matched to an imidazolium cation OFO at $E_B$ ~0.9 eV larger than the imidazolium cation HOFO. Furthermore, the imidazolium cation HOFO had a very strong contribution from the ring carbon atoms and a relatively weak contribution from the ring nitrogen atoms.

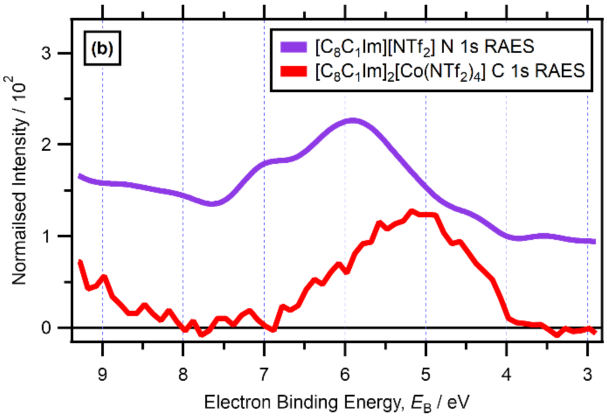

**Figure S47.** Subtracted RXP spectra for $N_{cation}$ for [$C_8C_1$Im][$NTf_2$] and $C_{cation}$ for [$C_8C_1$Im]$_2$[Co($NTf_2$)$_4$] (*hν* = 285.45 eV). These RXPS traces were produced by subtraction of resonant XP spectrum minus non-resonant XP spectrum using the procedure outlined in reference [1]. All electron spectra were charge referenced using procedures outlined in Section 2.5.

For [$C_4$Py][$NTf_2$] a broad feature due to resonant enhancement was observed at *hν* ≈ 401 eV and 4 eV < $E_B$($N_{cation}$ RXPS) < 7.5 eV (Figure 3a). *hν* ≈ 401 eV corresponded to absorption from the $N_{cation}$ 1s core state to pyridinium ring π* unoccupied valence state(s) (ESI Figure S46). The feature at 4 eV < $E_B$($N_{cation}$ RXPS) < 7.5 eV was from participator Auger transitions involving valence states with good overlap with the $N_{cation}$ 1s core hole. Consequently, for [$C_4$Py]$^+$-based ILs, valence states at 4 eV < $E_B$($N_{cation}$ RXPS) < 7.5 eV had strong contributions from $N_{cation}$ in the pyridinium ring, *i.e*. from $N_{cation}$ 2p-based AOs. For non-resonant laboratory valence XPS at $h\nu$ = 1486.6 eV for [$C_8$Py][$BF_4$], a feature due to cationic valence states at 4 eV < $E_B$ < 6.5 eV was observed (Figure 2c). Therefore, for [$C_n$Py][A] charge referenced to $E_B(C_{alkyl}\ 1s)$ = 285.0 eV, $E_B$(cation HOFO) = 5.3 ± 0.6 eV, independent of the identity of the anion $[A]^-$.

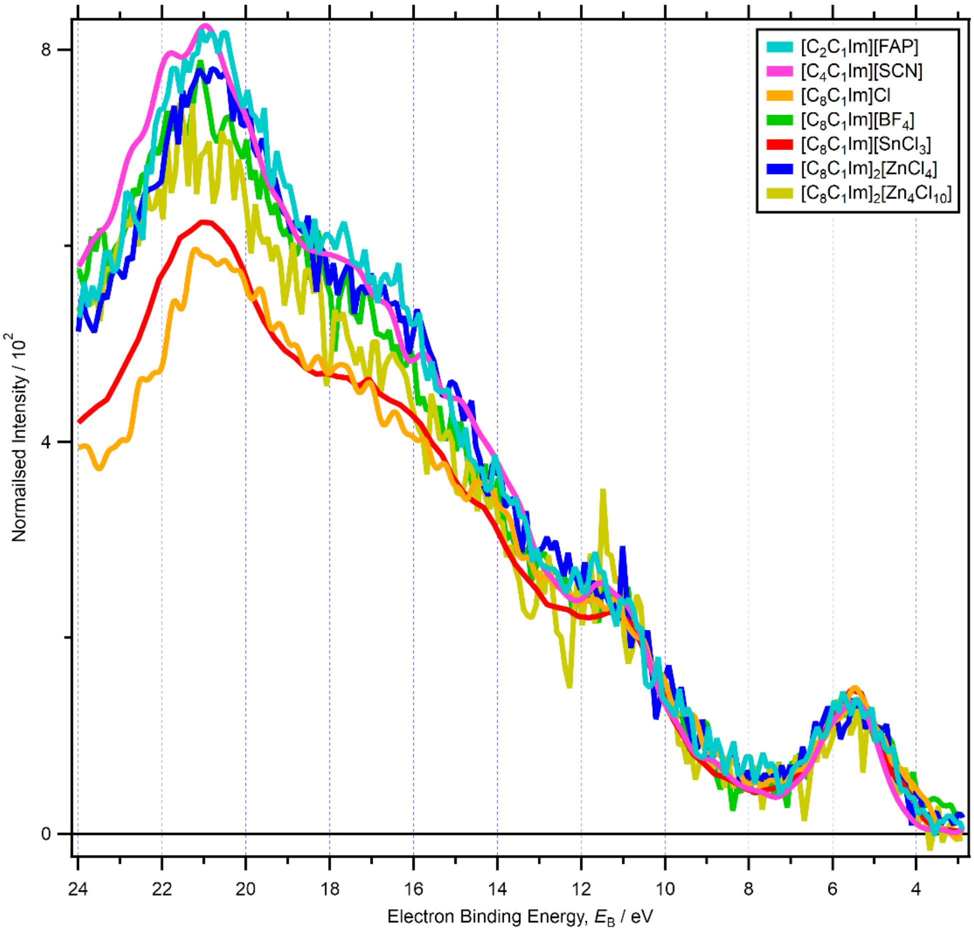

**ESI Figure S48.** Subtracted RXP spectra for $N_{cation}$ for seven [$C_nC_1$Im][A] ILs. These RXPS traces were produced by subtraction of resonant XP spectrum minus non-resonant XP spectrum using the procedure outlined in reference [1]. All electron spectra were charge referenced using procedures outlined in Section 2.4. [$C_8C_1$Im][$NTf_2$] was not included in this Figure due to spectator Auger contributions from $N_{anion}$.

## 9. Results. Quantifying the effect of countercation on anion $E_B$ and $E_i$

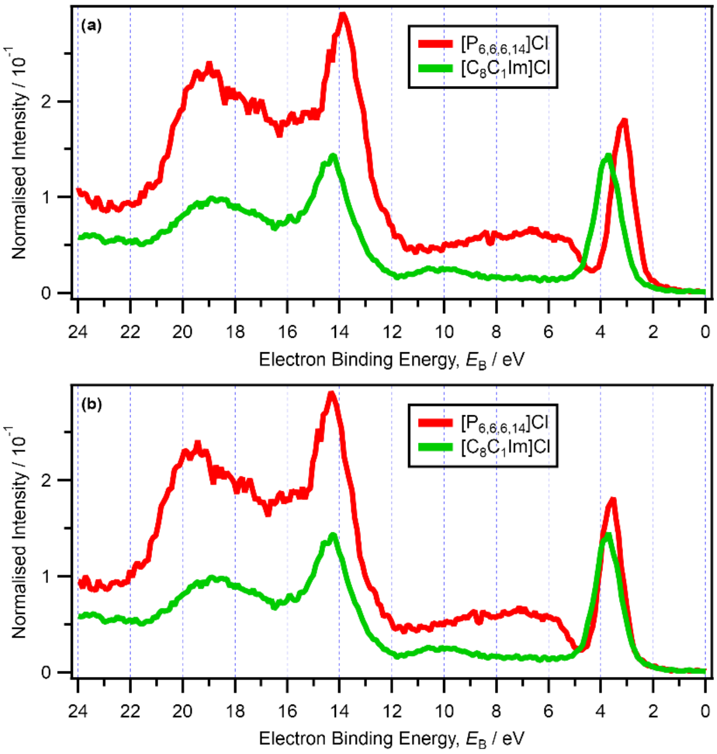

**ESI Figure S49.** Non-resonant laboratory XPS at $h\nu$ = 1486.6 eV for [$C_8C_1$Im]Cl and [$P_{6,6,6,14}$]Cl: (a) valence charge referenced to $E_B$($C_{alkyl}$ 1s) = 285.00 eV (*i.e.* using procedure 1 outlined in Section 2.4), (b) valence charge referenced to $E_B$(Cl $2p_{3.2}$) = 198.16 eV (*i.e.* using procedure 5 outlined in Section 2.4).

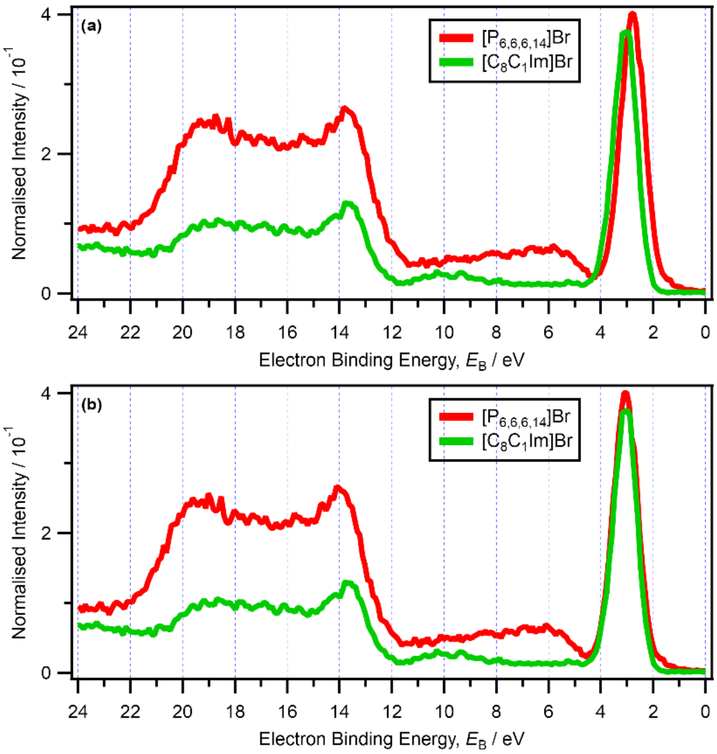

**ESI Figure S50.** Non-resonant laboratory XPS at $h\nu$ = 1486.6 eV for [C$_8$C$_1$Im]Br and [P$_{6,6,6,14}$]Br: (a) valence charge referenced to $E_B$(C$_{alkyl}$ 1s) = 285.00 eV (*i.e.* using procedure 1 outlined in Section 2.4), (b) valence charge referenced to $E_B$(Br 3d$_{5/2}$) = 67.41 eV (*i.e.* using procedure 5 outlined in Section 2.4).

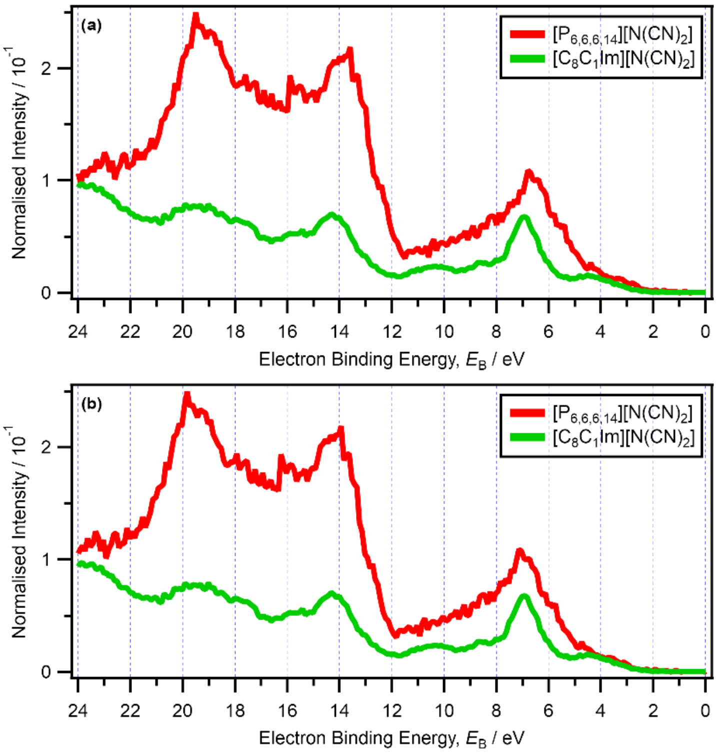

**ESI Figure S51.** Non-resonant laboratory XPS at $h\nu$ = 1486.6 eV for [C$_8$C$_1$Im][N(CN)$_2$] and [P$_{6,6,6,14}$][N(CN)$_2$]: (a) valence charge referenced to $E_B$(C$_{alkyl}$ 1s) = 285.00 eV (*i.e.* using procedure 1 outlined in Section 2.4), (b) valence charge referenced to $E_B$(N$_{terminal}$ 1s) = 398.36 eV (*i.e.* using procedure 5 outlined in Section 2.4).

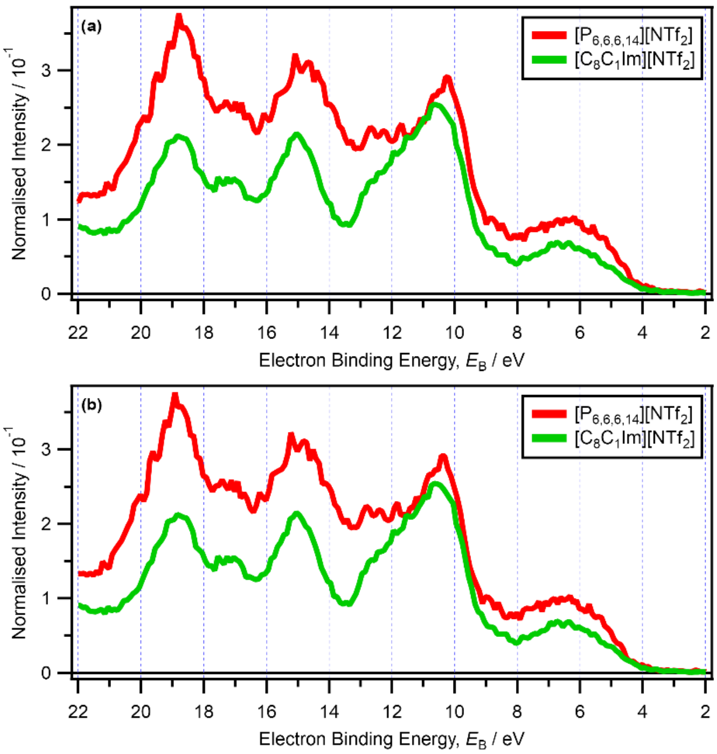

**ESI Figure S52.** Non-resonant laboratory XPS at $h\nu$ = 1486.6 eV for $[C_8C_1Im][NTf_2]$ and $[P_{6,6,6,14}][NTf_2]$: (a) valence charge referenced to $E_B(C_{alkyl}$ 1s) = 285.00 eV (*i.e.* using procedure 1 outlined in Section 2.4), (b) valence charge referenced to $E_B(N_{anion}$ 1s) = 399.46 eV (*i.e.* using procedure 5 outlined in Section 2.4).

## 10. Results. HOMO Identification and $E_\mathrm{i}$(ion) values

**Table S5.** $E_\mathrm{B}$(cation HOFO), $E_\mathrm{B}$(anion HOFO), HOFO identities, $E_\mathrm{B}$ difference between the respective ion onset $E_\mathrm{B}$ values, $\Delta E_\mathrm{B}$(ion onset) = $E_\mathrm{B}$(cation onset) – $E_\mathrm{B}$(anion onset), $E_\mathrm{B}$ difference between the respective ion HOFO $E_\mathrm{B}$ values, $\Delta E_\mathrm{B}$(ion HOFO) = $E_\mathrm{B}$(cation HOFO) – $E_\mathrm{B}$(anion HOFO) and HOMO identity. Entries are listed by $\Delta E_\mathrm{B}$(ion HOFO) [a]

| Ionic Liquid | $E_\mathrm{B}$(cation HOFO) / eV | $E_\mathrm{B}$(cation onset) / eV | Cation HOFO contribution | $E_\mathrm{B}$(anion HOFO) / eV | $E_\mathrm{B}$(anion onset) / eV | Anion HOFO contribution | $\Delta E_\mathrm{B}$(ion HOFO) / eV | $\Delta E_\mathrm{B}$(ion onset) / eV | HOMO identify |
|---|---|---|---|---|---|---|---|---|---|
| $[C_8C_1Im]_2[FeCl_4]$ | 4.8 ± 0.4 | 3.7 ± 0.3 | N 2p + C 2p | 1.4 ± 0.3 | 0.7 ± 0.2 | Cl 3p + Fe 3d | 3.4 ± 0.5 | 3.0 ± 0.4 | Anion |
| $[C_6C_1Im]I$ | 4.8 ± 0.4 | 3.7 ± 0.3 | N 2p + C 2p | 2.6 ± 0.1 | 1.7 ± 0.2 | I 5p | 2.2 ± 0.4 | 2.0 ± 0.4 | Anion |
| $[C_8C_1Im]_2[CoBr_4]$ | 4.8 ± 0.4 | 3.7 ± 0.3 | N 2p + C 2p | 2.7 ± 0.3 | 1.7 ± 0.2 | Br 4p + Co 3d | 2.1 ± 0.5 | 2.0 ± 0.4 | Anion |
| $[P_{6,6,6,14}]Br$ | 5.0 ± 0.4 | Unknown | C 2p | 2.9 ± 0.1 | 1.8 ± 0.2 | Br 4p | 2.1 ± 0.4 | Unknown | Anion |
| $[N_{4,1,1,0}][HSO_4]$ | 6.5 ± 1.0 | Unknown | C 2p | 4.5 ± 0.4 | 3.1 ± 0.3 | O 2p | 2.0 ± 1.4 | Unknown | Anion |
| $[C_8C_1Im][C(CN)_3]$ | 4.8 ± 0.4 | 3.7 ± 0.3 | N 2p + C 2p | 2.8 ± 0.2 | 1.8 ± 0.2 | N 2p | 2.0 ± 0.5 | 1.9 ± 0.4 | Anion |
| $[C_8C_1Im]_2[CoCl_4]$ | 4.8 ± 0.4 | 3.7 ± 0.3 | N 2p + C 2p | 2.9 ± 0.3 | 1.9 ± 0.2 | Cl 3p + Co 3d | 1.9 ± 0.5 | 1.8 ± 0.4 | Anion |
| $[C_4C_1Im][SCN]$ | 4.8 ± 0.4 | 3.7 ± 0.3 | N 2p + C 2p | 2.9 ± 0.1 | 1.9 ± 0.2 | N 2p + S 3p | 1.9 ± 0.4 | 1.8 ± 0.4 | Anion |
| $[C_8C_1Im][SCN]$ | 4.8 ± 0.4 | 3.7 ± 0.3 | N 2p + C 2p | 2.9 ± 0.1 | 1.9 ± 0.2 | N 2p + S 3p | 1.9 ± 0.4 | 1.8 ± 0.4 | Anion |
| $[C_8C_1Im][I_3]$ | 4.8 ± 0.4 | 3.7 ± 0.3 | N 2p + C 2p | 2.9 ± 0.3 | 1.8 ± 0.2 | I 5p | 1.9 ± 0.5 | 1.9 ± 0.4 | Anion |
| $[P_{6,6,6,14}]Cl$ | 5.0 ± 0.4 | Unknown | C 2p | 3.1 ± 0.1 | 2.2 ± 0.2 | Cl 3p | 1.9 ± 0.4 | Unknown | Anion |
| $[P_{6,6,6,14}][N(CN)_2]$ | 5.0 ± 0.4 | Unknown | C 2p | 3.2 ± 0.4 | 2.0 ± 0.3 | N 2p and/or C 2p | 1.8 ± 0.6 | Unknown | Anion |
| $[C_8C_1Im][SnCl_3]$ | 4.8 ± 0.4 | 3.7 ± 0.3 | N 2p + C 2p | 3.1 ± 0.2 | 2.1 ± 0.2 | Sn 5s + Sn 5p + Cl 3p | 1.7 ± 0.4 | 1.6 ± 0.4 | Anion |
| $[C_8C_1Im]Br$ | 4.8 ± 0.4 | 3.7 ± 0.3 | N 2p + C 2p | 3.1 ± 0.1 | 2.1 ± 0.2 | Br 4p | 1.7 ± 0.4 | 1.6 ± 0.4 | Anion |
| $[N_{8,1,1,0}][HSO_4]$ | 6.0 ± 1.0 | Unknown | C 2p | 4.5 ± 0.4 | 3.5 ± 0.3 | O 2p | 1.5 ± 1.1 | Unknown | Anion |
| $[C_8C_1Im]_2[NiCl_4]$ | 4.8 ± 0.4 | 3.7 ± 0.3 | N 2p + C 2p | 3.3 ± 0.3 | 2.2 ± 0.2 | Cl 3p + Ni 3d | 1.5 ± 0.5 | 1.5 ± 0.4 | Anion |
| $[P_{6,6,6,14}][NO_3]$ | 5.0 ± 0.4 | Unknown | C 2p | 3.5 ± 0.4 | 2.3 ± 0.3 | O 2p | 1.5 ± 0.6 | Unknown | Anion |
| $[C_4C_1Pyrr][NTf_2]$ | 6.5 ± 1.0 | Unknown | C 2p | 5.0 ± 0.4 | 4.0 ± 0.3 | O 2p/N 2p | 1.5 ± 1.1 | Unknown | Anion |
| $[C_8C_1Im]_2[ZnBr_4]$ | 4.8 ± 0.4 | 3.7 ± 0.3 | N 2p + C 2p | 3.5 ± 0.3 | 2.7 ± 0.2 | Br 4p | 1.3 ± 0.5 | 1.0 ± 0.4 | Anion |
| $[C_4C_1Im][N(CN)_2]$ | 4.8 ± 0.4 | 3.7 ± 0.3 | N 2p + C 2p | 3.5 ± 0.4 | 2.4 ± 0.3 | N 2p and/or C 2p | 1.3 ± 0.6 | 1.3 ± 0.4 | Anion |
| $[C_8C_1Im]Cl$ | 4.8 ± 0.4 | 3.7 ± 0.3 | N 2p + C 2p | 3.5 ± 0.1 | 2.6 ± 0.2 | Cl 3p | 1.3 ± 0.4 | 1.1 ± 0.4 | Anion |
| $[P_{6,6,6,14}]_2[ZnCl_4]$ | 5.0 ± 0.4 | Unknown | C 2p | 3.8 ± 0.3 | 2.9 ± 0.2 | Cl 3p | 1.2 ± 0.5 | Unknown | Anion |
| $[C_8C_1Im]_2[ZnCl_2Br_2]$ | 4.8 ± 0.4 | 3.7 ± 0.3 | N 2p + C 2p | 3.6 ± 0.3 | 2.8 ± 0.2 | Br 4p | 1.2 ± 0.5 | 0.9 ± 0.4 | Anion |
| $[S_{2,2,2}][NTf_2]$ | 6.0 ± 0.4 | Unknown | S 3p | 5.0 ± 0.4 | 4.2 ± 0.3 | O 2p/N 2p | 1.0 ± 0.6 | Unknown | Anion |
| $[S_{2,2,1}][NTf_2]$ | 6.0 ± 0.4 | Unknown | S 3p | 5.0 ± 0.4 | 4.3 ± 0.3 | O 2p/N 2p | 1.0 ± 0.6 | Unknown | Anion |
| $[C_8C_1Im]_2[Zn_2Br_6]$ | 4.8 ± 0.4 | 3.7 ± 0.3 | N 2p + C 2p | 3.8 ± 0.3 | 3.0 ± 0.2 | Br 4p | 1.0 ± 0.5 | 0.7 ± 0.4 | Anion |
| $[C_8C_1Im]_2[ZnCl_4]$ | 4.8 ± 0.4 | 3.7 ± 0.3 | N 2p + C 2p | 4.1 ± 0.3 | 3.3 ± 0.2 | Cl 3p | 0.7 ± 0.5 | 0.4 ± 0.4 | Anion |
| $[C_8C_1Im]_2[Zn_3Br_8]$ | 4.8 ± 0.4 | 3.7 ± 0.3 | N 2p + C 2p | 4.1 ± 0.3 | 3.2 ± 0.2 | Br 4p | 0.7 ± 0.5 | 0.5 ± 0.4 | Anion |
| $[C_8C_1Im]_2[Zn_4Br_{10}]$ | 4.8 ± 0.4 | 3.7 ± 0.3 | N 2p + C 2p | 4.2 ± 0.3 | 3.3 ± 0.2 | Br 4p | 0.6 ± 0.5 | 0.4 ± 0.4 | Anion |
| $[C_8C_1Im]_2[Zn_2Cl_6]$ | 4.8 ± 0.4 | 3.7 ± 0.3 | N 2p + C 2p | 4.4 ± 0.3 | 3.7 ± 0.2 | Cl 3p | 0.4 ± 0.5 | 0.0 ± 0.4 | Anion |
| $[C_4C_1Im][HSO_4]$ | 4.8 ± 0.4 | 3.7 ± 0.3 | N 2p + C 2p | 4.5 ± 0.4 | 3.2 ± 0.3 | O 2p | 0.3 ± 0.6 | 0.5 ± 0.4 | Anion |
| $[C_8C_1Im][HSO_4]$ | 4.8 ± 0.4 | 3.7 ± 0.3 | N 2p + C 2p | 4.5 ± 0.4 | 3.2 ± 0.3 | O 2p | 0.3 ± 0.6 | 0.5 ± 0.4 | Anion |
| $[C_4C_0Im][HSO_4]$ | 4.8 ± 0.4 | 3.7 ± 0.3 | N 2p + C 2p | 4.5 ± 0.4 | 3.4 ± 0.3 | O 2p | 0.3 ± 0.6 | 0.3 ± 0.4 | Anion |
| $[C_4C_1Im][MeSO_4]$ | 4.8 ± 0.4 | 3.7 ± 0.3 | N 2p + C 2p | 4.5 ± 0.4 | 3.1 ± 0.3 | O 2p | 0.3 ± 0.6 | 0.6 ± 0.4 | Anion |

| | | | | | | | | | |
|---|---|---|---|---|---|---|---|---|---|
| [C$_4$C$_1$Im][OcSO$_4$] | 4.8 ± 0.4 | 3.7 ± 0.3 | N 2p + C 2p | 4.5 ± 0.4 | 3.1 ± 0.3 | O 2p | 0.3 ± 0.6 | 0.6 ± 0.4 | Anion |
| [C$_2$C$_1$Im][MeSO$_3$] | 4.8 ± 0.4 | 3.7 ± 0.3 | N 2p + C 2p | 4.5 ± 0.4 | 3.0 ± 0.3 | O 2p | 0.3 ± 0.6 | 0.7 ± 0.4 | Anion |
| [C$_4$C$_1$Im][Me$_2$PO$_4$] | 4.8 ± 0.4 | 3.7 ± 0.3 | N 2p + C 2p | 4.5 ± 0.4 | 3.2 ± 0.3 | O 2p | 0.3 ± 0.6 | 0.5 ± 0.4 | Anion |
| [N$_{2,2,1,0}$][TfO] | Unknown | Unknown | Not identified | 5.0 ± 0.4 | 3.7 ± 0.3 | O 2p | Not determined | Unknown | Anion |
| [N$_{4,1,1,1}$][NTf$_2$] | Unknown | Unknown | Not identified | 5.0 ± 0.4 | 4.0 ± 0.3 | O 2p/N 2p | Not determined | Unknown | Anion |
| [N$_{3,2,1,1}$][NTf$_2$] | Unknown | Unknown | Not identified | 5.0 ± 0.4 | 3.9 ± 0.3 | O 2p/N 2p | Not determined | Unknown | Anion |
| [C$_4$Py][NTf$_2$] | 5.3 ± 0.6 | 4.3 ± 0.4 | N 2p + C 2p | 5.0 ± 0.4 | 3.9 ± 0.3 | O 2p/N 2p | 0.3 ± 0.6 | -0.2 ± 0.4 | Cation/Anion |
| [P$_{6,6,6,14}$][NTf$_2$] | 5.0 ± 0.4 | Unknown | C 2p | 4.8 ± 0.4 | 3.6 ± 0.3 | O 2p/N 2p | 0.2 ± 0.6 | Unknown | Cation/Anion |
| [N$_{8,8,8,1}$][NTf$_2$] | 5.0 ± 0.4 | Unknown | C 2p | 5.0 ± 0.4 | 3.8 ± 0.3 | O 2p/N 2p | 0.0 ± 0.6 | Unknown | Cation/Anion |
| [C$_4$C$_1$Im][TfO] | 4.8 ± 0.4 | 3.7 ± 0.3 | N 2p + C 2p | 5.0 ± 0.4 | 3.6 ± 0.3 | O 2p | -0.2 ± 0.6 | 0.1 ± 0.4 | Cation/Anion |
| [C$_8$C$_1$Im][TfO] | 4.8 ± 0.4 | 3.7 ± 0.3 | N 2p + C 2p | 5.0 ± 0.4 | 3.7 ± 0.3 | O 2p | -0.2 ± 0.6 | 0.0 ± 0.4 | Cation/Anion |
| [C$_4$C$_1$Im][NTf$_2$] | 4.8 ± 0.4 | 3.7 ± 0.3 | N 2p + C 2p | 5.0 ± 0.4 | 3.8 ± 0.3 | O 2p/N 2p | -0.2 ± 0.6 | -0.1 ± 0.4 | Cation/Anion |
| [C$_6$C$_1$Im][NTf$_2$] | 4.8 ± 0.4 | 3.7 ± 0.3 | N 2p + C 2p | 5.0 ± 0.4 | 3.8± 0.3 | O 2p/N 2p | -0.2 ± 0.6 | -0.1 ± 0.4 | Cation/Anion |
| [C$_8$C$_1$Im][NTf$_2$] | 4.8 ± 0.4 | 3.7 ± 0.3 | N 2p + C 2p | 5.0 ± 0.4 | 3.8 ± 0.3 | O 2p/N 2p | -0.2 ± 0.6 | -0.1 ± 0.4 | Cation/Anion |
| [C$_2$C$_0$Im][NTf$_2$] | 4.8 ± 0.4 | 3.7 ± 0.3 | N 2p + C 2p | 5.0 ± 0.4 | 3.9 ± 0.3 | O 2p/N 2p | -0.2 ± 0.6 | -0.2 ± 0.4 | Cation/Anion |
| [C$_4$C$_0$Im][NTf$_2$] | 4.8 ± 0.4 | 3.7 ± 0.3 | N 2p + C 2p | 5.0 ± 0.4 | 3.9 ± 0.3 | O 2p/N 2p | -0.2 ± 0.6 | -0.2 ± 0.4 | Cation/Anion |
| [C$_8$C$_1$Im]$_2$[Co(NTf$_2$)$_4$] | 4.8 ± 0.4 | 3.7 ± 0.3 | N 2p + C 2p | 5.0 ± 0.4 | 3.7 ± 0.3 | Co 3d/O 2p/N 2p | -0.2 ± 0.6 | 0.0 ± 0.4 | Cation/Anion |
| [N$_{2OH,2OH,2OH,1}$][TfO] | 4.8 ± 0.4 | 3.6 ± 0.3 | O 2p | 5.0 ± 0.4 | 3.6 ± 0.3 | O 2p | -0.2 ± 0.6 | 0.0 ± 0.4 | Cation/Anion |
| [C$_8$C$_1$Im]$_2$[Zn$_4$Cl$_{10}$] | 4.8 ± 0.4 | 3.7 ± 0.3 | N 2p + C 2p | 5.0 ± 0.3 | 4.0 ± 0.2 | Cl 3p | -0.2 ± 0.5 | -0.3 ± 0.4 | Cation/Anion |
| [C$_8$C$_1$Im][InCl$_4$] | 4.8 ± 0.4 | 3.7 ± 0.3 | N 2p + C 2p | 5.2 ± 0.3 | 4.5 ± 0.2 | Cl 3p | -0.4 ± 0.5 | -0.8 ± 0.4 | Cation |
| [C$_6$C$_1$Im][B(CN)$_4$] | 4.8 ± 0.4 | 3.7 ± 0.3 | N 2p + C 2p | 6.6 ± 0.6 | 5.3 ± 0.3 | N 2p and/or C 2p | -1.8 ± 0.7 | -1.6 ± 0.4 | Cation |
| [C$_8$Py][BF$_4$] | 5.3 ± 0.6 | 4.3 ± 0.4 | N 2p + C 2p | 7.6 ± 0.6 | 6.4 ± 0.4 | F 2p | -2.3 ± 0.7 | -2.1 ± 0.6 | Cation |
| [C$_8$C$_1$Im][BF$_4$] | 4.8 ± 0.4 | 3.7 ± 0.3 | N 2p + C 2p | 7.8 ± 0.6 | 6.4 ± 0.4 | F 2p | -3.0 ± 0.7 | -2.7 ± 0.6 | Cation |
| [C$_4$C$_1$Im][PF$_6$] | 4.8 ± 0.4 | 3.7 ± 0.3 | N 2p + C 2p | 8.0 ± 0.6 | 7.0 ± 0.4 | F 2p | -3.2 ± 0.7 | -3.3 ± 0.6 | Cation |
| [C$_2$C$_1$Im][FAP] | 4.8 ± 0.4 | 3.7 ± 0.3 | N 2p + C 2p | 8.6 ± 0.6 | 7.2 ± 0.4 | F 2p | -3.8 ± 0.7 | -3.5 ± 0.6 | Cation |
| [C$_8$C$_1$Im][SbF$_6$] | 4.8 ± 0.4 | 3.7 ± 0.3 | N 2p + C 2p | 8.9 ± 0.6 | 7.6 ± 0.4 | F 2p | -4.1 ± 0.7 | -3.9 ± 0.6 | Cation |

[a] The HOMO identity assignments for [N$_{2,2,1,0}$][TfO], [N$_{4,1,1,1}$][NTf$_2$] and [N$_{3,2,1,1}$][NTf$_2$] were based upon a combination of $E_B$(anion HOFO) for these ILs and $E_B$(cation HOFO) for [N$_{4,1,1,0}$][HSO$_4$]

**Table S6.** $E_B$(anion HOFO) and $E_i$(anion) for a range of anions in $[C_nC_1Im][A]$ ILs

| Anion | $E_B$(anion HOFO) / eV | $E_i$(anion)[a] / eV |
|---|---|---|
| $[FeCl_4]^{2-}$ | 1.4 ± 0.3 | 6.0 ± 0.3 |
| $I^-$ | 2.6 ± 0.1 | 7.2 ± 0.2 |
| $[CoBr_4]^{2-}$ | 2.7 ± 0.3 | 7.3 ± 0.3 |
| $[C(CN)_3]^-$ | 2.8 ± 0.2 | 7.4 ± 0.2 |
| $[SCN]^-$ | 2.9 ± 0.1 | 7.5 ± 0.2 |
| $[I_3]^-$ | 2.9 ± 0.3 | 7.5 ± 0.3 |
| $[CoCl_4]^{2-}$ | 2.9 ± 0.3 | 7.5 ± 0.3 |
| $[SnCl_3]^-$ | 3.1 ± 0.2 | 7.7 ± 0.2 |
| $Br^-$ | 3.1 ± 0.1 | 7.7 ± 0.2 |
| $[NiCl_4]^{2-}$ | 3.3 ± 0.3 | 7.9 ± 0.3 |
| $[N(CN)_2]^-$ | 3.5 ± 0.4 | 8.1 ± 0.4 |
| $Cl^-$ | 3.5 ± 0.1 | 8.1 ± 0.2 |
| $[ZnBr_4]^{2-}$ | 3.5 ± 0.3 | 8.1 ± 0.3 |
| $[ZnCl_2Br_2]^{2-}$ | 3.6 ± 0.3 | 8.2 ± 0.3 |
| $[NO_3]^-$ [b] | 3.8 ± 0.5 | 8.4 ± 0.4 |
| $[Zn_2Br_6]^{2-}$ | 3.8 ± 0.3 | 8.4 ± 0.3 |
| $[ZnCl_4]^{2-}$ | 4.1 ± 0.3 | 8.7 ± 0.3 |
| $[Zn_3Br_8]^{2-}$ | 4.1 ± 0.3 | 8.7 ± 0.3 |
| $[Zn_4Br_{10}]^{2-}$ | 4.2 ± 0.3 | 8.8 ± 0.3 |
| $[Zn_2Cl_6]^{2-}$ | 4.4 ± 0.3 | 9.0 ± 0.3 |
| $[HSO_4]^-$ | 4.5 ± 0.4 | 9.1 ± 0.4 |
| $[Me_2PO_4]^-$ | 4.5 ± 0.4 | 9.1 ± 0.4 |
| $[MeSO_3]^-$ | 4.5 ± 0.4 | 9.1 ± 0.4 |
| $[MeSO_4]^-$ | 4.5 ± 0.4 | 9.1 ± 0.4 |
| $[OcSO_4]^-$ | 4.5 ± 0.4 | 9.1 ± 0.4 |
| $[Zn_3Cl_8]^{2-}$ [c] | 4.7 ± 0.3 | 9.3 ± 0.3 |
| $[TfO]^-$ | 5.0 ± 0.4 | 9.6 ± 0.4 |
| $[Co(NTf_2)_4]^{2-}$ | 5.0 ± 0.4 | 9.6 ± 0.4 |
| $[NTf_2]^-$ | 5.0 ± 0.4 | 9.6 ± 0.4 |
| $[Zn_4Cl_{10}]^{2-}$ | 5.0 ± 0.3 | 9.6 ± 0.3 |
| $[InCl_4]^-$ | 5.2 ± 0.3 | 9.8 ± 0.3 |
| $[B(CN)_4]^-$ | 6.6 ± 0.6 | 11.2 ± 0.6 |
| $[BF_4]^-$ | 7.8 ± 0.6 | 12.4 ± 0.6 |
| $[PF_6]^-$ | 8.0 ± 0.6 | 12.6 ± 0.6 |
| $[FAP]^-$ | 8.6 ± 0.6 | 13.2 ± 0.6 |
| $[SbF_6]^-$ | 8.9 ± 0.6 | 13.5 ± 0.6 |

[a] For $E_i$(anion) the work function was 4.58 eV[17-21]

[b] For $[NO_3]^-$ the value was $E_B$(anion HOFO,pred.), estimated using $E_B$(anion HOFO) measured for $[P_{6,6,6,14}][NO_3]$ and other $E_B$(anion HOFO) values for $[P_{6,6,6,14}][A]$ and $[C_8C_1Im][A]$

[c] For $[Zn_3Cl_8]^{2-}$ the value was $E_B$(anion HOFO,pred.) not $E_B$(anion HOFO), estimated using $E_B$(anion HOFO) for other halozincate dianions

**Table S7.** $E_B$(cation HOFO) and $E_i$(cation) for a range of cations

| Cation | $E_B$(cation HOFO) / eV | $E_i$(cation)[a] / eV |
|---|---|---|
| $[C_2C_1Im]^+$ | 4.8 ± 0.4 | 9.4 ± 0.4 |
| $[C_4C_1Im]^+$ | 4.8 ± 0.4 | 9.4 ± 0.4 |
| $[C_6C_1Im]^+$ | 4.8 ± 0.4 | 9.4 ± 0.4 |
| $[C_8C_1Im]^+$ | 4.8 ± 0.4 | 9.4 ± 0.4 |
| $[C_2C_0Im]^+$ | 4.8 ± 0.4 | 9.4 ± 0.4 |
| $[C_4C_0Im]^+$ | 4.8 ± 0.4 | 9.4 ± 0.4 |
| $[N_{(2OH)3,1}]^+$ | 4.8 ± 0.4 | 9.4 ± 0.4 |
| $[P_{6,6,6,14}]^+$ | 5.0 ± 0.4 | 9.6 ± 0.4 |
| $[N_{8,8,8,1}]^+$ | 5.0 ± 0.4 | 9.6 ± 0.4 |
| $[C_4Py]^+$ | 5.3 ± 0.6 | 9.9 ± 0.6 |
| $[C_8Py]^+$ | 5.3 ± 0.6 | 9.9 ± 0.6 |
| $[S_{2,2,1}]^+$ | 6.0 ± 0.4 | 10.6 ± 0.4 |
| $[S_{2,2,2}]^+$ | 6.0 ± 0.4 | 10.6 ± 0.4 |
| $[N_{4,1,1,0}]^+$ | 6.5 ± 1.0 | 11.1 ± 1.0 |
| $[N_{8,1,1,0}]^+$ | 6.5 ± 1.0 | 11.1 ± 1.0 |

[a] For $E_i$(cation) the work function was 4.58 eV[17-21]

## 11. Results. FWHM for HOMO Identification

The FWHM for the peak due to the HOMO for $[SCN]^-$, $Cl^-$, $I^-$ and $[C(CN)_3]^-$ ranged from 0.75 eV to 1.02 eV. ILs with these anions were chosen as they all gave peaks due to the HOMO that could be readily fitted ($Br^-$ was not included due to the influence of spin-orbit coupling, which was too small to be important for $Cl^-$ and large enough in $I^-$ to be accounted for when fitting). Therefore, a total FWHM value of 0.9 eV was used to estimate the experimental contribution to the FWHM. The equation used to estimate the sample contribution to the FWHM was:[14, 15]

$$[\mathrm{FWHM(total)}]^2 = [\mathrm{FWHM(apparatus)}]^2 + [\mathrm{FWHM(lifetime)}]^2 + \mathrm{FWHM(sample)}]^2 \qquad \text{(Equation 1)}$$

## 12. Results. Predictions

**Table S8.** Predictions for [C$_n$C$_1$Im][A] ILs of $E_\mathrm{B}$(cation HOFO) and $E_\mathrm{i}$(cation) using $E_\mathrm{B}$(cation HOFO) = $E_\mathrm{B}$(N$_\mathrm{cation}$ 1s) - 397.1 eV and $E_\mathrm{i}$(cation) = $E_\mathrm{B}$(cation HOFO) + 4.58 eV. The error in $E_\mathrm{B}$(N$_\mathrm{cation}$ 1s) is ±0.1 eV, and the errors in $E_\mathrm{B}$(cation HOFO,pred.) and $E_\mathrm{i}$(cation,pred.) are both ±0.2 eV

| Ionic Liquid | $E_\mathrm{B}$(N$_\mathrm{cation}$ 1s) / eV | $E_\mathrm{B}$(cation HOFO,pred.) / eV | $E_\mathrm{i}$(cation,pred.) / eV |
|---|---|---|---|
| [C$_8$C$_1$Im]Cl | 401.7 | 4.6 | 9.2 |
| [C$_4$C$_1$Im][OcSO$_4$] | 401.7 | 4.6 | 9.2 |
| [C$_8$C$_1$Im]Br | 401.7 | 4.6 | 9.2 |
| [C$_4$C$_1$Im][HSO$_4$] | 401.8 | 4.7 | 9.3 |
| [C$_8$C$_1$Im][HSO$_4$] | 401.8 | 4.7 | 9.3 |
| [C$_8$C$_1$Im]$_2$[NiCl$_4$] | 401.8 | 4.7 | 9.3 |
| [C$_8$C$_1$Im]$_2$[CoCl$_4$] | 401.8 | 4.7 | 9.3 |
| [C$_8$C$_1$Im]$_2$[FeCl$_4$] | 401.8 | 4.7 | 9.3 |
| [C$_8$C$_1$Im]$_2$[ZnCl$_4$] | 401.8 | 4.7 | 9.3 |
| [C$_8$C$_1$Im]$_2$[ZnCl$_2$Br$_2$] | 401.8 | 4.7 | 9.3 |
| [C$_6$C$_1$Im]I | 401.9 | 4.8 | 9.3 |
| [C$_8$C$_1$Im]$_2$[ZnBr$_4$] | 401.9 | 4.8 | 9.4 |
| [C$_4$C$_1$Im][SCN] | 401.9 | 4.8 | 9.4 |
| [C$_8$C$_1$Im][SCN] | 401.9 | 4.8 | 9.4 |
| [C$_8$C$_1$Im]$_2$[CoBr$_4$] | 401.9 | 4.8 | 9.4 |
| [C$_4$C$_1$Im][TfO] | 402.0 | 4.9 | 9.4 |
| [C$_8$C$_1$Im][TfO] | 402.0 | 4.9 | 9.4 |
| [C$_8$C$_1$Im]$_2$[Zn$_2$Br$_6$] | 402.0 | 4.9 | 9.4 |
| [C$_8$C$_1$Im]$_2$[Zn$_2$Cl$_6$] | 402.0 | 4.9 | 9.4 |
| [C$_8$C$_1$Im][BF$_4$] | 402.0 | 4.9 | 9.5 |
| [C$_8$C$_1$Im][SnCl$_3$] | 402.0 | 4.9 | 9.5 |
| [C$_4$C$_1$Im][N(CN)$_2$] | 402.0 | 4.9 | 9.5 |
| [C$_8$C$_1$Im]$_2$[Zn$_3$Br$_8$] | 402.0 | 4.9 | 9.5 |
| [C$_8$C$_1$Im]$_2$[Zn$_4$Br$_{10}$] | 402.1 | 5.0 | 9.5 |
| [C$_8$C$_1$Im]$_2$[Zn$_4$Cl$_{10}$] | 402.1 | 5.0 | 9.5 |
| [C$_6$C$_1$Im][B(CN)$_4$] | 402.1 | 5.0 | 9.5 |
| [C$_8$C$_1$Im][C(CN)$_3$] | 402.1 | 5.0 | 9.5 |
| [C$_4$C$_1$Im][NTf$_2$] | 402.1 | 5.0 | 9.6 |
| [C$_6$C$_1$Im][NTf$_2$] | 402.1 | 5.0 | 9.6 |
| [C$_8$C$_1$Im][NTf$_2$] | 402.1 | 5.0 | 9.6 |
| [C$_4$C$_1$Im][PF$_6$] | 402.1 | 5.0 | 9.6 |
| [C$_8$C$_1$Im][I$_3$] | 402.1 | 5.0 | 9.6 |
| [C$_8$C$_1$Im][SbF$_6$] | 402.1 | 5.0 | 9.6 |
| [C$_8$C$_1$Im][InCl$_4$] | 402.2 | 5.1 | 9.7 |
| [C$_8$C$_1$Im]$_2$[Co(NTf$_2$)$_4$] | 402.2 | 5.1 | 9.7 |
| [C$_2$C$_1$Im][FAP] | 402.3 | 5.2 | 9.8 |

## 13. References

1. R. M. Fogarty, R. G. Palgrave, R. A. Bourne, K. Handrup, I. J. Villar-Garcia, D. J. Payne, P. A. Hunt and K. R. J. Lovelock, *Phys. Chem. Chem. Phys.*, 2019, **21**, 18893-18910.
2. S. Men, K. R. J. Lovelock and P. Licence, *Phys. Chem. Chem. Phys.*, 2011, **13**, 15244-15255.
3. S. Men, D. S. Mitchell, K. R. J. Lovelock and P. Licence, *ChemPhysChem*, 2015, **16**, 2211-2218.
4. I. J. Villar-Garcia, S. Fearn, G. F. De Gregorio, N. L. Ismail, F. J. V. Gschwend, A. J. S. McIntosh and K. R. J. Lovelock, *Chem. Sci.*, 2014, **5**, 4404-4418.
5. L. S. Longo, E. F. Smith and P. Licence, *ACS Sustain. Chem. Eng.*, 2016, **4**, 5953-5962.
6. S. A. Men, K. R. J. Lovelock and P. Licence, *Chem. Phys. Lett.*, 2017, **679**, 207-211.
7. C. J. Clarke, S. Hayama, A. Hawes, J. P. Hallett, T. W. Chamberlain, K. R. J. Lovelock and N. A. Besley, *J. Phys. Chem. A*, 2019, **123**, 9552-9559.
8. J. M. Seymour, E. Gousseva, R. M. Fogarty, L. Frankemoelle, R. Rowe, C. J. Clarke, D. A. Duncan, R. A. Bennett, R. G. Palgrave, P. A. Hunt and K. R. J. Lovelock, 2021, To be submitted in June 2021.
9. J. X. Mao and K. Damodaran, *Ionics*, 2015, **21**, 1605-1613.
10. I. J. Villar-Garcia, E. F. Smith, A. W. Taylor, F. L. Qiu, K. R. J. Lovelock, R. G. Jones and P. Licence, *Phys. Chem. Chem. Phys.*, 2011, **13**, 2797-2808.
11. T. Cremer, C. Kolbeck, K. R. J. Lovelock, N. Paape, R. Wölfel, P. S. Schulz, P. Wasserscheid, H. Weber, J. Thar, B. Kirchner, F. Maier and H. P. Steinrück, *Chem.-Eur. J.*, 2010, **16**, 9018-9033.
12. J. M. Pi, M. Stella, N. K. Fernando, A. Y. Lam, A. Regoutz and L. E. Ratcliff, *J. Phys. Chem. Lett.*, 2020, **11**, 2256-2262.
13. M. O. Krause and J. H. Oliver, *J. Phys. Chem. Ref. Data*, 1979, **8**, 329-338.
14. J. Liu, H. Zhang, Y. M. Li and Z. Liu, *J. Phys. Chem. B*, 2018, **122**, 10600-10606.
15. J. C. Vickerman and I. S. Gilmore, eds., *Surface Analysis: The Principal Techniques*, John Wiley & Sons, Chichester, 2009.
16. C. Ehlert, M. Holzweber, A. Lippitz, W. E. S. Unger and P. Saalfrank, *Phys. Chem. Chem. Phys.*, 2016, **18**, 8654-8661.
17. G. Greczynski and L. Hultman, *ChemPhysChem*, 2017, **18**, 1507-1512.
18. G. Greczynski and L. Hultman, *Appl. Surf. Sci.*, 2018, **451**, 99-103.
19. G. Greczynski and L. Hultman, *Angew. Chem.-Int. Edit.*, 2020, **59**, 5002-5006.
20. D. R. Baer, K. Artyushkova, H. Cohen, C. D. Easton, M. Engelhard, T. R. Gengenbach, G. Greczynski, P. Mack, D. J. Morgan and A. Roberts, *Journal of Vacuum Science & Technology A*, 2020, **38**, 031204.
21. G. Greczynski and L. Hultman, *Prog. Mater Sci.*, 2020, **107**, 100591.